MICROMETEOROLOGY GROUP
Faculty of Biology, Chemistry and Earth Sciences
University of Bayreuth

Experimental evaluation of the significance of the pressure transport term to the Turbulence Kinetic Energy budget across contrasting forest architectures

Master Thesis in Geoecology

Laura Ehrnsperger

supervised by

Prof. Dr. Christoph THOMAS

February 28, 2017

Contact details of author:
Laura Ehrnsperger (B.Sc. Geoecology)
Matriculation number: 1248081
E-mail: laura.ehrnsperger@geoecology.org

Supervisor:
Prof. Dr. Christoph Thomas
(Micrometeorology Group, University of Bayreuth)

Co-Supervisor:
Dr. Wolfgang Babel
(Micrometeorology Group, University of Bayreuth)

Contents

List of Figures

List of Tables

List of Abbreviations and Symbols

Abbreviations

ASCII2	American Standard Code for Information Interchange, character encoding standard
agl	Above Ground Level
asl	Above Sea Level
B	Buoyancy term of the TKE budget
BayCEER	Bayreuth Center of Ecology and Environmental Research
BL	Boundary Layer
CO_2	Chemical abbreviation for carbon dioxide
COM	Interface for serial connection with data logger
CR3000	Type of data logger by Campbell Scientific
CSAT3	3-D sonic anemometer type by Campbell Scientific
EC	Eddy Covariance Method
FFT	Fast-Fourier transform method
FLUXNET	Global measurement network for observations from micrometeorological tower sites
GPS	Global Positioning System
H_2O	Chemical abbreviation for water
Hz	Hertz = $\frac{1}{s}$
I1	IRGA installed at 36m height
I2	IRGA installed near the soil surface
INTRAMIX	INvestigation and TRAnsport of MIXing within a forest canopy

IRGA	Infra-red gas analyzer
LAI	Leaf Area Index
LES	Large Eddy Simulation
Li-7500	Open-path infra-red gas analyzer by LI-COR Environmental
MODIS	Moderate Resolution Imaging Spectroradiometer, Instrument to measure electromagnetic radiation mounted on NASA-satellite
MS	Mechanical shear term of the TKE budget
OD	Omnidirectional
P1	Pressure transducer at 36m height
P2	Pressure transducer at 18m height
P3	Pressure transducer at 4m height
P4	Pressure transducer within the soil
PAI	Plant Area Index
PT	Pressure transport term of the TKE budget
RS-232	Serial interface at data logger
QAQC	Quality Assessment and Quality Control
S1	Sonic anemometer at 36m height
S2	Sonic anemometer at 18m height
S3	Sonic anemometer at 4m height
S4	Sonic anemometer near the soil surface
S5	Sonic anemometer at 4m height at satellite station a)
S6	Sonic anemometer at 4m height at satellite station b)
SDM	Connection interface at data logger
TEMS	Measurement network
TKE	Turbulence Kinetic Energy
TKE tdc	TKE tendency of the TKE budget
TOA5	File format
TT	Turbulent transport term of the TKE budget

USA-1	3-D sonic anemometer type by Metek

Symbols

$\overline{e}$	Mean turbulence kinetic energy
g	Gravity acceleration
L	Monin-Obukhov length
Q_{v0}	Kinematic virtual temperature flux at the surface
T_v	Virtual temperature
$\overline{u}$	Mean horizontal wind speed
u'	Perturbations of horizontal along-wind component
u*	Friction velocity
$\overline{u'u'}$	Covariance of perturbations of the horizontal along-wind component
v'	Perturbations of horizontal cross-wind component
$\overline{v'v'}$	Covariance of perturbations of the horizontal cross-wind component
w'	Perturbations of vertical wind component
$\overline{w'u'}$	Momentum flux
$\overline{w'w'}$	Covariance of the perturbations of the vertical wind component
$\overline{w'\theta'_v}$	Buoyancy flux
z	Height above the ground, e.g. measurement height
$\frac{\delta\overline{e}}{\delta t}$	TKE tendency
$\frac{\delta\overline{w'p'}}{\delta z}$	Flux divergence of pressure transport
$\frac{\delta\overline{w'\overline{e}}}{\delta z}$	Flux divergence of turbulent transport transport
ϵ	Viscous dissipation
ζ	Obukhov stability parameter
θ_v	Virtual potential temperature

κ	von K*á*rman constant
κ_L	$= \mathrm{RL/cp} = 2/7 = 0.286$
ρ	Air density $[m^3]$

Erklärung zur selbständigen Anfertigung der Arbeit

Ich erkläre hiermit, dass ich die vorliegende Masterarbeit selbstständig angefertigt, sowie alle verwendeten Quellen und Hilfsmittel im Literaturverzeichnis angegeben habe. Des Weiteren versichere ich, dass ich alle wörtlichen und sinngemäßen Übernahmen aus anderen Werken als solche gekennzeichnet habe. Die Arbeit hat in gleicher oder ähnlicher Form noch keiner anderen Prüfungsbehörde vorgelegen.

Bayreuth, 28.02.2017

_____

Laura Ehrnsperger

Abstract

Forests are one of the dominant vegetation types on Earth and an important sink for carbon on our planet. Forests are moreover special ecosystems due to their great canopy height und complex architecture consisting of a subcanopy and a canopy layer, which changes the mechanisms of turbulent exchange within the plant canopy. To date, the sinks and sources of turbulence in forest canopies are not completely understood, especially the role of the pressure transport remains unclear. The INTRAMIX experiment was conducted in a mountainous Norway spruce (*Picea abies*) forest at the Fluxnet Waldstein site (DE-Bay) in Bavaria, Germany, for a period of ten weeks in order to experimentally evaluate the significance of the pressure transport to the turbulence kinetic energy (TKE) budget for the first time. It was expected that the pressure transport is more important in the subcanopy layer of the forest where the fluxes caused by mechanical shear and buoyancy are relatively low. The INTRAMIX data of the dense forest was compared to observations from a sparse Ponderosa pine (*Pinus ponderosa*) stand in Oregon, USA, to study the influence of forest architecture. It was hypothesized that the pressure transport is more important in dense forest canopies as the crown decouples the subcanopy from the buoyancy- and shear-driven airflow above the canopy. It was also investigated how atmospheric stability influences the TKE budget. Based upon model results from literature it was expected that the pressure transport acts as a source for TKE especially under unstable dynamic stability.

The results revealed that pressure transport was of the same magnitude in all three layers of the dense forest, but was most important in the subcanopy as expected. The pressure transport was a continuous source of TKE during the day and a slight sink at night throughout the whole Norway spruce forest. The pressure transport in the sparse Ponderosa Pine forest was in contrast to that a source term for TKE in the top of the canopy and subcanopy layer, but was a sink within the canopy. Moreover, the pressure transport was generally larger in the sparse forest compared to the dense Norway spruce forest. Nonetheless, the pressure transport was less important in the sparse forest canopy due to the high magnitude of the remaining TKE budget terms. These distinct differences between

the forests show that forest architecture significantly influences the TKE budget. Dynamic stability had also a great impact on the TKE budget and especially on the pressure transport term. Pressure transport was largest under unstable atmospheric conditions being a source for TKE at all layers of the dense forest, while under near-neutral or stable conditions the pressure transport term was slightly positive or negative, respectively. Under weak-wind conditions the pressure transport increased with canopy height, while under the strong-wind regime pressure transport showed a minimum in the canopy layer. The pattern of the pressure transport under the strong wind regime was remarkably similar to vertical profile of the Ponderosa pine forest indicating that the differences of the pressure transport term were mainly caused by the influence of the respective forest architecture on wind speeds in the canopy.

Zusammenfassung

Wälder gehören zu den wichtigsten Vegetationstypen der Erde und sind eine wichtige Senke für Kohlenstoff auf unserem Planeten. Wälder sind zudem wegen ihrer großen Bestandeshöhe und komplexen Architektur, die aus einer unteren Schicht mit Unterwuchsvegetation und einer Kronenschicht besteht, spezielle Ökosysteme. Dieser besondere Aufbau verändert die Mechanismen des turbulenten Austausches von Energie und Materie im Wald. Bis heute sind die Quellen und Senken für Turbulenzen in Wäldern nicht vollständig verstanden, besonders der Einfluss des Drucktransports ist unklar. Das INTRAMIX-Experiment wurde in einem subalpinen Fichtenbestand (*Picea abies*) an dem Fluxnet-Standort Waldstein (DE-Bay) in Bayern, Deutschland, für die Dauer von zehn Wochen durchgeführt. Ziel war es die Bedeutung des Drucktransportterms für das Turbulente Kinetische Energie (TKE)-Budget das erste Mal experimentell zu untersuchen. Die INTRAMIX-Daten des dichten Bestandes wurden außerdem mit den Messungen in einem lichten Gelb-Kiefer-Wald (*Pinus ponderosa*) in Oregon, USA, verglichen, um den Einfluss der Waldarchitektur auf das TKE-Budget zu untersuchen. Es wurde angenommen, dass der Drucktransport in dichten Wäldern wichtiger ist, da die Baumkrone den Unterbestand von den durch Auftrieb und Scherung getriebenen Flüssen über der Krone entkoppeln. Es wurde außerdem untersucht, welchen Einfluss atmosphärische Stabilität auf das TKE-Budget hat. Basierend auf Ergebnissen aus Modellen, wurde erwartet, dass der Drucktransport besonders unter instabiler dynamischer Stabilität als Quelle für TKE fungiert.

Die Ergebnisse zeigten, dass der Drucktransport in allen drei Schichten des dichten Waldes in derselben Größenordnung lag, jedoch im Unterwuchs am bedeutendsten war. Der Drucktransport war eine kontinuierliche Quelle für TKE während des Tages und eine leichte Senke während der Nacht im gesamten Fichtenwald. Dagegen war der Drucktransport im lichten Gelb-Kiefer-Wald eine Quelle für TKE in der oberen Baumkrone und im Unterwuchs, während er eine Senke innerhalb der Krone war. Allerdings war der Drucktransport im lichten Wald generell größer als im dichten Fichtenwald. Nichtsdestotrotz war der Drucktransportterm im

lichten Bestand weniger bedeutend, da die Größenordnung der restlichen TKE-Terme höher war. Diese deutlichen Unterschiede zwischen den Wäldern zeigen, dass die Waldarchitektur das TKE-Budget signifikant beeinflusst. Dynamische Stabilität hat ebenfalls großen Einfluss auf das TKE-Budget und besonders auf den Drucktransportterm. Der Drucktransport war unter labiler Schichtung am größten, wobei er eine Quelle für TKE war, wohingegen der Drucktransport unter neutralen bzw. labilen Bedingungen leicht positiv bzw. negativ war. Unter Schwachwind-Bedingungen nahm der Drucktransport mit steigender Höhe im Bestand zu, während der Drucktransport unter dem Starkwind-Regime innerhalb der Baumkrone abnahm. Das vertikale Profil des Drucktransport unter den verschiedenen Windregimen war erstaunlich ähnlich zu dem Muster der zwei verschiedenen Wälder. Dies deutet darauf hin, dass die Unterschiede im Drucktransportterm hauptsächlich von den durch die Waldarchitektur veränderten Windregimen verursacht wurden.

1. Introduction

Forests are one of the dominant ecosystems covering 30% of the Earth's land surface (reference!!!), which significantly influence the global cycling of carbon and water. Measurements of turbulence in forested ecosystems are therefore needed to understand the dispersal of trace gases, smoke, pollen and pesticides within the canopy (Baldocchi and Hutchison, 1987). Therefore, it is important to understand the transport processes that control the distribution of energy and matter within plant canopies. Nevertheless, it is still difficult to determine the turbulence characteristics above and within vegetation. This is due to the fact that vegetated surfaces modify the surface boundary layer as the high surface roughness of plant canopies creates additional turbulence at the atmosphere-vegetation-interface (Dwyer et al., 1997; Leclerc et al., 1990; Raupach et al., 1986). The structure of the plant canopy thereby significantly influences the characteristics of turbulent motion by extracting momentum from the flow, converting kinetic energy of the mean flow into turbulence kinetic energy, convectively transferring sensible heat at the atmosphere-vegetation boundary and breaking down large-scale turbulent motions into smaller scales (Baldocchi and Hutchison, 1987; Wilson and Shaw, 1977). Forests are an additionally extreme case due to their large vertical extent and high surface roughness.

Forests are typically structured into an upper canopy layer extending from lower boundary of the crown to the top of the canopy and a lower subcanopy layer ranging from the surface to the upper trunk space. This extensive canopy structure creates a special microclimate due to altered temperature and wind regimes within the stand. Legg and Monteith (1975) pointed out that this causes a rapid change of flow statistics with canopy height. The temperatures are lower in the subcanopy of a forest due to the shading effect of the crown. Furthermore, the wind speed within a forest canopy does not increase logarithmically with height like it would be the case without vegetation. The higher density of the crown compared to the trunk space slows down the airflow and leads to a second wind maximum in the subcanopy (Gao et al., 1989; Meyers and Baldocchi, 1991). As the structure and

density of the crown and understory vegetation and the overall architecture of the stand influence the airflow, knowledge of the architecture of a forest is important to understand turbulent motions within this ecosystem.
Turbulence itself is essential for the transport of energy and mass in forest canopies, so it is important to examine the mechanisms that contribute to its production or consumption. The budget of turbulence kinetic energy is a method to estimate the relative importance of physical processes like shear or buoyancy on the characteristics of turbulence (Dwyer et al., 1997). To date, only three of the five terms of the TKE budget equation can be measured, the buoyancy term, the mechanical shear and the turbulent transport, while pressure transport and viscous dissipation cannot be sampled directly (Wyngaard and Coté, 1971). Mechanical shear, buoyancy and vertical turbulent transport are commonly measured in field studies (Baldocchi and Hutchison, 1987; Leclerc et al., 1990; Meyers and Baldocchi, 1991; Vickers and Thomas, 2013), wind-tunnel experiments (Brunet et al., 1994; Raupach et al., 1986) and modeled in Large Eddy Simulation (LES) studies (Dwyer et al., 1997), but only a few studies tried to experimentally evaluate the pressure transport term so far to complete the TKE budget equation (Sigmon et al., 1983). A Large Eddy Simulation study of Dwyer et al. (1997) found that pressure transport in the model was of opposite sign to the turbulent transport in the upper canopy, but smaller in magnitude. Both vertical turbulent and pressure transport have been found to be responsible for half of the TKE dissipation in the upper canopy layer and were the dominant source for TKE in the lower two-thirds of the canopy in this LES (Dwyer et al., 1997). So far, the TKE budget is unbalanced, indicating that pressure transport might be a major sink near the surface.
In order to balance to the TKE budget, four of the five terms on the right hand side of the TKE budget equation (mechanical shear generation, buoyancy production, turbulent and pressure flux divergence) will be calculated for this master thesis and the viscous dissipation term will be approximated as the remaining residual. The pressure transport term will be quantified here for the first time concerning its magnitude in two forest canopies and its significance to the TKE budget in comparison to the other terms of the TKE budget equation. Besides the sole quantity also the direction of pressure transport within a forest canopy is of importance as it determines whether the pressure flux divergence is a sink or source term for turbulence kinetic energy in a forest.
High foliage density in the crown layer inhibits the airflow through mechanical shear and wake production. This leads to lower wind speeds in the subcanopy

space, where mechanical shear plays only a minor role due to the weak-wind conditions. Besides slowing down the wind speed, the shading effect of the crown layer also causes less radiative forcing in the subcanopy. This reduces the buoyancy flux beyond the canopy layer of the forest. So in the subcanopy space, where shear generation and buoyancy production play only minor roles, pressure transport is probably more important. Mcbean and Elliott (1975) supposed that pressure transport has to be of opposite sign to the flux divergence of turbulent transport. As vertical turbulent transport is a major source in the subcanopy, pressure transport therefore has to be a major sink near the ground. This leads to the first hypothesis that the pressure transport term is more important in the subcanopy than in the upper canopy and acts as a major sink of TKE near the surface that compensates for buoyancy and mechanical shear as it exports TKE from the subcanopy.

Not only the layers within one forest probably show a different pattern of TKE distribution but also contrasting forests show differences in the dominating transport processes. Meyers and Baldocchi (1991) found in a LES study that the forest architecture significantly influences the distribution patterns of TKE. TKE is often produced in the upper canopy layer and additionally of greater magnitude than in the subcanopy. In the upper canopy, mechanical shear is a major source, while dissipation is the dominant sink due to the large foliage density (Dwyer et al., 1997). The foliage density and the distances between the trees significantly influence the turbulent flow. Depending on these characteristics the forest canopy may act as a source or sink for heat caused by temperature differences between the layers and the surrounding air above the canopy (Dwyer et al., 1997). It was expected that there would be significant differences in the buoyancy term of the TKE budget equation across the different forest architectures, particularly in the subcanopy space. Although LES studies cannot replace accurate field measurements of pressure fluctuations, they are useful to estimate the role of pressure transport in the dynamics of the airflow within a forest canopy (Dwyer et al., 1997). Dwyer et al. (1997) conducted a LES for a sparse forest with a Leaf Area Index (LAI) of only 2 and a forest with a dense crown and a LAI of 5 and a canopy height of 20m for both cases. These LAI values are very close to the leaf area indices of the two different forest investigated here (see Chapter 2 for details). A dense crown probably creates a greater pressure flux divergence between the canopy layers and thereby transports a pressure pulse from above the canopy more effectively than a sparse canopy. This leads to the second hypothesis that the denser the forest, the more efficiently is TKE transported through pressure flux divergence between

the canopy layers.
Furthermore, the meteorological parameters like atmospheric stability influence the turbulence characteristics. Lesnik (1974) proofed that shear production was the major source at the canopy top in a 20-year old pine forest under different stability conditions. The effects of atmospheric thermal stratification in a deciduous forest on the TKE budget were investigated by Leclerc et al. (1990). They showed that normalized shear production and a residual, which was assumed to be the viscous dissipation, increased with decreasing level of convective instability and even further increased with the onset of stable conditions. A LES study by Dwyer et al. (1997) investigated the TKE budgets across near-neutral to strongly unstable conditions. The magnitude of pressure transport was larger, the more unstable the atmospheric conditions were. Pressure transport seems to be especially important under convective and unstable conditions, where it acts as a source of TKE (Wyngaard and Coté, 1971) (Figure 1.0.1). Now that the pressure transport was actually measured, the influence of atmospheric stability on the pressure flux divergence and the TKE budget can finally be examined regarding three different stability regimes. Based on former simulation studies it is hypothesized that pressure transport is a source of TKE under unstable atmospheric conditions, as it redistributes TKE in the opposite direction as the turbulent flux divergence (Figure 1.0.1), and increases with increasing dynamic stability.

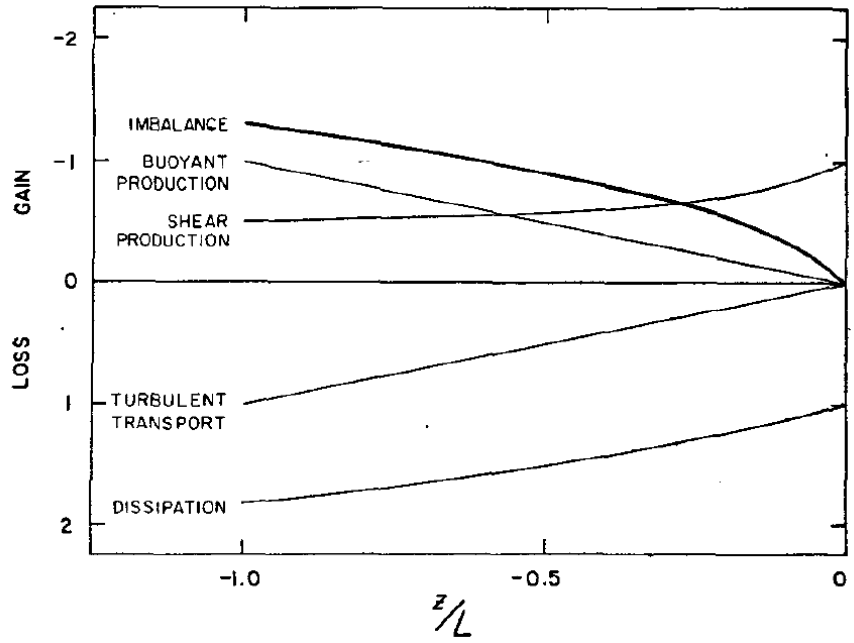

FIGURE 1.0.1: Dimensionless turbulent energy budget under unstable conditions. The pressure transport term is identical with the imbalance here. Positive values indicate a source of TKE, while negative values are sink terms. The TKE terms are plotted against z/L, which is the dimensionless stability parameter ζ (for further details see Chapter 3) (source: Wyngaard and Coté (1971)).

2. Material and Methods

2.1 Theoretical framework

2.1.1 Calculation of Turbulence Kinetic Energy

Turbulence is an omnipresent process occurring across all scales at every soil-vegetation-atmosphere-interface, but it is still difficult to determine its characteristics. Turbulence kinetic energy is used as a measure of intensity of turbulence per unit mass and is calculated from the mean of the perturbations of the horizontal along-wind component u', the horizontal across-wind component v' and the vertical wind component w' following Equation 2.1 (Stull and Ahrens, 2000).

$$\overline{e} = \frac{1}{2} \cdot (\overline{u'u'} + \overline{v'v'} + \overline{w'w'}) \tag{2.1}$$

2.1.2 TKE Budget Equation

To examine which atmospheric processes contribute to the production or consumption of turbulence kinetic energy, the TKE budget equation is commonly used. Assuming horizontal homogeneity and steady-state conditions, this equation defines the tendency of TKE (right-hand side of the equation) as the sum of buoyancy production (first left-hand side term), mechanical shear generation (second left-hand side term), turbulent transport (third left-hand side term), pressure transport (fourth left-hand side term) and viscous dissipation (fith left-hande side

term) (see Equation 2.2) (Vickers and Thomas, 2013).

$$\frac{\delta \overline{e}}{\delta t} = \frac{g}{\theta_v} \cdot \overline{w'\theta'_v} - \overline{w'u'} \cdot \frac{\delta \overline{u}}{\delta z} - \frac{\delta \overline{w'\overline{e}}}{\delta z} - \frac{1}{\rho} \cdot \frac{\delta \overline{w'p'}}{\delta z} - \epsilon \tag{2.2}$$

where g is gravity acceleration, θ_v is the virtual potential temperature, $\overline{w'\theta'_v}$ is the buoyancy flux, $\overline{w'u'}$ is the momentum flux, $\frac{\delta \overline{u}}{\delta z}$ is the spatial gradient of the mean horizontal along-wind, $\frac{\delta \overline{w'\overline{e}}}{\delta z}$ is the flux divergence of turbulent vertical mixing of TKE, $\frac{1}{\rho}$ is the ratio of mass density of dry air, $\frac{\delta \overline{w'p'}}{\delta z}$ is the flux divergence of pressure transport and ϵ is the viscous dissipation, which converts TKE into internal energy. A positive sign stands for a source or production term of TKE, whereas negative terms indicate consumption of turbulence kinetic energy and thereby a sink. The turbulent and the pressure transport terms are flux divergence terms that cannot create or consume, but only redistribute TKE. Still they can be sources or sinks of TKE by transferring turbulent energy to other regions of the canopy. Turbulence in the boundary layer (BL) is mainly produced mechanically by wind shear and the buoyant movement of air due to thermal gradients (Stull and Ahrens, 2000). The sinks that compensate for buoyant and mechanical sources of turbulence kinetic energy are turbulent transport and dissipation. Several studies (Leclerc et al., 1990; Raupach et al., 1996; Vickers and Thomas, 2013; Wyngaard and Coté, 1971) have already focused on the determination of the buoyancy term, turbulent transport and shear production, as these terms can be measured with means of the eddy covariance method (EC) at multiple heights, while pressure transport and viscous dissipation cannot be sampled directly so far. Near the surface in the surface roughness sublayer, the production of turbulence kinetic energy is mostly dominated by shear that occurs above the tree canopy (Vickers and Thomas, 2013). Mechanical shear is especially important when the wind speed is high or the wind direction is frequently changing. In forest canopies, the shear term is a dominant source for TKE in the upper crown and above the canopy, while it is only of minor importance in the subcanopy layer Vickers and Thomas (2013).

While mechanical shear is usually a production term, buoyancy can either be a source or sink in forest canopies. Buoyancy comes especially into play during weak-wind conditions and high positive heat flux, being a main source of TKE in the upper canopy and above the crown where the income of solar radiation is highest. This is mostly the case under unstable regimes. In the subcanopy, where wind speeds are low anyway, buoyancy also acts as a production term often exceeding mechanical shear.

The vertical turbulent transport term redistributes TKE in the forest canopy. This vertical redistribution of turbulence kinetic energy is more distinct in periods with strong vertical mixing like under unstable stratifications. Vertical turbulent transport is often directed from the upper layer of the canopy into the subcanopy space. This coupling of the above and below canopy layer under unstable conditions is a major source of TKE in the subcanopy (Vickers and Thomas, 2013).

High shear generation does not only lead to a high production of TKE, but also increases dissipation near the surface. Viscous dissipation is the transformation of turbulence kinetic energy into heat and is the ultimate sink term in lower layers of the atmosphere. As viscous dissipation cannot be measured directly, it is commonly quantified as a residual, which includes possible measurement errors from other processes. As the heat production due to viscous dissipation is too low to account for the observed loss of TKE, other processes have to be responsible for this discrepancy. One of the possibly responsible sinks is the pressure transport term that is usually summed up in the dissipation term together with measurement errors of other terms. While the mechanical shear, buoyancy and turbulent transport term have been studied a lot, the pressure transport was often neglected in studies, due to difficulties in measuring barometric pressure at high frequencies (Vickers and Thomas, 2013; Wyngaard and Coté, 1971).

2.2 Site description of the Waldstein-Weidenbrunnen

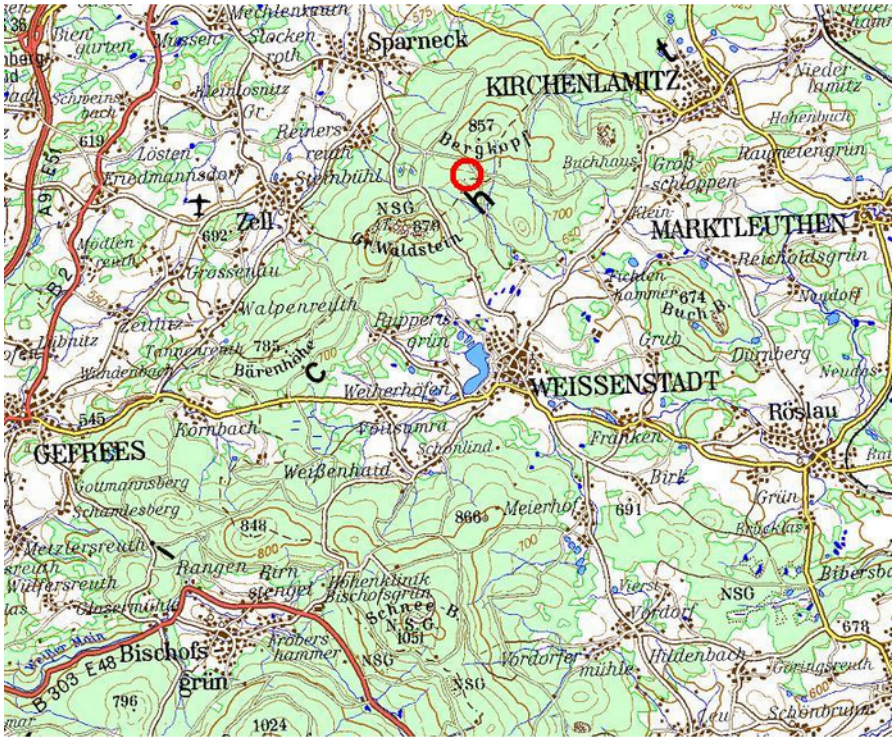

FIGURE 2.2.1: Map of the Fichtelgebirge region in northern Bavaria, Germany. The location of the Waldstein experimental site of the University of Bayreuth is indicated by a red circle (source: Bundesamt für Kartographie und Geodäsie (2005) ATKIS® DTK200-V, © Bundesamt für Kartographie und Geodäsie 2005).

To determine the contribution of the different terms to the budget of turbulence kinetic energy, an experimental set-up was established within a dense mountainous Norway spruce forest. The measurements took place at the Waldstein-Weidenbrunnen site in the Fichtelgebirge mountains 40 km northeast of Bayreuth (50° 08' 31" N, 11° 52' 01" E) (Figure 2.2.1). The experimental site was established in 1996 by the University of Bayreuth and is part of the FLUXNET (ID: DE-Bay), MODIS and TEMS networks (BayCEER, 2011). It is located at an elevation of 775 m above sea level (asl) and dominated by a moist-temperate continental climate with a mean annual temperature of 5.3 °C and a mean annual precipitation of 1162.5 mm (mean of period 1971-2000) (BayCEER, 2011; Foken and Staudt, 2007; Matzner, 2004). The dominant vegetation type is an evergreen coniferous forest consisting of 62 year old Norway spruces (*Picea abies*) with a mean canopy height of 25 m with a dense understory vegetation covering 60-80% of the ground (BayCEER, 2011; Matzner, 2004) (Figure 2.2.2). The

canopy extents from approximately 10 m to 25 m with the majority of the plant tissue concentrated in this area and a mean LAI of 5.2 (Figure 2.2.3). The stand is relatively dense with 1007 trees/ha. The mean wind direction at the site is west to southwest with a mean wind speed of 3 m/s. Atmospheric measurements are conducted at the site using a 32 m walk-up eddy covariance tower for profile measurements and a 36 m slim triangle tower for flux measurements. The slim turbulence tower that was involved in this experiment is usually equipped with two eddy covariance complexes consisting of one ultrasonic anemometer and one infra-red gas analyzer (IRGA), respectively.

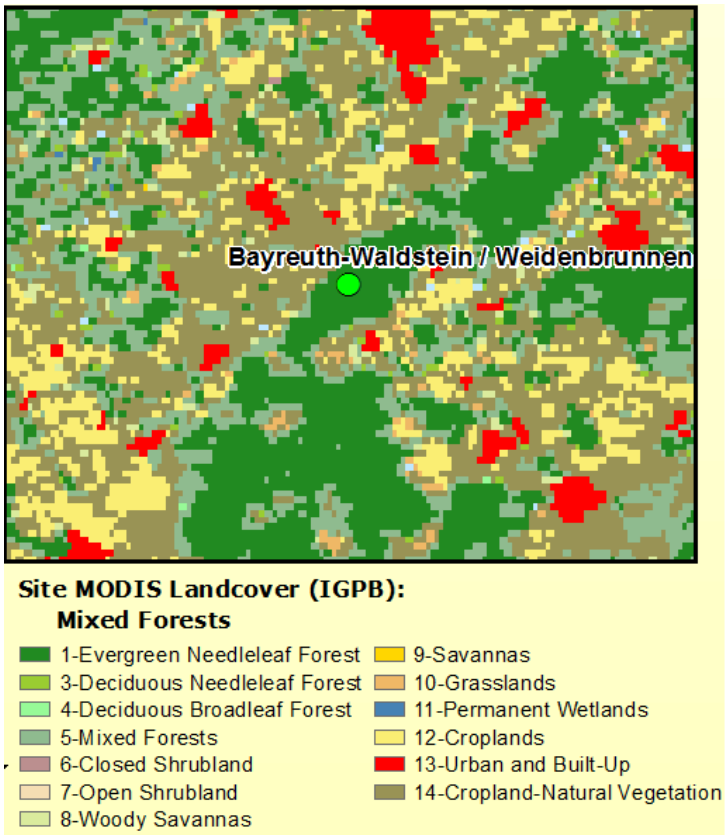

FIGURE 2.2.2: Map of land cover in the Fichtelgebirge region surrounding the Waldstein experimental site (source: http://fluxnet.ornl.gov/sites/ default/files/mapbook/405.png (Date: 10/25/2015)).

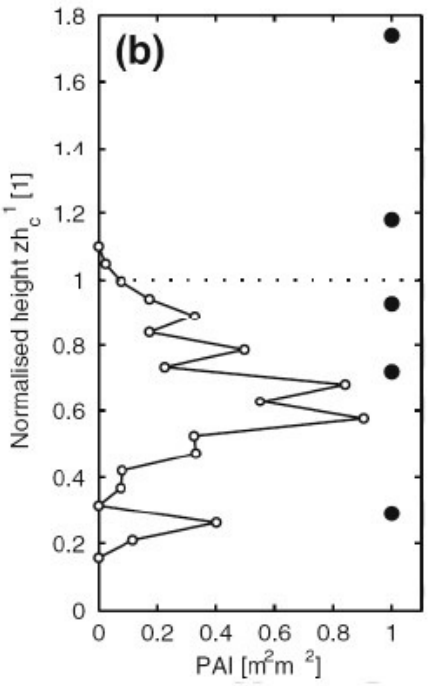

FIGURE 2.2.3: Distribution of Plant Area Index (PAI) [m^2/m^2] with normalized canopy height z/h at the Waldstein-Weidenbrunnen site (open circles with solid line). Filled circles indicate measurement heights of Foken and Staudt (2007). Dashed line is top of canopy (source: Foken and Staudt (2007)).

2.3 Experimental set-up of INTRAMIX

Measurements have been conducted for a period of ten weeks at the Waldstein site from May 2016 to July 2016. The experiment was named INvestigation of TRAnsport and MIXing within a forest (INTRAMIX) and undertaken together with Tobias Wunder, another master student at the micrometeorology group of the University of Bayreuth, who focuses on coherent structures at within the forest. The instrumentation consisted of six three-dimensional (3-D) ultrasonic anemometers (four CSAT3s, Campbell Scientific, Shepshed, UK; two USA-1 Meteks, VSHT, Elmshorn, Germany) to measure wind speed, wind direction and temperature, two infra-red gas analyzers (Li-7500, LI-COR Environmental) for CO_2 and H_2O concentrations and four fast-response pressure transducers for high resolution measurements of static atmospheric pressure (216B, Paroscientific, Redmond, USA) (Figure 2.3.2, Figure 2.3.3). One sonic anemometer was installed at 36 m above ground level (agl) on top of the turbulence tower (S1 above the crown, Figure 2.3.3a), one at 18 m agl where the PAI of the forest is at maximum (S2, Figure 2.2.3, Figure 2.3.2c) and at 4 m agl above the inflection point of the wind profile to measure counter gradient fluxes (S3, Figure 2.3.2d) (Figure 2.3.1). The

sonic anemometer S4 has been established within a distance of 6 m to the main tower directly above the ground. To study the influence of the canopy structure on the TKE budget, three vertical layers were defined. The top of the canopy layer was located between 36.20 m and 18.56 m agl with a vertical extend of 17.64 m, the canopy layer was situated between 18.56 m and 4.32 m agl with an extend of 14.24 m and the subcanopy layer laid between 4.32 m and 0.16 m agl with an extend of 4.16 m. The booms of all sonic anemometers were oriented to the respective dominant wind direction to minimize transducers shadowing errors (Baldocchi and Hutchison, 1987). One IRGA has been installed at the top of the main tower at 36 m (I1, Figure 2.3.3a), while the second one (I2) measured the flux of CO_2 and water vapor near the ground above the soil pressure sensor (Figure 2.3.3b). Besides the main tower (Figure 2.3.2a) with the vertical profile measurements, two satellite stations with 6 m triangle towers (Figure 2.3.2b, Figure 6.0.1) have been established each in a distance of 36 m to the main tower. One of the satellite stations was established at a spot with a dense high understory vegetation (station a)), Figure 2.3.1) consisting of young Norway spruces (*Picea abies*) with heights ranging from 2-4 m, mosses and dwarf shrubs, mainly blueberry (*Vaccinium myrtillus*), while the second tower was only surrounded by dwarf shrubs (*Vaccinium myrtillus*) and mosses (station b)), Figure 2.3.1). The two satellite stations had one sonic anemometer installed at 4 m height (S5, S6), respectively, to measure submeso-scale motions. Horizontal coherent structures in the subcanopy will not be subject to this thesis, but are the main aspect of Tobias Wunder's master thesis. The pressure transducers were, analogous to the sonic anemometers, located above, within and beneath the canopy together with one sonic anemometer, respectively. Each transducer was equipped with one pressure port consisting of four disks to align the airflow and a perforated inlet orthogonal to the flow to measure static pressure perturbations (Figure 2.3.2c). To ensure that the same portion of air was measured, the middle of the path length of the sonic anemometers and the infra-red gas analyzers were at the same height as the inlet of the pressure transducers.

The last pressure transducer was placed within the soil at the boundary between Oh- and Ah-soil horizons to determine how deep the pressure pulses in the atmosphere penetrate into the soil. To prevent the intrusion of litter and soil organisms, the soil pressure sensor is located in a box of steel mesh of approximately 20x20 cm, which assures the location of the pressure sensor at a certain depth. The perforation is necessary to allow the pressure signal to pass through the litter layer. This set-up enabled us to follow the pressure pulse from above

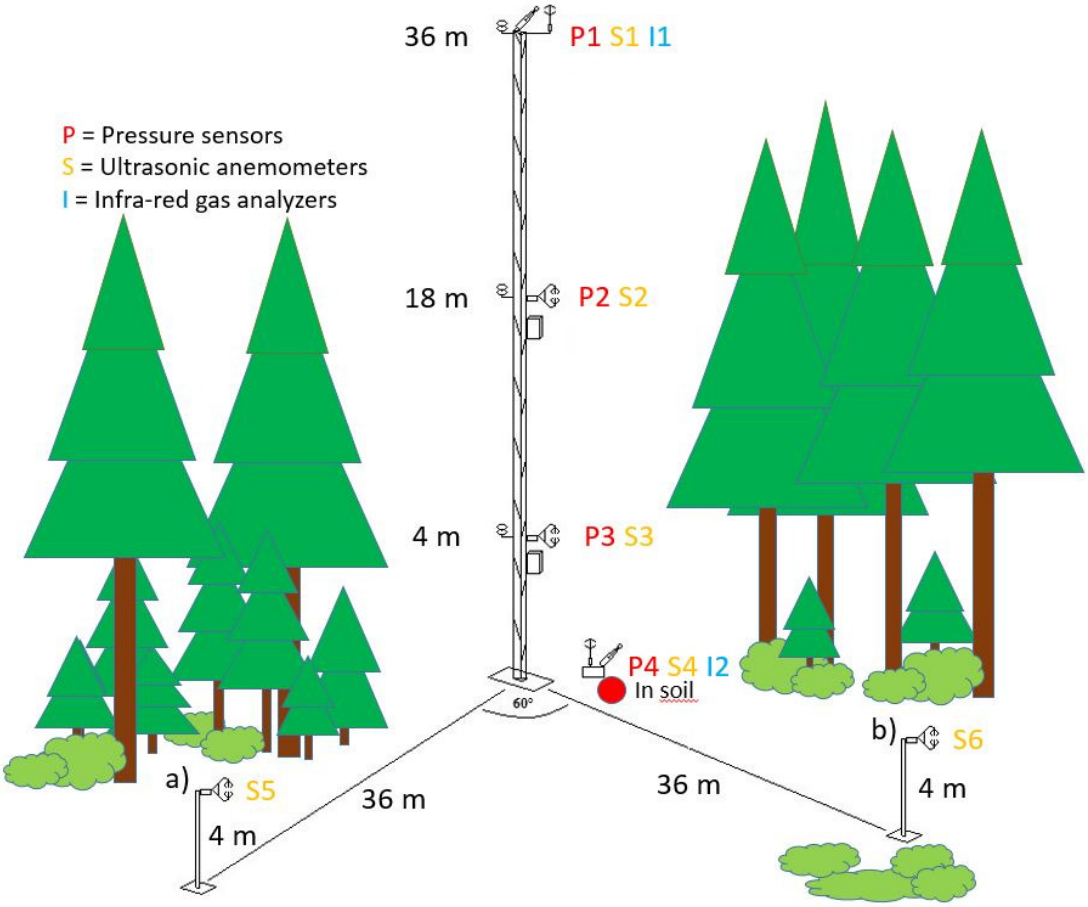

FIGURE 2.3.1: Schematic structure of the experimental set-up of INTRAMIX at the Waldstein site. The design includes the main tower for vertical flux measurements and two satellite stations (a) and b) to resolve horizontal structures. The stations form an isosceles triangle with a side length of approximately 36m.

the canopy into the ground. The measurement at multiple heights are necessary to balance over three vertical layers, the top of the canopy layer between the upper portion of the canopy and the atmosphere above the crown, a middle canopy layer between the upper trunk space the lower crown and a lower subcanopy layer extending between the trunk space and the ground. The layers were defined to average the point data at different height to mean fluxes in the respective layer. Data was collected with three CR3000 Data Logger at a frequency of 20 Hz from the sonic anemometers, IRGAs and pressure sensors. Only the P4 pressure sensor was sampled at 10 Hz as the serial connection to the logger was limited.

The four pressure sensors were all connected to one CR3000 logger, while data of three anemometers and one IRGA was transferred to one data logger, respectively. The CR3000 data logger of the pressure sensors was additionally connected to a GPS antenna. For this experiment, it was important that the signals of sonic anemometers and pressure sensors were synchronized precisely using the GPS-signal that was transmitted to all loggers to avoid a time lag between the signals of the different sensors. This was of utmost importance as the signals of pressure and wind velocity are time-dependent. Normally a lag correction is done in post-processing, but in this case, this correction may eliminate a physical lag between the pressure pulse and turbulent motions. To detect this physical lag, the time stamps of the data loggers had to be in accordance with each other. Further details on instrumentation type and connection of the complexes can be overlooked at Table 2.3.1. P1, S2, P2, S3, P3 and S6 were directed towards southwest following the main wind direction. S1 and I1 were omnidirectional (OD) as they were located above the tower top and were therefore not affected by any shading or disturbing effects of the turbulence tower. S5 was pointed to northwest towards a clearance. The different orientations of the subcanopy sonic anemometers S3, S5 and S6 should have no effect on the comparability of the data as the wind direction under the weak-wind conditions of the subcanopy is anyway changing frequently (Anfossi et al., 2005). So it is of lesser importance that the sonics point into the mean wind. S4 and I2 were orientated towards southwest, too, but for the soil measurement field primarily the vertical winds were of interest.
The CSAT3 sonic anemometers were connected to the data logger via SDM (S3, S2, S5, S6), while the two USA-1 Meteks had a serial connection via RS232 (S1, S4). The IRGA I2 at the soil measurement complex was connected through SDM. A SDM connection was also tried to be established with the infra-red gas analyzer I1, but due to a defect SDM chip the type of connection was altered to a serial one. Three of the four pressure transducers were also connected via SDM together with

(A) Main complex with three measurement heights at the turbulence tower at Waldstein-Weidenbrunnen.

(B) Satellite station a) with sonic anemometer S5 at 4m height within the high understory vegetation.

(C) Canopy measurement complex: Pressure port P2 (right) and CSAT3 S1 (left) (photo: Laura Ehrnsperger).

(D) Subcanopy measurement complex: Pressure port P3 (left) and CSAT3 (right) (photo: Laura Ehrnsperger).

FIGURE 2.3.2: Measurement towers and complexes with one CSAT3 and one pressure transducer each at the Waldstein-Weidenbrunnen site during the INTRAMIX experiment.

(A) Top of the canopy measurement complex: Pressure port P1 (left), Metek USA-1 S1 (in the back) and IRGA I1 (left) (photo: Laura Ehrnsperger).

(B) Soil measurement complex with pressure transducer P4, Metek USA-1 S4 and IRGA I2 (photo: Laura Ehrnsperger).

FIGURE 2.3.3: Measurement complexes consisting of one Metek USA-1, one pressure transducer and one Li-7500 each at the Waldstein-Weidenbrunnen site during the INTRAMIX experiment.

the GPS antenna. The last pressure sensor was connected serial as all COM ports were occupied with other sensors. This led to frequent data gaps as the sensor had to be connected via RS232 at a lower frequency of 10 Hz. But as mainly the pressure transport in the atmospheric layers within and directly above the forest were of interest, this discontinuity in the data was accepted to guarantee a reliable GPS-signal for all fast-response sensors.

2.4 Data acquisition

The data loggers were located near the ground (Logger 3) and at 18 m at the turbulence tower (Logger 1, Logger 2), respectively. The logger programs for the three CR3000 data loggers were written using the CRBasic Editor, a tool of the Loggernet software of Campbell Scientific. The names of the programs were $S1-3\_I1.CR3000$, $S4-6\_I2\_serialoutput2.CR3000$ and $P1-4.CR3000$. The data of sonic anemometers S1, S2, S3 and IRGA I1 were organized in a data table together. Furthermore, the sonics S4, S5, S6 and IRGA I2 data were written into one table, as was the data of the four pressure transducers P1, P2, P3, P4.
For recording the data, SD storage cards with a size of 2 GB or 4 GB were used. Data was harvested approximately once a week at all three loggers at the Waldstein-Weidenbrunnen site. Due to difficulties with the SDM chip, the IRGA with the serial number 0270 had to be replaced with 1632, and was finally replaced by 1270. Furthermore, the time series of S4, S5 and S6 starts only the 05/17/2016 instead of 05/12/2016, when the system was set up, as the SDM speed was too

Table 2.3.1: Description of the experimental set-up with structure of the complexes, heights and data logger connections.

Sensor ID	**Type**	**Height [m]**	**Azimuth [°]**	**Logger ID**
Main complex				
S1	USA-1	36.20	OD	Logger 1
S2	CSAT3	18.56	155	Logger 1
S3	CSAT3	04.32	130	Logger 1
I1	Li-7500	36.20	OD	Logger 1
P1	216B	36.00	155	Logger 2
P2	216B	18.60	130	Logger 2
P3	216B	04.32	130	Logger 2
Satellite stations a) and b)				
S5	CSAT3	04.30	275	Logger 3
S6	CSAT3	04.60	133	Logger 3
Soil measurement field				
S4	USA-1	0.16	31	Logger 3
I2	Li-7500	0.07	32	Logger 3
P4	216B	-0.05	Within soil	Logger 2

high for the relatively long cable length of 45 m of the satellite stations. After slowing down the SDM speed in the logger program of the satellite stations, data was collected at logger 3. All in all, data is available for a period of 62 days between 05/17/2016 and 07/19/2016.

2.5 Mature pine data set

The Norway spruce forest at the Waldstein-Weidenbrunnen site is a dense stand with small shrubs and trees building the understory vegetation. To evaluate the impact of different forest architectures on TKE it is helpful to look at other forest types. A field campaign similar to the aforementioned INTRAMIX experiment was conducted for 34 days from 06/25/2014 to 08/05/2014 in a mature Ponderosa Pine (*Pinus ponderosa*) forest in central Oregon (44° 27' 12" N, 121° 33' 42" W), USA, during the ARCFLO experiment. The climate of the Mature pine site is

TABLE 2.5.1: Site characteristics of the two examined catchments, a Norway spruce forest at Waldstein-Weidenbrunnen, BY, Germany (from Foken and Staudt (2007), and a mature pine forest, OR, USA (from Vickers and Thomas (2013).

Parameter	**Norway spruce forest**	**Ponderosa pine forest**
Location	50°08'31"N, 11°52'01"E	44°27'12"N, 121°33'42"W
Elevation	775 m	1253 m
Annual precipitation	1156.5 mm	-
Mean annual temperature	5.3 °C	-
Vegetation type	Norway spruce (*Picea abies*)	Ponderosa Pine (*Pinus ponderosa*)
Mean canopy height	25 m (2008)	16 m (2013)
Age of stand	62 years	90 years
LAI	5.2	3.3
Understory (% of area covered)	Dense understory with low canopy height (60-80%)	Sparse vegetation with low canopy height (-)

semi-arid. Analogous to the experimental setup for this master thesis, the static pressure was measured with pressure transducers (Paroscientific 216B) and wind direction and speed were sampled with 3-D-sonic anemometers (Young 81000) at four locations at 30.65 m agl, 16.75 m agl and 5.80 m agl and near the surface at 0.125 m. The mature pine forest has a less extended and sparser crown extending from 10 m to 16 m agl and a total LAI of 3.3 (Vickers and Thomas, 2013). The understory vegetation accounts for 17% of the overall LAI and consists mainly of 1 m tall shrubs (Vickers and Thomas, 2013). The 90-year old stand is generally more open than the Norway spruce forest at the Waldstein-Weidenbrunnen with only 325 trees/ha and is located on a flat saddle region at a height of 1253 m asl (Vickers and Thomas, 2013). Table 5.2.1 gives an overview of the two different forest sites. Data is continuously available for 1616 30-minute periods except for two data gaps between 07/12/2014 09:00 and 07/14/2014 10:00 and /07/14/2014 10:00 and 07/16/2014 09:30. Analogously to the INTRAMIX site, the forest canopy is divided into three layers. A top of the canopy layer between 30.65 m agl and 16.75 m agl with a vertical extend of 13.90 m, a canopy layer between 16.75 m agl and 5.80 m agl with a vertical extend of 10.95 m and a subcanopy layer between 5.80 m agl and 0.125 m agl with a vertical extend of 5.68 m.

2.6 Data processing

2.6.1 Data converting

In a first step, the raw binary data on the storage cards was converted to TOA5 format, an ASCII2 format by Campbell Scientific, using the "Card Convert" tool of Loggernet, a Campbell Scientific program associated with the CR3000 data loggers. The "stats" and "gps_stats" tables containing the 1min statistics for different parameters were converted into one file for each event of card exchange, respectively. The time series data ("ts_data") was split into tables of one hour of data each for the whole period as the time series tables would have been too big to handle otherwise. Afterwards the TOA5 files were converted into csv- or Matlab-files and finally gzipped using the BmmCamptoAsciiConverter for Windows written by Christoph Thomas.

2.6.2 Merging of data

As a next step the csv-files containing the data of the six sonic anemometers, two infra-red gas analyzers and four pressure sensors were merged into one data table using the time stamp of the data as a reference value. Besides the time stamp, the frequency at which the data was recorded had to be inserted to properly merge the different data tables. In this case the measurement frequency was 20Hz, as mentioned before. The merging into one data table enables one to calculate the fluxes of energy and matter and to directly relate the transport processes with the pressure fluctuations that occurred at that time. The merging was done using the "terra_merge" tool in Matlab, a script written by Christoph Thomas. The data of the mature pine site were already merged and available from the micrometeorology archive server.

2.6.3 Flux calculation with Bmmflux

Before the analysis with Bmmflux could start, a configuration file that is adjusted to the specific characteristics of the site and to each specific sensor had to be prepared. In the configuration files information concerning the position of the pressure transducer, the sonic anemometer and the IRGA was provided, together with details about the investigated system like canopy height, roughness length and displacement height. After merging the data of barometric pressure, wind

speed and wind direction, the covariances, means and standard deviations of the scalars, the stability parameter ζ and the mean TKE were computed together with various other quantities using the Bmmflux software, an Matlab analysis tool for flux data written by Christoph Thomas. During the computation process a number of corrections were applied to the raw data. The first correction is the coordinate or tilt rotation following Wilczak et al. (2001). For the 30-minute intervals a 3-D-rotation was applied using the given orientation of the respective sensor head to north. By rotating the anemometer coordinate system into the mean wind, the correction assures that the mean vertical wind is zero for each 30 minute interval. Thus the 3-D rotation corrects for sensor tilt and inherent flow distortion. Additionally, the time series data was despiked using the algorithm of Vickers and Mahrt (1997). Furthermore, the Moore correction was applied to the time series. The Moore correction is a frequency response correction in the high and low frequency range for EC systems (Moore, 1986). The Moore correction improves the spectral representation of perturbations and compensates for path-length averaging, the separation distance between sensors, attenuation in sampling tubes and for dynamic electronic filtering in sensors and data acquisition system. The WPL (also known as Webb) correction for open-path instruments was performed to correct for observed density perturbations in measured scalars, which are caused by air density fluctuations (Burba et al., 2008). Bmmflux also includes the Schotanus correction, which converts the buoyancy flux into the sensible heat flux (Liu et al., 2001). Additionally, Quality Assessment Quality Control (QAQC) flags were calculated according to Lee et al. (2005). Fast-Fourier transform (FFT) power spectra and cospectra were also calculated by the Bmmflux software (see Chapter 6).

2.6.4 Quality Assessment and Quality Control

Before the calculations of the TKE terms were done, the data had to be controlled and checked for outliers and reasonability. The time series data of the four measurement heights (At soil, 4 m, 18 m, 36 m) had to be aligned to the same length, as the data was not covering exactly the same time period due to later installing of one site. The data was intersecting for 2972 30-minute averaging periods or 62 days, so it was assured that in that period data was available for all four heights. To check the data for their reasonability hard plausibility thresholds were applied to exclude physically not meaningful data from the analysis. These thresholds

TABLE 2.6.1: Hard thresholds of fricton velocity u*, air density ρ, sensible heat flux H, the mean horizontal wind speed $\overline{u}$, the mean TKE and the stability parameter ζ.

Parameter	**Hard threshold**
u^* $[ms^{-1}]$	0−1.5
ρ [kg m^{-3}]	1−1.2
H [W m^{-2}]	-200-800
$u_{meanrot}$ $[ms^{-1}]$	0−8
TKE $[m^2s^{-2}]$	0−7
ζ [-]	-5−5

were decided upon with respect to usual limits of the different parameters. For details concerning the thresholds of the different parameters, see Table 2.6.1. The calculated QAQC flags could not be used unfortunately as the did not remove all physically not meaningful data.

2.6.5 Statistical analysis with R

The open source statistical software R (version 3.2.5) was used for statistical data analysis. The packages required for the computations and graphical analysis were "lubridate" and "zoo". R was used to calculate four of the five terms of the TKE budget equation. The terms of the TKE budget were determined following Vickers and Thomas (2013). The full Equation 2.2 can be seen in Section 2.1. The left-hand side term of the TKE budget equation is the TKE tendency and as 30 minute averages were calculated, δt equals 1800 seconds.
To calculate the buoyancy term, the virtual potential temperature θ_v had to be calculated first. The virtual potential temperature is the potential temperature of dry air if it had the same density as moist air (American Meteorological Society, 2017). θ_v is used instead of the measured temperature to compare measurements made at different temperatures and densities of air. It was assumed that the differences between sonic temperature and virtual temperature were negligible, so it could be assumed that $T_s = T_v$ and the equation 2.3 could be used for calculation of the virtual potential temperature.

$$\theta_v = T_s \cdot (\frac{p_0}{p})^{\kappa_L} \tag{2.3}$$

After this initial calculation the buoyancy term could be calculated for the three forest layers together with the mechanical shear, turbulent transport and pressure transport term and the TKE tendency. If the Turbulence Kinetic Energy budget would be balanced, the TKE tendency term would be zero. If the sources exceed the sink terms, then the TKE tendency is positive and the other way round. Finally, equation 2.2 was resolved to estimate the viscous dissipation term. As this term is not measured and various factors like measurement errors contribute to it, it will be called 'residual' in the following text.
In order to see the diurnal trends of the TKE terms, the ensemble averages of each parameter were computed. For that the mean and standard deviation of every quantity for every 30-minute interval was calculated, so all in all you get 48 30-intervals for the diel cycle, two per hour of the day.
Several conditional sampling analyses were performed to compare the data of the INTRAMIX experiment concerning differences in turbulence characteristics due to different stability regimes, differences between the subcanopy, canopy and above canopy layer, differences between an open and a dense forest and the influence of wind regimes.

3. Dynamic atmospheric stability regimes

3.1 Obukhov stability parameter

To investigate the influence of dynamic stability of the atmosphere on the terms of the TKE budget equation, three stability regimes have been established. The three regimes were classified as stable stratification, neutral stratification and unstable stratification. Dynamic atmospheric stability regimes are determined by the present wind speed and heat flux. Very low wind speeds and a negative heat flux are typical for stable stratification, which occur mostly at night, while moderate wind speeds and a positve heat flux are typically observed during the day under unstable regime (Eigenmann et al., 2009). High wind speeds and low net radiation characterize neutral conditions. A common parameter to define the dynamic stability is the dimensionless Obukhov stability parameter ζ, which can be calculated from the height above the ground z and the Monin-Obukhov length L as follows:

$$\zeta = \frac{z}{L} \tag{3.1}$$

The Obukhov length itself is derived from the following equation:

$$L = \frac{-u_*^3 \cdot T_v}{\kappa \cdot g \cdot Q_{v0}} \tag{3.2}$$

Where L is the Monin-Obukhov length, u* is the friction velocity, T_v is the virtual temperature, κ is the von Kármán constant, g is gravitational acceleration and

TABLE 3.2.1: Overview of the total number of 30-min intervals of the respective stability regime for the dense and the sparse forest.

Stability regime	**Dense forest**	**Sparse forest**
Stable	461	450
Neutral	1221	478
Unstable	926	656

Q_{v0} is a kinematic virtual temperature flux at the surface. The dimensionless stability parameter ζ is an expression of the relative roles of shear and buoyancy in the production or consumption of turbulence kinetic energy.

3.2 Classification of dynamic stability regimes

The Obukhov stability parameter is typically in the range of -5 and 5 (Foken, 2006). A negative ζ indicates thereby unstable to convective conditions depending on how negative ζ is. The more negative the Obukhov stability parameter is, the stronger is the instability of the atmosphere until free-convective conditions are reached at very negative ζ. In this study only unstable conditions were considered as free-convective conditions are usually observed at greater height z than the canopy height of a forest (Eigenmann et al., 2009). Similarly, a increasingly positive ζ indicates a more distinct stable stratification. A Obukhov stability parameter $<$ -0.0625 indicates the unstable regime. Around zero between -0.0625 and 0.125 the atmospheric stratification is assumed to be neutral. If ζ is more positive than 0.125, the stratification is stable. After applying the ζ thresholds by Foken (2006) 2608 30-minute intervals of the dense forest remained for further analysis. In the sparse forest 1584 30-minute periods were analyzed. Table 3.2.1 shows which portion of the data is classified stable, near-neutral and unstable, respectively.

Generally, the magnitude of ζ was greater in regions of the canopy, where the winds speeds were larger like at the top of the canopy and in the subcanopy (see Figure 6.0.3, Figure 6.0.4). The variabilty of zeta was also larger in the sparse pine forest compared to the dense stand.

4. Weak- and strong-wind regimes

4.1 Classification of wind regimes

The influence of the dynamic stability regimes was additionally compared to the impact of wind speed on the TKE budget terms. The wind speed at the top of the canopy and in the subcanopy show very large differences as the airflow is attenuated due to the tree crown. Therefore, two wind regimes were defined, a weak-wind and a strong-wind regime. The threshold for the weak-wind regime was based on the findings of Tobias Wunder who identified $< 0.6\ m\ s^{-1}$ as a critical threshold in the subcanopy space. All mean horizontal wind speed exceeding $0.6\ m\ s^{-1}$ were classified as strong-wind. This was threshold was applied to the mean horizontal wind speed $\overline{u}$ of upper boundary of the subcanopy layer. So the weak-wind conditions are only definitely present in the subcanopy, but the same amount of data is sampled for all layers.

The total number of 30-minute intervals that were classified weak- or strong-wind, respectively, and the relative percentage based on the absolute number of 2608 valid 30-minute intervals can be seen in Table 4.1.1 below. As the threshold of the subcanopy wind speed was taken for classification, it is not guaranteed that the wind regime found in the subcanopy at a certain time was also apparent in the canopy and top of the canopy layer. Moreover the number of 30-minute intervals that are sampled differ for each layer. Nevertheless, the vertical profile for this

Table 4.1.1: Overview of the total number of 30-min intervals and percentage of the respective wind regime in the subcanopy layer.

Wind regime	**Number of 30-min intervals**	**Relative percentage**
Subcanopy		
Weak-wind	1668	0.64
Strong-wind	941	0.36

scenario was plotted, too (see Figure 6.0.5).

5. Results and Discussion

The TKE budget equation is a measure for the intensity of turbulence and helps to evaluate which quantities contribute to the production or consumption of turbulence. Following the convention, TKE terms that are positive implicate a source of turbulence kinetic energy either through production or import of TKE, while a negative sign stands for a sink of TKE due to consumption or export of turbulence kinetic energy.

5.1 Differences between the canopy layers of a forest

It was hypothesized that the pressure transport term of the TKE budget is most important in the subcanopy, where it acts as a sink, compared to the canopy and top of canopy layer, where shear generation and buoyancy production probably dominate. This assumption is verified in this section and the overall influence of the forest architecture of the Norway spruce stand at the Waldstein site on the TKE budget was assessed by looking at the three different canopy layers: The top of the canopy layer, the canopy layer and the subcanopy layer. Table 5.1.1 shows the means over the whole measurement period for the TKE budget terms, the TKE tendency and mean turbulence kinetic energy itself and Figure 5.1.1 displays the vertical profile of the same quantities. The three data points per plot represent the layer average of each canopy layer and are located at the midpoint of the respective layer. The measurement height was normalized by the canopy height to compare data from other forests with differing canopy height and there by facilitates comparisons with results from literature. Additionally to the layer averages, also the ratio between each lower layer and the top of the canopy layer

TABLE 5.1.1: Means over the entire measurement period and the ratio (respective lower layer divided by the top of the canopy layer following Vickers and Thomas (2013)) for the TKE budget terms. Positive TKE terms contribute to a positive TKE tendency and negative values to a negative TKE tendency. Analogous to Vickers and Thomas (2013) for the TKE the direct measurements of the 36 m height (top of the canopy layer), 18 m height (canopy layer) and 4 m height (subcanopy layer) are taken, respectively.

Quantity	**Subcanopy**	**Canopy**	**Top of canopy**	**Ratio Sub-canopy**	**Ratio Canopy**
Mechanical shear $[m^2 s^{-3}]$	4.0×10^{-4}	-1.8×10^{-6}	3.3×10^{-2}	0.01	-0.00006
Buoyancy production $[m^2 s^{-3}]$	2.8×10^{-5}	5.5×10^{-4}	1.5×10^{-3}	0.02	0.36
Turbulent transport $[m^2 s^{-3}]$	2.1×10^{-4}	8.0×10^{-3}	-3.9×10^{-3}	-0.05	-2.1
Pressure transport $[m^2 s^{-3}]$	2.4×10^{-5}	1.5×10^{-5}	5.3×10^{-5}	0.44	0.28
Residual $[m^2 s^{-3}]$	-6.0×10^{-4}	-7.4×10^{-3}	-2.6×10^{-2}	0.02	0.28
TKE tendency $[m^2 s^{-3}]$	3.2×10^{-7}	1.9×10^{-7}	-7.4×10^{-7}	-0.43	-0.25
TKE $[m^2 s^{-2}]$	0.16	0.37	1.4	0.12	0.27

was calculated to compare the magnitudes of the TKE budget terms of the three different layers (Table 5.1.1).

Mechanical shear is the transfer of kinetic energy from the mean flow to the turbulent flow (Leclerc et al., 1990). The shear generation was the dominant source of turbulence kinetic energy in the top of the canopy layer and in the subcanopy layer (see Table 5.1.1, Figure 5.2.2, Figure 5.2.7). This was an expected result for the top of the canopy, but not for the subcanopy layer, where shear seemed to play only a minor role in former studies. Vickers and Thomas (2013) found that the shear generation was the smallest term of the three measured TKE budget terms in the lower layer of the canopy being less than a half of the buoyancy and turbulent transport term. This contradicting result could be due to the site characteristics with only a low understory canopy height around the main measurement tower.

So only the trunks of the trees significantly slowed down the airflow and led to the comparable high shear generation in the subcanopy. Moreover, a nearby clearing could act as an inlet for winds at the subcanopy level, which cause this maximum in the trunk space. Second wind maxima are commonly observed in forests with a low understory vegetation (Baldocchi and Hutchison, 1987).
Yet the magnitude of the mechanical shear term in the three layers differed. The mechanical shear was two orders of magnitude greater in the top of the canopy layer with a mean of 3.3x10^{-2} m^2s^{-3} compared to 4.0x10^{-4} m^2s^{-3} in the subcanopy layer and even four magnitudes greater than in the canopy layer with a mean of only -1.8x10^{-6} m^2s^{-3} (see Table 5.1.1, Figure 5.1.1). This huge differences are caused by high wind speeds at the top of the forest, while the dense crown prevents high wind velocities and also decouples the more open trunk space from the top of the canopy. Dwyer et al. (1997) and Shaw (1977) also identified shear production as the principal source for TKE in the upper canopy of their models. The magnitude of the top of the canopy mechanical shear of this experiment is in line with the results that Vickers and Thomas (2013) found for a Ponderosa pine forest. They observed that shear generation was the most important term in the upper part of the canopy with a mean value of 2.1x10^{-2} m^2s^{-3}, while in the lower layer the mechanical shear term was also two orders of magnitude smaller. As the experimental study from Vickers and Thomas (2013) divided the forest canopy only into two layers instead of three like it was done here, one has to take a closer look on the distribution of the tree crown in the layer. The crown contributed to the upper layer in their study, so the mechanical shear in the upper part of the canopy of the Ponderosa pine forest may be slightly underestimated. But the foliage density was much lower than for the Waldstein site with a LAI of 3.3, so the differences between subcanopy and crown space are probably much lower anyway.

Besides the differences between the three canopy layers, there was also a diel cycle visible in the top of the canopy layer (see Figure 5.1.2, top chart). During the day, the shear generation was nearly twice as high with a maximum value of 5.2x10^{-2} m^2s^{-3} compared to the nighttime peaks of mechanical shear, which were only about 3.0x10^{-2} m^2s^{-3}. Although the magnitude of the mechanical shear term was smaller during the night, it never got negative over the course of the day like it did occasionally in the lower two layers. From 01:00 to approximately 03:00 mechanical shear decreased to the minimum value of 2.0x10^{-2} m^2s^{-3}. Afterwards the mechanical shear term increased until it finally reached its maximum around 14:00. Then the shear generation rapidly decreased until approximately 19:00 reaching the second minimum, which was also 2x10^{-2} m^2s^{-3}. From 19:00

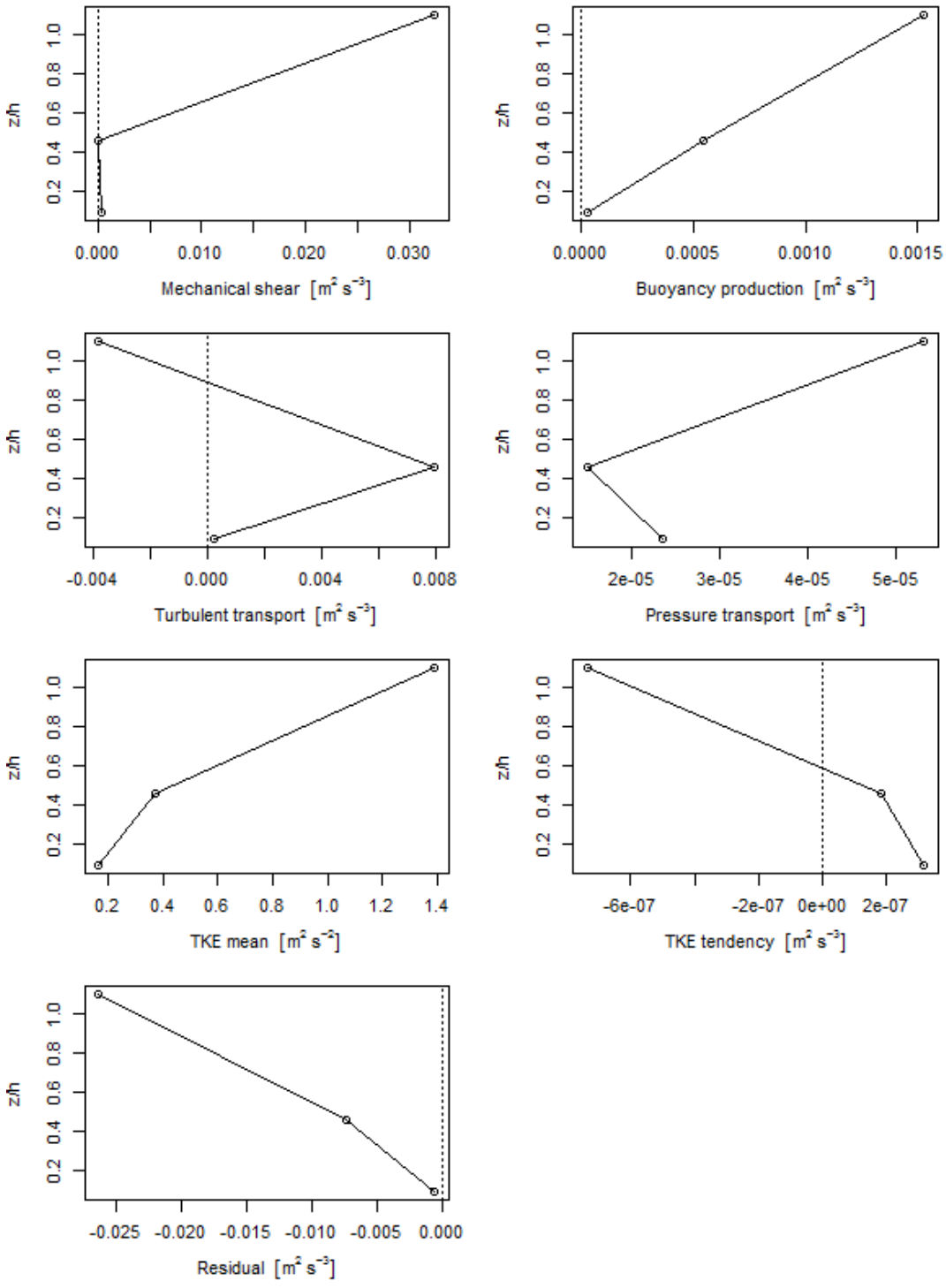

FIGURE 5.1.1: Vertical profile of the TKE terms. The open circles (○) indicate the mean of the respective layer and are located at the midpoint of each layer. Measurement height z is normalized by the canopy height h.

on the mechanical shear term in the top of the canopy increased until it reached its nocturnal maximum.

In contrast to the top of the canopy, shear played only a minor role in the canopy layer of the dense Norway spruce forest, where the mechanical shear had only 0.00006% of the shear generation above the crown (see Table5.1.1). There was also no diurnal cycle apparent in crown space, but the mechanical shear term in the canopy was the only one to become negative and showed narrow peaks of both signs, which occurred intermittently (see Figure 5.1.2, mid chart). The variations were in the range of $\pm 1\text{x}10^{-3}\ m^2 s^{-3}$ and occurred mainly between 04:00 and 08:00. It is not clear why these perturbations occurred just at during this period, perhaps the sunrise led to fast changing wind speeds or they were just measurement artefacts. Except for this period, the mechanical shear term in the canopy layer leveled around zero being slightly negative in the morning and slightly positive in the afternoon and evening hours. The very small magnitude of the shear generation in the canopy layer is probably caused by the high density of the foliage in this layer. The leaves slow down the airflow and therefore lead to very low wind speeds and low mechanical shear generation. Baldocchi and Hutchison (1987) also found that the mean tangential momentum transfer $\overline{w'u'}$ decreases with depth into the canopy of a uniform almond orchard due to the absorption of momentum by canopy elements. This absorption of momentum was strongest in the upper half of the almond canopy, where about 80% of the momentum was absorbed. This corresponds well with the results of this study.

In the subcanopy the mechanical shear term was the most important source for TKE and also was higher than in the canopy layer showing a diel cycle comparable to the one in the top of the canopy layer (see Figure 5.2.7). The relatively high shear generation in the subcanopy indicates a secondary wind maximum below the crown. This phenomena was frequently observed elsewhere in plant canopies (Gao et al., 1989; Meyers and Baldocchi, 1991; Shaw, 1977; Wilson and Shaw, 1977). Nevertheless, the mechanical shear in the subcanopy layer was only 1% of the shear generation at the top of the canopy (see Table 5.1.1). The foliage in the canopy layer attenuates or deflects vertical wind gusts from the top of the canopy and thus prevents them from penetrating deep into the subcanopy (Baldocchi and Hutchison, 1987). The mechanical shear increased between 06:00 and 19:00, when the energy by solar radiation is greatest and is approximately zero during nighttime (see Figure 5.1.2). This is due to the fact that the wind speeds during the night are very low (Mahrt, 2007). Shear generation had its maximum around noon with $1.3\text{x}10^{-3}\ m^2 s^{-3}$ comparable to the top of the canopy layer, but

the increase and decrease of TKE was less steep in the subcanopy.

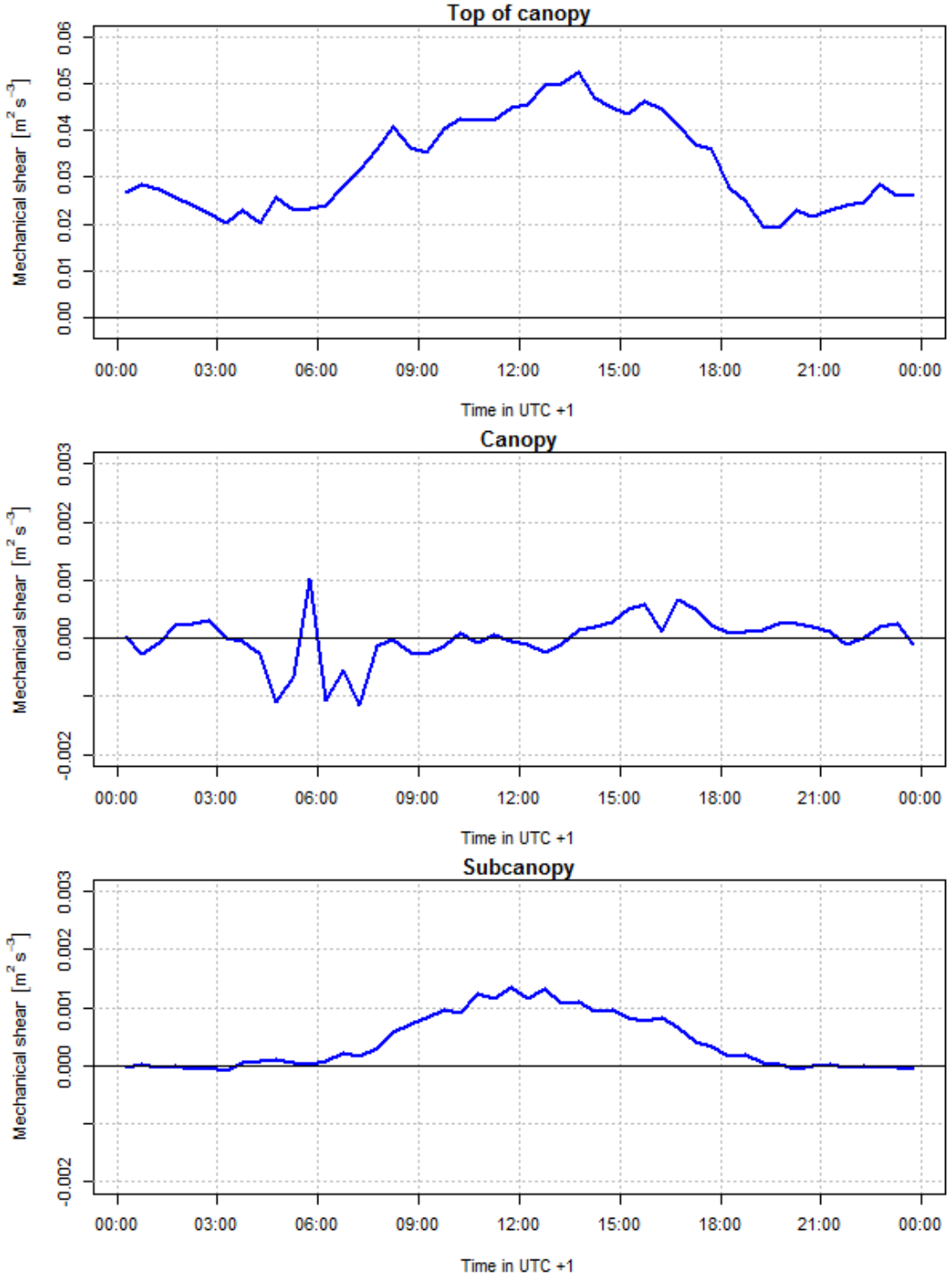

FIGURE 5.1.2: Ensemble average for mechanical shear of the TKE budget (blue line). The diel cycle of the top of the canopy (top), canopy (middle) and subcanopy (bottom) is displayed. Please note that the y-axis of the plots differ by one order of magnitude.

The buoyancy term of the TKE budget produces turbulence kinetic energy by converting potential energy (Leclerc et al., 1990). Buoyancy acted as a source for TKE in all layers of the forest during the day as the term is driven by temperature and thereby solar radiation (see Figure 5.1.3). During the night the buoyancy term was negative and therefore a sink of turbulence kinetic energy in all three layers of the canopy. This is a typical behavior of the buoyancy term that was previously seen in other studies (Vickers and Thomas, 2013). The increase of the buoyancy term occurred simultaneously in the upper two layers around 06:00 corresponding to sunrise. In the subcanopy occurred also a slight increase at that time, but the major rise did not occur before 09:00. This delay is perhaps due to the shading effect of the tree crown leading to a slower temperature rise in the subcanopy compared to the upper canopy. All in all, the shape of the buoyancy term over the course of the day was similar for all layers of the canopy.

What differed was the magnitude of buoyancy production across the layers of the forest. The buoyancy term decreased by one order of magnitude per layer (see Figure 5.1.1). At the top of the canopy, buoyancy production had a mean of 1.5x10^{-3} m^2s^{-3}, followed by an average of 5.5x10^{-4} m^2s^{-3} in the canopy layer and 2.8x10^{-5} m^2s^{-3} in the subcanopy (see Table 5.1.1).

The buoyancy production was largest at the top of the canopy as this layer is most exposed to radiative forcing. The buoyancy term in the top of the canopy layer increased between 06:00 and 11:00 reaching a plateau from 11:00 to approximately 13:30 (see Figure 5.1.3). From there on the buoyancy term in the top of the canopy steeply decreased until around 18:00, where it changed sign. After changing its sign to negative the buoyancy term decreased less steep in the evening compared to the rapid decrease during the afternoon. The same was true for the early morning hours. The nighttime minimum of -0.8x10^{-3} m^2s^{-3} was only 14% of the daytime maximum of around 5.8x10^{-3} m^2s^{-3}. In the canopy layer, the buoyancy production was less distinct being only 36% of the magnitude of the buoyancy term at the top of the canopy (see Table 5.1.1). The peak was reached around 12:00, but the increase was less steep than at the top of the canopy.

Analogously to the top of the canopy layer, the buoyancy term in the canopy layer became negative between 18:00 and 06:00, but its magnitude was with approximately -0.2x10^{-3} m^2s^{-3} four times smaller than in the top of the canopy layer (see Figure 5.1.3). The decrease was additionally more steady than in the layer above with no period of higher increase or decrease around sunrise or sunset, respectively. As shear generation played only a minor role in the canopy layer, buoyancy production gained importance. Thus, the buoyancy term was the second largest

source for TKE in the canopy layer and a slight sink for turbulence kinetic energy at night (see Figure 5.2.4).
In the subcanopy, the buoyancy production was even two orders of magnitude smaller compared to the top of the canopy layer being only 2% of the top of the canopy buoyancy with a maximum of only 2.8x10^{-4} m^2s^{-3} at 12:00 (see Table 5.1.1, Figure 5.1.3). The course of the buoyancy term showed furthermore more variations. All in all, the buoyancy term was positive during the day being a source of TKE in the subcanopy, but there was a sudden decrease between 07:30 and 08:00, where the buoyancy production equaled zero. Afterwards the buoyancy term rose again until noon, then it rapidly decreased to zero and changed sign after another small positive peak at 17:00. A reason for this variations is probably the unsteady income of net radiation. In the subcanopy, the buoyancy flux can change frequently due to shading by the crown and changing position of the sun (see Figure 6.0.2), which lead to rapid changes in buoyancy production. The buoyancy term in subcanopy layer, which was observed in this study, was one order of magnitude smaller than the buoyancy production found in the lower layer of a sparse Pine forest (Vickers and Thomas, 2013). That the buoyancy production is so small in the subcanopy could be due to the massive shading effect of the tree crown, which is greater, the denser the canopy is. During the night the buoyancy term was slightly negative, so it acted as a small sink for TKE in the subcanopy layer.

Turbulent transport is important for the redistribution of turbulence kinetic energy in the forest canopy. This redistribution of TKE could be observed for the upper two layers, which showed turbulent transport of the same magnitude, but of opposite sign (see Figure 5.1.4). This indicates that TKE was transported downwards from the top of the canopy, where it was a sink of turbulence kinetic energy, into the lower canopy layer, where turbulent transport acted as a source of TKE. A similar pattern of coupling between an upper and a lower layer was found by Vickers and Thomas (2013), Leclerc et al. (1990) and Shaw (1977). The results are also supported by one of the first evaluations of the TKE budget, where turbulent transport was also found to import TKE from upper parts of the canopy into lower canopy levels (Lesnik, 1974). Shaw (1977) estimated that the major source of TKE in the lower two-thirds of a corn canopy is caused by transport from higher levels. It was thus assumed that a high amount of the turbulence in the lower parts of the forest is not generated locally like former studies state (Finnigan, 2000; Shaw, 1977; Vickers and Thomas, 2013).

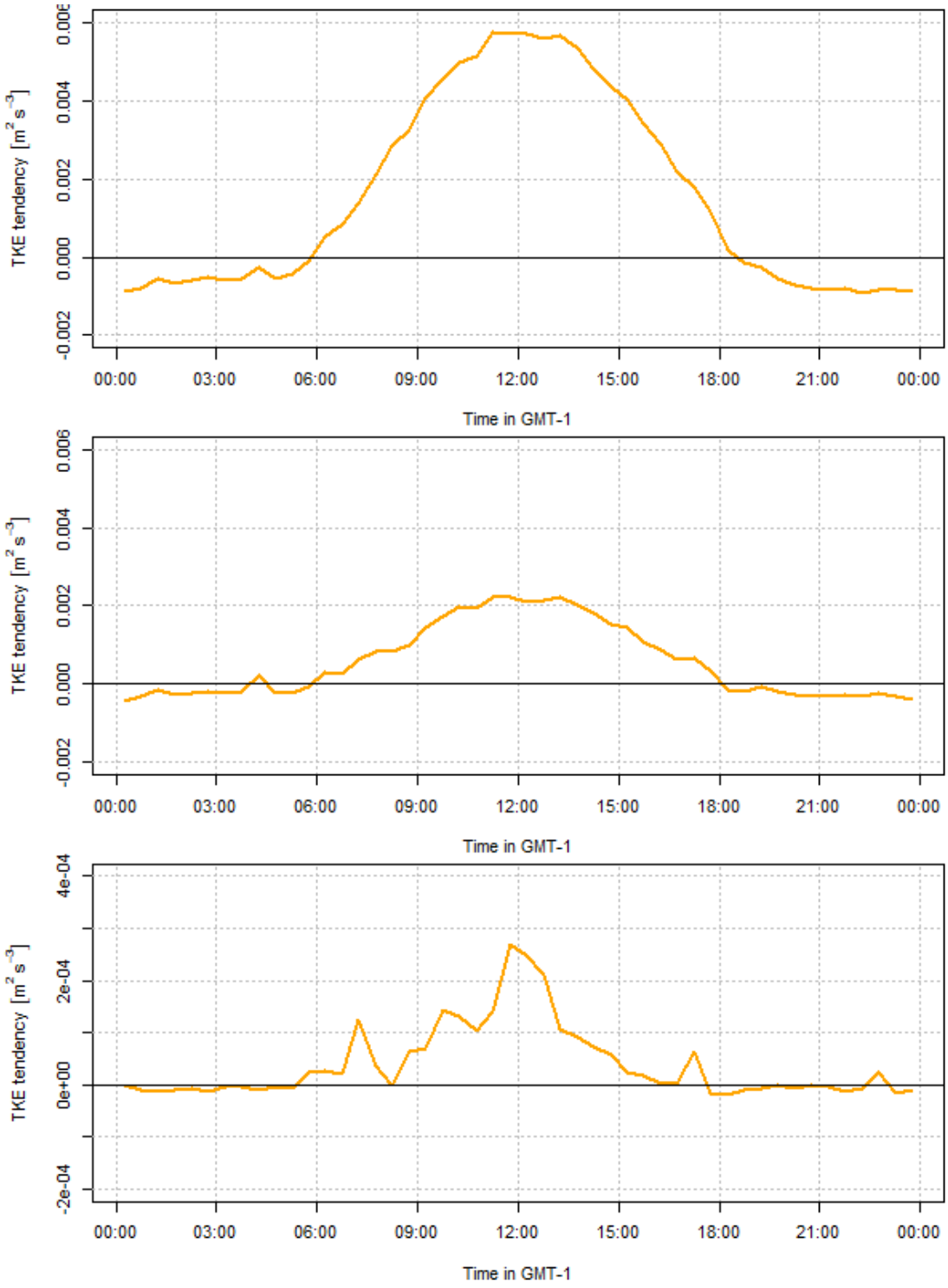

FIGURE 5.1.3: Ensemble average for buoyancy term of the TKE budget (orange line). The diel cycle of the top of the canopy (top), canopy (middle) and subcanopy (bottom) is displayed. Please note that the y-axis of the plots differ by one order of magnitude.

At the top of the canopy, the turbulent transport term was negative during the whole course of the day, but showed a slight diurnal course with a minimum of -1.0x10^{-2} m^2s^{-3} around noon (see Figure 5.1.4). Turbulent transport was the second largest sink for TKE after the residual term at the canopy top (see Figure 5.2.2). The turbulent transport term in the top of the canopy layer decreased during the day between 06:00 and 18:00. During the night the values and variations of the turbulent transport were smaller. The maximum values occurred around noon simultaneously to the negative peak in the top of the canopy layer.

In contrast to the layer above, in the canopy layer the turbulent transport term was always positive and was the largest source for TKE (see Figure 5.2.4). The turbulent transport in the canopy layer was greatest of all layers with a maximum of 1.6x10^{-2} m^2s^{-3} and was in average more than twice as high as in the top of the canopy layer with 8.0x10^{-3} m^2s^{-3} compared to -3.9x10^{-3} m^2s^{-3} in the top of the canopy layer (see Table 5.1.1). Leclerc et al. (1990) also found that within the tree crown turbulent transport is gaining importance due to canopy elements that obstruct the mean flow. This is supported by Raupach et al. (1996) who observed that turbulent transport becomes more important within the canopy and is often the largest source term for TKE. Also Meyers and Baldocchi (1991) identified the turbulent transport as the most important source for turbulence kinetic energy within the canopy between z/h = 0.6-0.9. In the sparse pine forest that Vickers and Thomas (2013) investigated turbulent transport was a large source for turbulence kinetic energy together with buoyancy. A LES study by Raupach et al. (1986) also identified turbulent transport as a source term for TKE in the canopy.

Certainly, the transfer of TKE from the top layer into the subcanopy was weaker having only 5% of the turbulent transport the top of the canopy, but still a small amount of TKE reached the subcanopy (see Table 5.1.1). The downward turbulent transport from the upper layers into the subcanopy is probably inhibited by the high density of the tree crown of the Norway spruce forest. The turbulent transport in the subcanopy layer is the second largest source for TKE besides mechanical shear, but showed no clear diurnal cycle (see Figure 5.2.7). So TKE is transported continuously downwards into the subcanopy space independent of the time of the day. Turbulent transport was a source for turbulence kinetic energy during most of the day, except for one short period between 01:00 and 03:00, where the turbulent transport term is negative (see Figure 5.1.4). Except for two narrow peaks at 09:00 and shortly before 18:00, which reached up to 6.0x10^{-4} m^2s^{-3}, the turbulent transport term is mostly below 5x10^{-4} m^2s^{-3}. All in all,

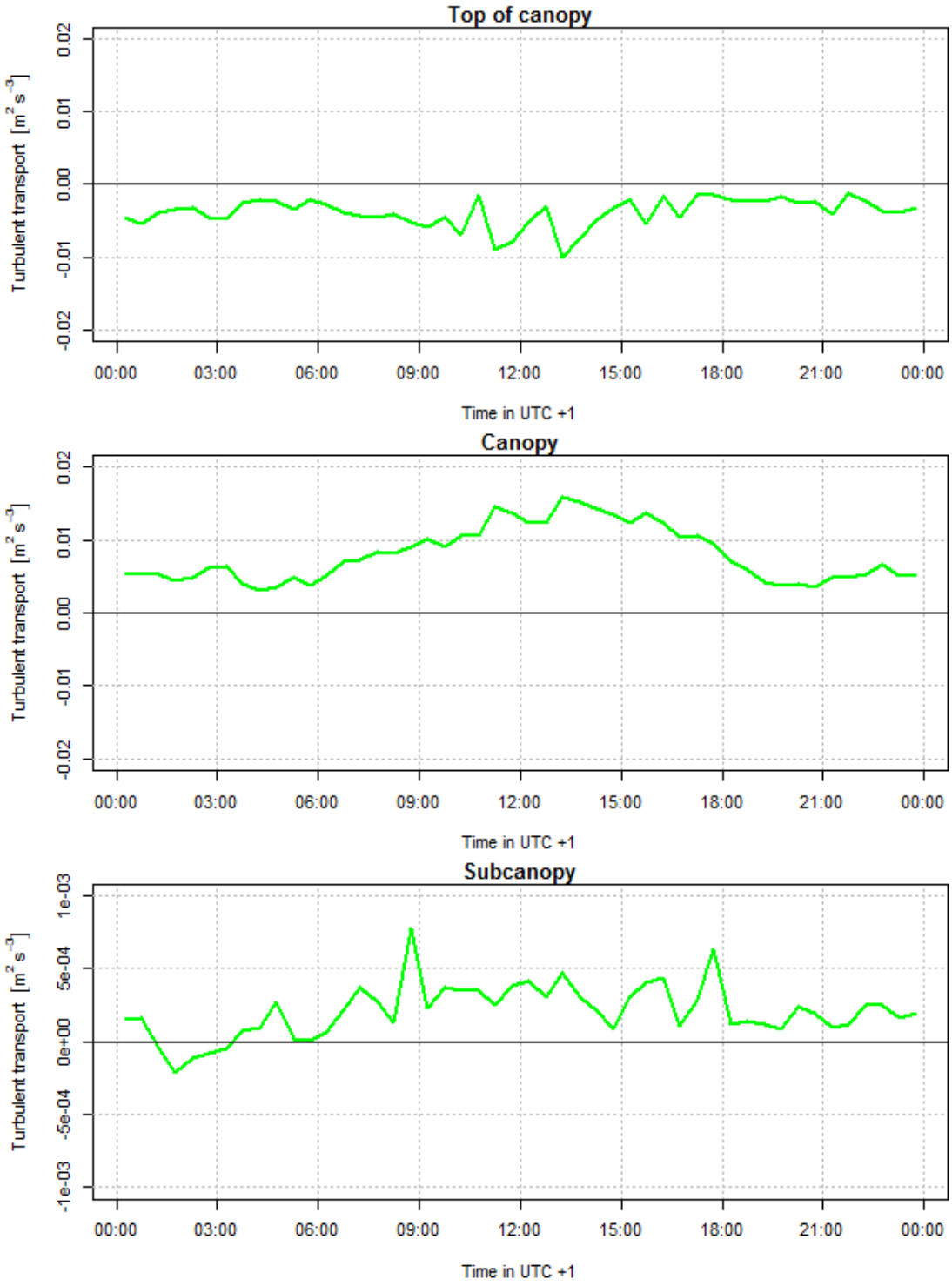

FIGURE 5.1.4: Ensemble average for turbulent transport of the TKE budget (green line). The diel cycle of the top of the canopy (top), canopy (middle) and subcanopy (bottom) is displayed. Please note that the y-axis of the plots differ by one order of magnitude.

a lot of studies support the result that turbulent transport is a major source for TKE in the canopy and subcanopy of a forest due to the import of TKE from the top of the canopy and is thus a dominant sink at the canopy top. (Brunet et al., 1994; Leclerc et al., 1990; Lesnik, 1974; Vickers and Thomas, 2013).

Pressure transport is the second flux divergence term in the TKE budget. Like turbulent transport it redistributes turbulence kinetic energy within the forest canopy. However, to date the effects of turbulent pressure fluctuations are still uncertain Vickers and Thomas (2013); Dwyer et al. (1997). The expectation on whether pressure transport is a source or sink are contradicting though (Leclerc et al., 1990; Mcbean and Elliott, 1975). It was hypothesized here that the pressure transport term is especially important in the subcanopy where it acts as a sink, as the heat production due to viscous dissipation is too low to account for the observed loss of TKE in this layer. The direct measurements of this study revealed that the pressure transport was a continuous source of TKE across the dense forest canopy (see Figure 5.1.1). The courses of the pressure transport term were less smooth for all three layers compared the other terms of the TKE budget. The results support the prediction of Leclerc et al. (1990) who found that pressure transport must have significantly contributed to the positive residual they found and therefore has to be a source for TKE within the canopy. A wind-tunnel study by Raupach et al. (1986) also found that pressure diffusion is a source above the crown and that pressure transport is also a source within the canopy together with turbulent transport. So the assumption that the pressure transport term is a sink in the subcanopy space was disproved. It was also interesting that the pressure transport was the only term which did not change its magnitude across the three layers of the forest. Pressure transport had the same magnitude for all layers with a mean of 5.3x10^{-5} m^2s^{-3} at the top of the canopy, 1.5x10^{-5} m^2s^{-3} in the canopy and 2.4x10^{-5} m^2s^{-3} in the subcanopy (see Table 5.1.1).
In the top of the canopy, the pressure transport term was greatest around noon with 1.8x10^{-4} m^2s^{-3} (see Figure 5.1.5). It showed a clear diurnal cycle with a constant rise from 06:00 until noon and a rapid decrease until 18:00. During the night and early morning between 18:00 and 06:00 the pressure transport was slightly positive or negative for most of the time ranging between -3.0x10^{-5} m^2s^{-3} and 7x10^{-5} m^2s^{-3}.

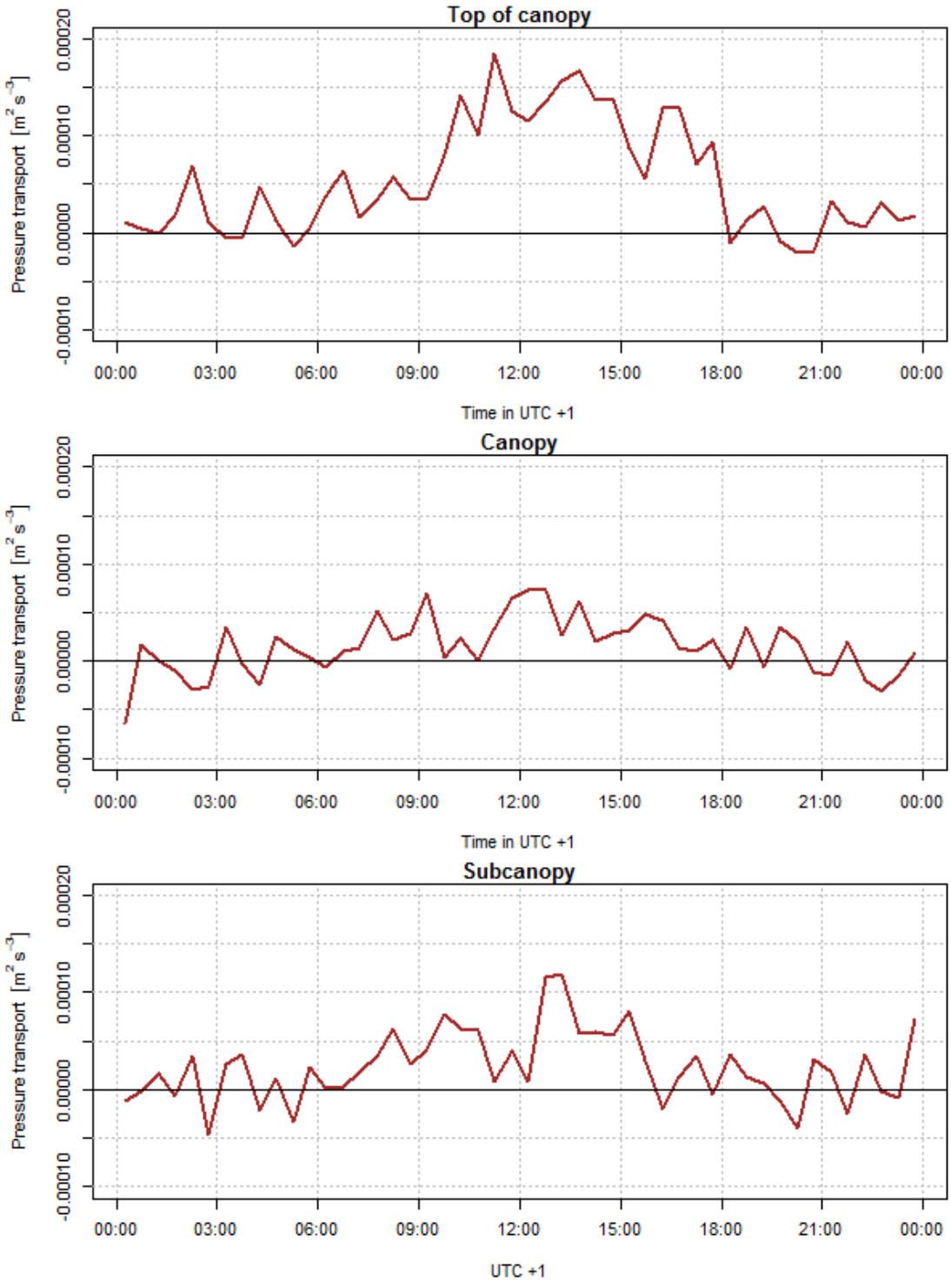

FIGURE 5.1.5: Ensemble average for the pressure transport of the TKE budget (brown line). The diel cycle of the top of the canopy (top), canopy (middle) and subcanopy (bottom) is displayed.

In the canopy layer, pressure transport was also a source for TKE, but smaller with a peak of 8.0x10-5 around 12:00 and only 28% of the value of pressure transport

above the crown (see Table 5.1.1, Figure 5.1.5). Pressure transport was positive during the day between 06:00 and 18:00 and then became slightly negative with occasional positive peaks during the night. In the top of the canopy and the canopy layer, pressure transport was only of minor importance as the terms of the TKE budget equation are by far greater. This supports the hypothesis that the pressure transport term is mainly important in the subcanopy of the forest.
In the subcanopy, pressure transport was indeed of the same magnitude like in the upper layers, but the other fluxes of turbulence kinetic energy were smaller and so the pressure transport term gained importance. This corresponds well to the prediction of Shaw and Zhang (1992) who found a strong correlation between longitudinal velocity measured in the trunk space and surface pressure. They presented this relationship as evidence that turbulence in the lower part of the forest canopy is mostly driven by pressure fluctuations. This would explain why the pressure transport term is greatest at the top of the canopy where the wind speeds are highest. It also fits to the observation that the pressure transport is larger in the subcanopy than in the canopy layer. The wind speed and therefore mechanical shear was higher in the subcanopy than within the canopy leading to higher pressure transport in this region. Maitani and Seo (1985) found in contrast to that a not negligible downward pressure driven flux of TKE in a plant canopy. Their study was experimental, however they only had pressure measurements at the soil surface of a wheat canopy and approximated the canopy layer using these surface measurements. So their results can only be compared to this study by limited extend as the canopy height was very low compared to a forest canopy. Here, pressure transport was a small source for turbulence kinetic energy in the trunk space comparable to the buoyancy term of the subcanopy layer (see Figure 5.2.7). However, the pressure transport term was not the largest source for TKE in the subcanopy like Dwyer et al. (1997) predicted in their LES study. The period during which the pressure transport term was positive was shorter in the subcanopy layer stretching only between 06:00 and 16:00 (see Figure 5.1.5). During the night the pressure transport is smaller, but more unsteady changing its sign quickly. This could be to the fact that wind speeds are generally smaller during the night. Shaw et al. (1990) could show by comparing surface pressure measurements with pressure fluctuations retrieved from a Poisson equation that the pressure fluctuations at the surface are primarily created by velocity perturbations in high shear region at the top of the forest canopy. So high wind speeds promote high pressure perturbations within the forest canopy. So all in all, the first hypothesis can be partly accepted. Pressure transport was no sink in the

subcanopy, but was most important in the trunk space as expected, because the magnitude of the other terms of the TKE budget was also low in the sucanopy region.

Viscous dissipation is assumed to be the most important sink of turbulence kinetic energy by transforming TKE into internal energy due to friction at a surface (Meyers and Baldocchi, 1991). The canopy elements convert large eddies into high-frequency motions (small eddies), which get dissipated quickly. However, viscous dissipation could not be measured directly during the INTRAMIX experiment, but was estimated as residual of the TKE budget equation after calculation of the remaining terms of the TKE budget equation. Therefore, the so-called residual (or residuum) has to be evaluated very carefully. Physically, viscous dissipation should always be a sink for turbulence kinetic energy. Positive values indicate measurement errors of the other TKE terms due to inaccuracy of the sensors or calculations, which contribute mistakenly to the dissipation term. Leclerc et al. (1990) found for example a positive residual to which viscous dissipation, the pressure transport and accumulated errors contributed. The residual term was the largest sink for turbulence kinetic energy in the TKE budget as it compensates for the source terms to balance the budget. The residual decreased in magnitude with decreasing height being -2.6x10^{-2} m^2s^{-3} in the top of the canopy, –7.4x10^{-3} m^2s^{-3} in the canopy layer and -6.0x10^{-4} m^2s^{-3} in the subcanopy (see Table 5.1.1, Figure 5.1.1).

At the top of the canopy, the residuum was negative throughout the day, but showed a clear diel cycle (see Figure 5.1.6). From 03:00 the dissipation decreased until 12:00, then was stable until 16:00 and increased during the evening until 19:30. During the night the residuum slightly decreased again.

In the canopy layer the residuum term was also negative during all time, but had only 28% of the value at the top of the canopy (see Table 5.1.1). Only the decrease in the early morning hours occurred later than at the top of the canopy at 04:30 and there was no clear stable period around noon (see Figure 5.1.6). In the afternoon the residuum term also increased until approximately 19:30 and showed a nocturnal minimum, too. A reason for these minima in the top of the canopy and canopy layer are presumably the small maxima of the turbulent transport term, for which the residuum compensates by getting more negative.

In the subcanopy the residual term had only 2% of the residuum above the tree crown, but was still the most important sink for TKE in the trunk space. The residuum of the subcanopy layer also showed a distinct diel cycle with a steep

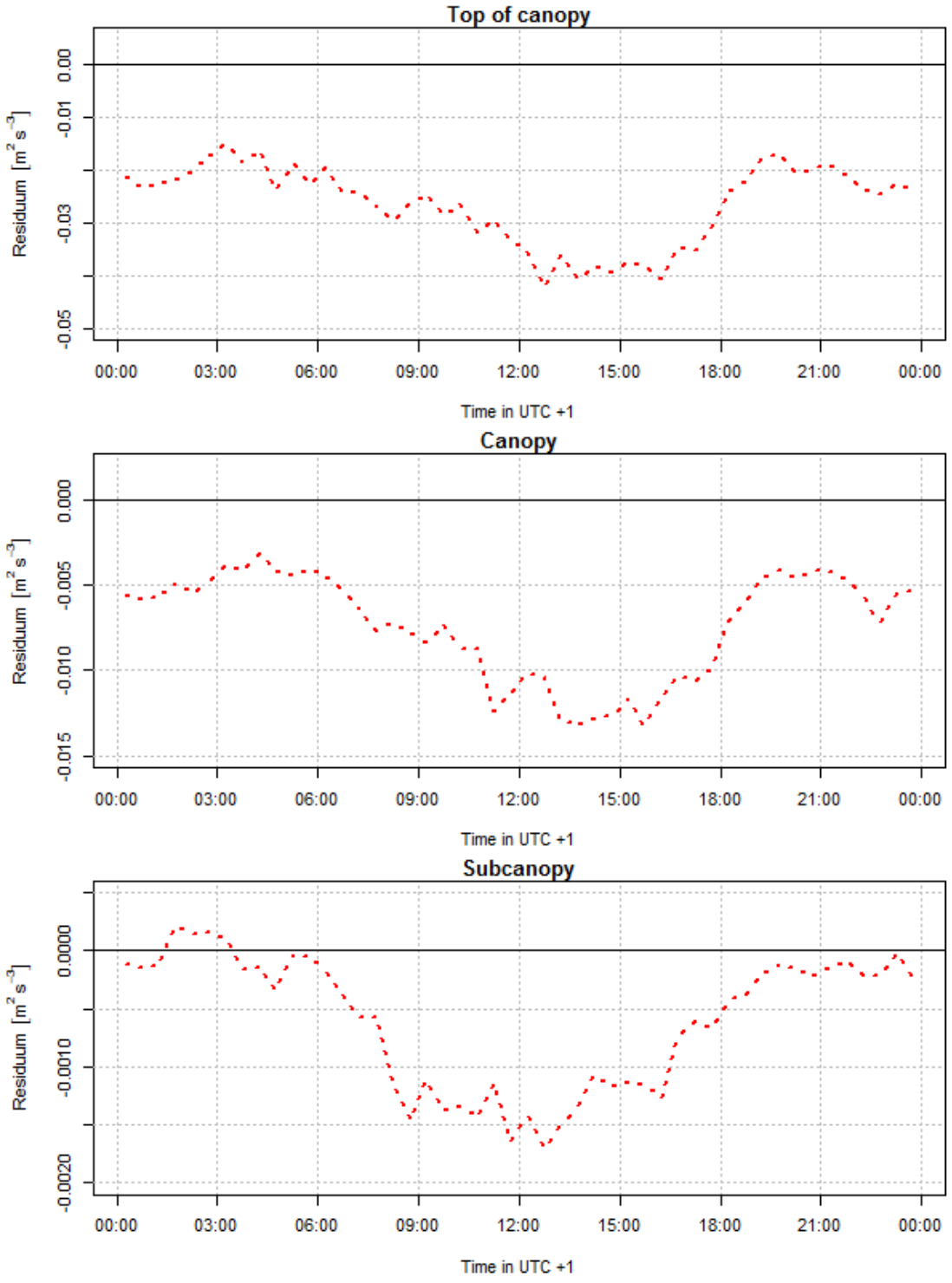

FIGURE 5.1.6: Ensemble average for the residual term of the TKE budget (dashed red line). The diel cycle of the top of the canopy (top), canopy (middle) and subcanopy (bottom) is displayed. Please note that the y-axis of the plots differ by one order of magnitude.

decrease between 05:30 and 12:00 and an increase from 12:00 to 20:00. During the night the residuum term in the subcanopy is closer to zero than the residuum in the upper two layers. Around 02:00 the residual of the subcanopy layer is even slightly positive 3:30.

The TKE tendency term shows if turbulence kinetic energy if TKE production or consumption dominates in the layer. So if TKE is increasing, the TKE tendency is positive and the other way round. This can be clearly seen in Figure 5.1.7 below. Generally, the turbulence intensity is smallest in the subcanopy (see Figure 5.1.1), where TKE was always lower than 0.5 m^2s^{-2} (see Figure 5.1.7). Former studies also showed that the turbulence intensities are highest in the upper canopy and decrease with height (Baldocchi and Hutchison, 1987; Cionco, 1972). Between 06:00 and 14:00 when the turbulence kinetic energy rose at 36 m, the TKE tendency of the top of the canopy layer was also positive. When TKE started to decrease at 14:00, the TKE tendency term got also negative and further decreased. During the night the turbulence kinetic energy showed a slight increase again, which was also followed by a change in sign of the TKE tendency. A reason for this nighttime increase at 36 m could be the nocturnal maxima of mechanical shear and turbulent transport that were observed (see Figure 5.1.2, Figure 5.1.4). With decreasing measurement height, the magnitude of turbulence kinetic energy got smaller. TKE at 36 m height reached up to 2.25 m^2s^{-2}, while in at 18 m it only peaked at 0.5 m^2s^{-2} (see Figure 5.1.7). In the subcanopy and at the ground the TKE is even lower with 0.3 m^2s^{-2} and 0.1 m^2s^{-2}, respectively. The diurnal pattern got also weaker with decreasing measurement height. This can also be seen in the lower panel of Figure 5.1.7, where the TKE tendency term of the canopy and subcanopy layer were smaller in magnitude compared to the top of the canopy.

All in all, the terms of the TKE budget equation were largest in the top of the canopy layer and decreased with height in the canopy and subcanopy, except for turbulent transport, which had its maximum in the canopy layer (Table 5.1.1, Figure 5.2.10a). The first hypothesis stated that pressure transport is more important in the subcanopy than in the upper parts of the canopy where other terms of the TKE budget dominate. This part of the hypothesis can be considered true based on the results of this study. In the top of the canopy layer, mechanical shear and buoyancy were the major sources for TKE. Pressure transport was only a small source being two orders of magnitude smaller than the other terms. The turbulent transport, the residuum and the buoyancy term during the night were the dominant sinks for turbulence kinetic energy in the top of the canopy layer.

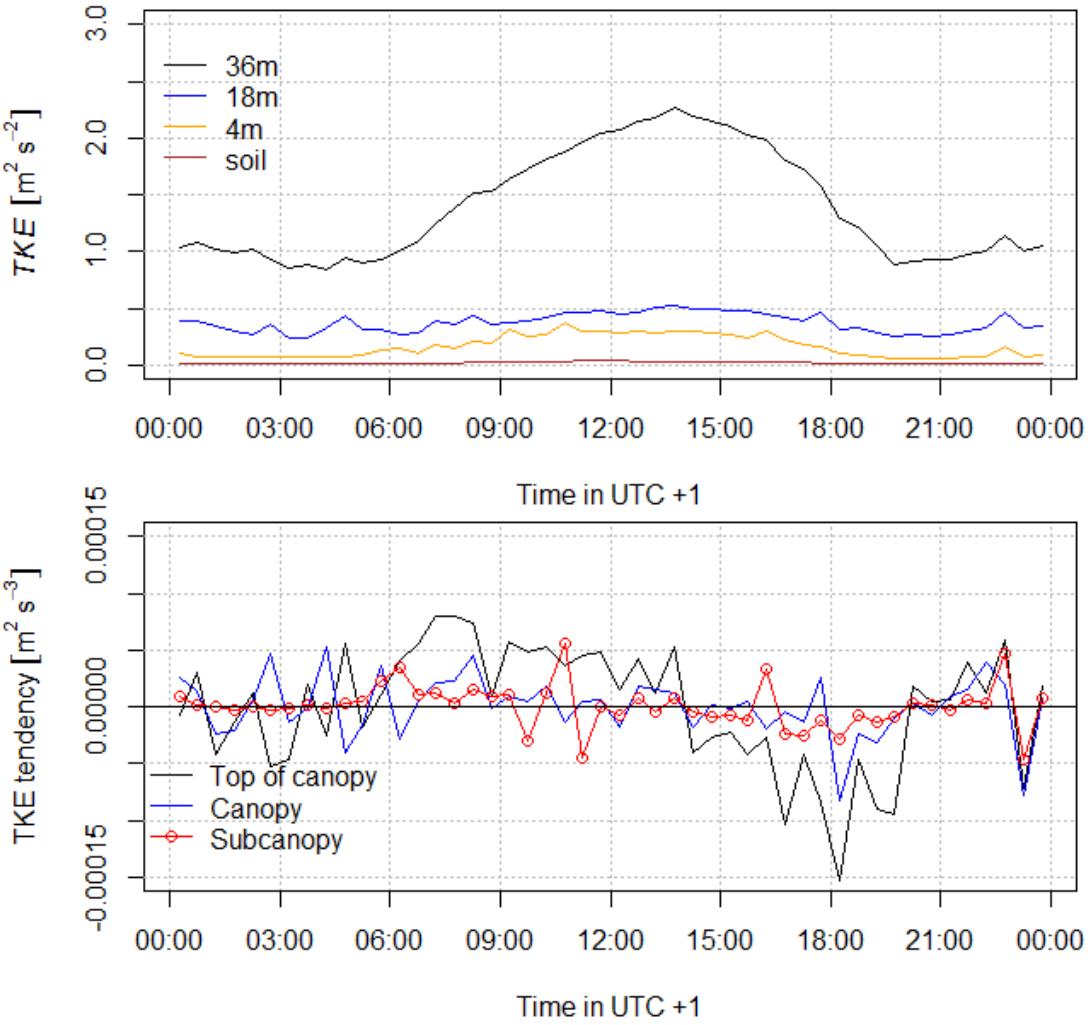

FIGURE 5.1.7: Ensemble average of the mean TKE for the four measurement heights (upper plot) plotted as diel cycle. The lower plot shows the TKE tendency for the three canopy layers. A increasing TKE is associated with positive TKE tendency and reversely. Please note that the y-axis of the plots differ.

Pressure transport was also a small sink for TKE at the top of the canopy during the night, but compared to the other sinks it was almost negligible.
In the canopy layer, other sources than at the top of the canopy dominated. Turbulent transport was by far the greatest source for TKE in the crown, followed by buoyancy production. Mechanical shear was very low in the canopy layer probably due to the very low wind speeds there caused by the high foliage density. Pressure transport was a small source for TKE, but compared to turbulent transport and buoyancy it was very small. The major sink for turbulence kinetic energy in the canopy layer was the viscous dissipation being of the same magnitude, but of opposite sign than turbulent transport.
In the subcanopy, mechanical shear was the greatest source for TKE due to a second wind maximum, followed by turbulent transport. This was surprising, because turbulent transport is usually the greatest source in the subcanopy (Vickers and Thomas, 2013). Buoyancy production and pressure transport acted as small sources for TKE. Like in the canopy layer, dissipation was the dominant sink for turbulence kinetic energy in the subcanopy layer. In summary, it can be stated that pressure transport is important in the subcanopy, where it is a source comparable to the buoyancy term, but in the upper layers of a forest canopy it can be mostly neglected.

5.2 Comparison of contrasting forest architectures

Studies about turbulence kinetic energy have been conducted for various ecosystems like agriculture (Brunet et al., 1994; Maitani and Seo, 1985; Wilson and Shaw, 1977) and forests (Amiro, 1990; Baldocchi and Hutchison, 1987; Dwyer et al., 1997; Leclerc et al., 1990; Vickers and Thomas, 2013) and even for urban areas (Christen et al., 2004, 2009; Giometto et al., 2015). Forest are especially interesting, but difficult measurement sites as the parameters have to be measured at several locations across the vertical extent of the canopy to adequately represent the forest. Different characteristics of the dominating species like leave type and size, foliage density, branch distribution and the composition of the understory vegetation influence the air flow within the forest together with the overall stand density. Figure 5.2.1 shows the vertical profiles of each TKE budget term of the two different forests. Each point is the midpoint of the respective layer, while the symbols indicate the dense and sparse forest, respectively. To compare the results measured at different heights in forest with differing canopy height, the mid-layer height was normalized using the canopy height of the respective forest.

The Norway spruces (*Picea abies*) of the Waldstein site formed a dense canopy which led to a high magnitude of the mechanical shear term of the TKE budget at the top of the canopy and very low values of mechanical shear in the two lower layers (see Figure 5.2.1). The shear generation was two orders of magnitude smaller in the subcanopy than in the top layer (see Table 5.1.1). In the canopy layer, mechanical shear was smallest with a mean of -1.8x10^{-6} m^2s^{-3} being four orders of magnitude smaller compared to the top of the canopy (see Table 5.1.1). Meyers and Baldocchi (1991) found a similar pattern of mechanical shear in a dense deciduous forest where shear generation was the largest source for TKE at the top of the canopy around z/h=1.0. Actually, it was expected that the mechanical shear term was even smaller in the subcanopy. The relatively high values of shear there are probably due to the only sparse understory vegetation around the measurement tower and a nearby clearing where winds can enter the subcanopy space leading to a second wind maximum. Within the crown the dense foliage slows down the airflow immensely leading to the minimum of shear generation in the canopy layer (see Figure 5.2.1). This assumption is proved by the distribution of shear generation in the sparse Ponderosa pine forest. Here the mechanical shear term also increased with increasing height (see Figure 5.2.1) and shear generation was smallest in the subcanopy with a mean value of 5.6x10^{-4} m^2s^{-3} (see Table 5.2.1). In the top of the canopy and canopy layer, the mechanical shear

term were two orders of magnitude higher than in the subcanopy with averages of 4.6x10^{-2} m^2s^{-3} and 1.0x10^{-2} m^2s^{-3}, respectively (see Table 5.2.1). This supports the model results of Dwyer et al. (1997) who found that dominant production mechanism of TKE is mechanical shear with a maximum just below the tree top height. Lesnik (1974) also found that the mechanical shear term was most important at the top of the canopy where the wind shear gradient was largest. As most of the mechanical shear is generated in the upper canopy, it is only logical that the forest architecture impacts the role of the shear term. During the day the mechanical shear term at the top of the sparse forest increased between 05:00 and 11:00 and then decreased in the afternoon and evening until 22:00 (see Figure 5.2.3). The maximum of mechanical shear in the Ponderosa Pine forest was reached shortly before noon and the value was about one third higher than in the dense forest. The course of mechanical shear is also less smooth than in the Norway spruce forest. There is no nocturnal maximum, which occurred in the dense forest, in the sparse Pine forest.
The canopy layers of the two forests showed a completely different pattern. While in the dense forest mechanical shear was not important as mentioned above, in the canopy layer of the Ponderosa Pine forest shear generation was the second largest source for TKE with a maximum of 2.0x10^{-2} m^2s^{-3} occurring around 13:00 (see Figure 5.2.5). Mechanical shear showed a diel cycle and was smallest during the night, when the mechanical shear was less than 1x10^{-2} m^2s^{-3}. This difference is caused by the strong influence of canopy elements, which suppress resolved-scale turbulent motion and attenuate the mean flow (Dwyer et al., 1997). Nonetheless, the mechanical shear in the canopy layer had only 22% of the top of the canopy shear generation (see Table 5.2.1).

The mechanical shear in the subcanopy layer of the sparse forest was by far smallest accounting only for 1% of the shear generation in the top of the canopy layer (see Table 5.2.1). The shear term showed also no diel cycle in contrast to the subcanopy shear generation in the dense spruce forest (see Figure 5.2.8). While mechanical shear was the most important source for TKE in the subcanopy of the Norway spruce forest, it was only the third largest source term in the sparse forest (see Table 5.2.1). This supports former results from Vickers and Thomas (2013) who also observed that in the lower layer of a pine canopy shear generation is less important than turbulent transport and buoyancy. Dwyer et al. (1997) also found that shear production is negligible below about half of the canopy height for both Large Eddy Simulations with LAI = 2 and LAI = 5 they did, respectively. The findings of this master thesis show that the forest architecture of a forest

TABLE 5.2.1: Averages over the entire measurement period and the ratio (respective lower layer divided by the top of the canopy layer following Vickers and Thomas (2013)) for the TKE budget terms of the sparse Ponderosa pine forest. Positive tendency terms contribute to positive TKE tendency and negative values to a negative TKE tendency. Analogous to Vickers and Thomas (2013) for the TKE the direct measurements of the 30 m height (top of the canopy layer), 16 m height (canopy layer) and 6 m height (subcanopy layer) are taken, respectively.

Quantity	**Subcanopy**	**Canopy**	**Top of canopy**	**Ratio Sub-canopy**	**Ratio Canopy**
Mechanical shear $[m^2 s^{-3}]$	5.6x10^{-4}	1.0x10^{-2}	4.6x10^{-2}	0.01	0.22
Buoyancy production $[m^2 s^{-3}]$	5.0x10^{-4}	1.4x10^{-3}	2.1x10^{-3}	0.24	0.67
Turbulent transport $[m^2 s^{-3}]$	2.6x10^{-3}	2.4x10^{-2}	-2.1x10^{-2}	-0.12	-1.1
Pressure transport $[m^2 s^{-3}]$	4.4x10^{-5}	-4.2x10^{-4}	3.5x10^{-4}	0.12	-1.2
Residual $[m^2 s^{-3}]$	-2.6x10^{-3}	-3.2x10^{-2}	-2.1x10^{-2}	0.12	1.5
TKE tendency $[m^2 s^{-3}]$	1.1x10^{-7}	2.7x10^{-7}	-3.9x10^{-7}	-0.28	-0.70
TKE $[m^2 s^{-2}]$	0.17	0.96	1.7	0.10	0.56

significantly influences its TKE budget. A dense forest with an open trunk space apparently favors a second wind maximum, while in a sparse forest the mechanical shear simply with depth into the canopy. Meyers and Baldocchi (1991) also examined a significant second wind maximum in the middle and lower canopy of dense deciduous forest with a LAI of about 5. For this study two needle leaf forests were observed, but probably deciduous forests with a different distribution of leaf area will show a different pattern. Meyers and Baldocchi (1991) e.g. observed very high values of shear in the high dense crown of a deciduous forest.
All in all, the mechanical shear term was larger in the sparse forest, where it increased towards the canopy top, than in the Norway spruce stand. In the spruce forest the dense crown layer caused a minimum of shear generation in the canopy layer.

At the top of the canopy, buoyancy term was an important source for TKE during the day and a small sink during nighttime for both forests (see Figure 5.2.2, Figure 5.2.3). In the dense Norway spruce forest buoyancy was greatest in the top of the canopy layer being the second largest source of TKE with a mean of 1.5x10^{-3} m^2s^{-3} (see Table 5.1.1). As expected the turbulence kinetic energy production through buoyancy decreased towards the surface by one magnitude per layer. The buoyancy production in the top of the canopy layer of the sparse Ponderosa Pine forest was comparable to the dense Waldstein forest with a mean of 2.1x10^{-3} m^2s^{-3} (see Table 5.2.1).
The buoyancy production was also the second largest source for TKE in the top of the canopy layer of the pine forest, but small compared to the other terms of the TKE budget. This corresponds well to what Vickers and Thomas (2013) observed in a sparse canopy, where buoyancy production was the second largest source for TKE, too. The buoyancy term peaked earlier at about 09:00 compared to the dense forest (see Figure 5.2.3), where the maximum was reached around 12:00 (see Figure 5.2.2). This early peak was caused by the location of the Ponderosa pine forest, which is further south than the Norway spruce forest. Additionally, more radiation can penetrate through the open canopy and heats the forest floor earlier leading to a high buoyancy flux. The forest floor of the pine stand is moreover consisting of dark vulcanic ash and dark Ponderosa pine needles, which heat up fast.
In the canopy layer of the pine forest the buoyancy production was in the same order of magnitude like at the top of the canopy with a mean of 1.4x10^{-3} m^2s^{-3} still representing 67% of the value at the top of the forest (see Table 5.2.1). This was

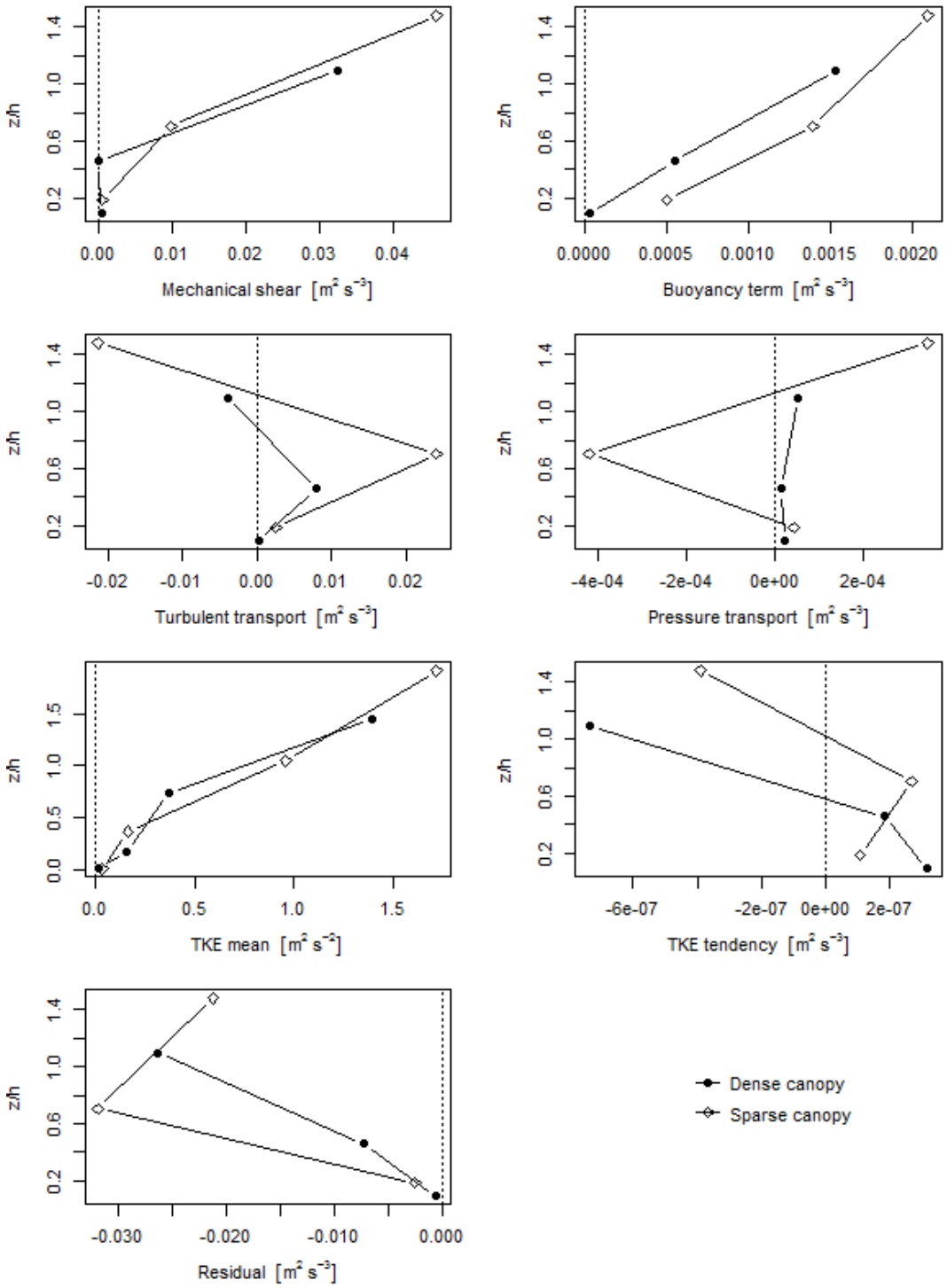

FIGURE 5.2.1: Vertical profile of the TKE terms across contrasting forest architectures. The symbols indicate the mean of the respective layer and are located at the midpoint of each layer. The filled circles (●) represent the dense forest, while the open diamonds (◇) stand for the sparse canopy. Measurement height z is normalized by the canopy height h.

one order of magnitude greater than the buoyancy production in the dense forest, where the buoyancy term in the canopy layer had only 36% of the value above the crown (see Table 5.1.1). The higher buoyancy term was probably caused by the more southward latitude of the Ponderosa pine forest and specific characteristics of the open forest with its dark forest floor and only scarce understory vegetation. Despite its smaller magnitude in the dense forest, the buoyancy production was still the second largest source for TKE there (see Figure 5.2.4). In the sparse pine stand buoyancy production was only the third largest source for TKE within the canopy after turbulent transport and mechanical shear (see Figure 5.2.5). The pattern of the buoyancy term in the canopy layer was very similar to the top of the canopy. The midday maximum of the canopy layer buoyancy production was already reached at 09:00 (see Figure 5.2.5), three hours earlier than in the dense Norway spruce forest. During the night the buoyancy term in the canopy layer was also slightly negative representing a sink for TKE.

The buoyancy term decreased in the subcanopy layer by one order of magnitude with an average of 5.0x10^{-4} m^2s^{-3} (see Table 5.2.1). The smaller gradient between the layers compared to the dense stand shows that the sparse crown of the Ponderosa pine forest has a much smaller shading effect on the subcanopy space than the dense crown of the Norway spruce forest at the Waldstein site. Analogously to the other layers of the Ponderosa pine forest, the peak of the buoyancy term occurred earlier in the sparse forest at around 10:00. The buoyancy production was also more important in the forest with the open crown where was the second largest source for TKE in the subcanopy (see Figure 5.2.8), while in the dense spruce forest it was one of the smaller sources together with pressure transport (see Figure 5.2.7). The results suggest that the forest architecture significantly influences the role of the buoyancy term in the TKE budget equation. The sparser the tree crown of a forest, the greater is the importance of buoyancy production. Our findings show that the heat flux they assumed for their simulations was probably too low. The comparison of subcanopy ratio shows this clearly as the buoyancy term in the subcanopy of the dense forest had only 2% of the magnitude of the buoyancy production at the top of the canopy (see Table 5.1.1), while in the pine forest with the open crown the buoyancy term of the subcanopy layer had 24% of the buoyancy term at the top of the forest canopy (see Table 5.2.1). This is in contrast to what Dwyer et al. (1997) found in their LES study of both a sparse and dense forest, where buoyancy is not even shown due to its small magnitude.

To sum up, the buoyancy production was larger in the sparse Ponderosa pine forest compared to the dense spruce stand. The comparably large buoyancy term in the

subcanopy of the sparse forest is probably due to the warming of the forest floor, which mainly consists of volcanic ash and dark needles of the pine trees. Vickers and Thomas (2013) found that buoyancy production in the lower layer of the same sparse pine forest was even 61% of the value of the upper crown. Additionally, the open forest is located further south leading to a generally higher net radiation compared to the mountainous Norway spruce forest in Northern Bavaria.

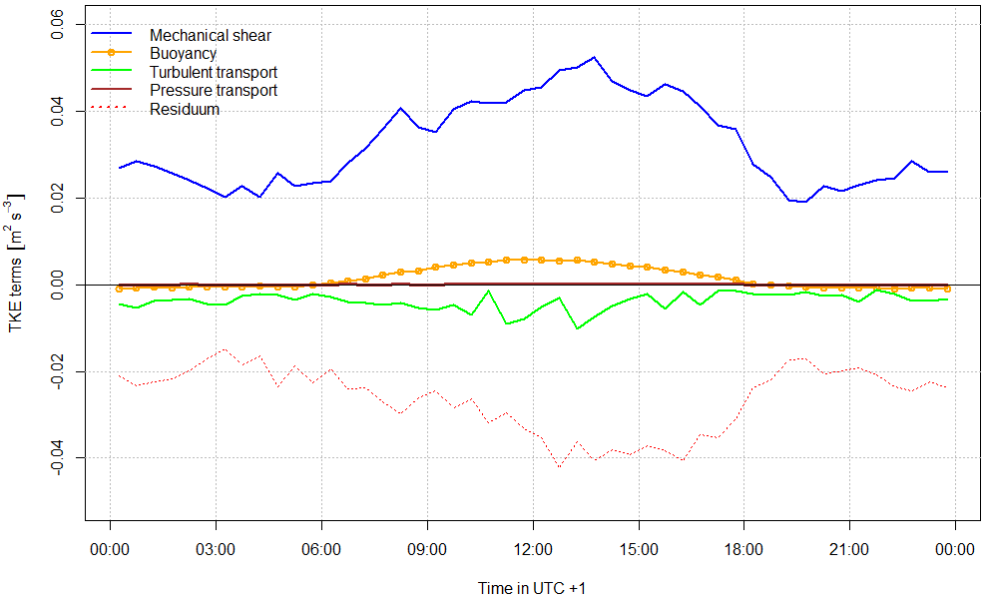

FIGURE 5.2.2: Ensemble averages of the TKE terms of the top of the canopy layer of the dense forest. Mechanical shear (solid blue line), buoyancy production (orange line with filled circles), turbulent transport (solid green line), pressure transport (solid brown line) and the residual term (dashed red line) are plotted versus the time of the day. The TKE tendency was left out in this plot as the term was very small, but can be seen in Figure 5.1.7

Turbulent transport is important for the redistribution of TKE within a forest canopy. But is the vertical turbulent transport affected by the forest architecture? In the dense spruce forest, turbulent transport was the second largest sink for turbulence kinetic energy at the top of the canopy after the residuum (see Figure 5.2.2), while in the canopy and subcanopy layer the turbulent transport term was the largest and second largest source for TKE, respectively (see Figure 5.2.4, Figure 5.2.7). Turbulent transport in the sparse Ponderosa pine forest was generally by one order of magnitude greater than in the dense forest, but the distribution pattern was similar (see Figure 5.2.3). The turbulent transport term was greater in the sparse Ponderosa Pine forest than in the dense forest canopy with a mean of -2.1x10^{-2} m^2s^{-3} at the top of the canopy, 2.4x10^{-2} m^2s^{-3} in the

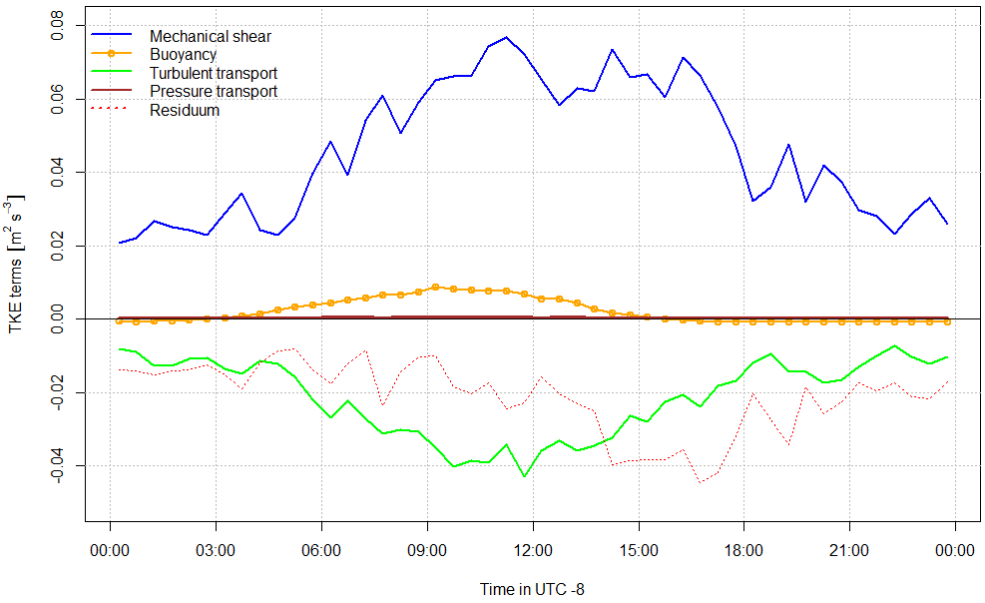

FIGURE 5.2.3: Ensemble averages of the TKE terms of the top of the canopy layer of the sparse forest. Mechanical shear (solid blue line), buoyancy production (orange line with filled circles), turbulent transport (solid green line), pressure transport (solid brown line) and the residual term (dashed red line) are plotted versus the time of the day. The TKE tendency was left out in this plot as the term was very small, but can be seen in Figure 5.2.9

.

canopy layer and 2.6x10^{-3} m^2s^{-3} in the subcanopy (see Table 5.2.1). The ratios of the subcanopy and canopy turbulent transport to the one above the crown were nevertheless comparable to the dense forest with -0.12 and -1.1, respectively (see Table 5.2.1). A LES study by Dwyer et al. (1997) predicted a similar vertical pattern of turbulent transport across forest canopies comparable to the one observed here. Their model result for a sparse forest showed a clear source for TKE within the canopy and a large sink of TKE with a peak just above the canopy top. A dense forest with a LAI of 5 was also simulated and turbulent transport in this dense canopy had almost the same magnitude like in the sparse forest, which contradicts to the findings of this study, where turbulent transport was larger in the sparse Ponderosa pine forest. Meyers and Baldocchi (1991) also identified turbulent transport as a sink at the canopy top and a source within the canopy of a dense deciduous forest using both experimental and model results.

Vertical turbulent transport was a continuous sink for TKE in the top of the canopy layer of the sparse forest sometimes even exceeding the residuum (see Figure 5.2.3). In the dense forest, the turbulent transport sink was less distinct and never reached the level of the residual term (see Figure 5.2.2, Figure 5.2.1).

In the canopy layer of the pine forest turbulent transport was of the same magnitude, but of opposite sign to the turbulent transport in the layer above being by far the most important source for TKE (see Figure 5.2.5). This is consistent with the dense forest, where turbulent transport was also the greatest source term within the canopy (see Figure 5.2.4). This indicates, analogously to what was observed in the dense Norway spruce forest, that TKE is transported downwards from the top of the canopy into the canopy layer in the open forest. Raupach et al. (1986) also identified turbulent transport as a source for TKE within the canopy in their wind-tunnel study. Nevertheless, the turbulent transport in the canopy layer of the open stand was twice as high as in the canopy of the dense spruce forest (see Figure 5.2.1).
Turbulent transport was the largest source of TKE in the subcanopy of the Ponderosa pine forest (see Figure 5.2.8), while it was only the second largest source term in the subcanopy layer of the dense forest (see Figure 5.2.7). The turbulent transport term of the Ponderosa pine site had also a clear diel cycle, while the subcanopy turbulent transport in the dense forest was only slightly higher during the day. Also the magnitude between the two forest sites differed strongly. At the pine forest the turbulent transport reached up to 6x10^{-3} m^2s^{-3}, while in the dense forest the largest peak was around 7x10^{-4} m^2s^{-3}. The transfer of TKE through turbulent is probably inhibited by the high foliage density in the dense Norway spruce forest and therefore only a small amount of the TKE that is exported from the top of the canopy reaches the subcanopy. The results of the sparse forest support the findings of former studies who identified the turbulent transport as the most important source of TKE below the crown (Meyers and Baldocchi, 1991; Raupach et al., 1996; Vickers and Thomas, 2013).
The vertical profile of TKE was very similar across the two different forest architectures, but the sink at the canopy top as well as the source in the lower region of the forest were more distinct in the open crown (see Figure 5.2.10b). Apparently a dense tree layer inhibits the vertical turbulent flow within a forest.

One of the main aspects of this master thesis was to investigate how the architecture of a forest influences the pressure transport. This is of special importance as there are only assumptions or modelling results that try to determine the role of the pressure transport to the TKE budget. Often this model results or approximations of the pressure transport term by surface pressure or wind-tunnel experiments are contradicting though (Dwyer et al., 1997). Raupach et al. (1986) stated e.g. that pressure transport is a source throughout the whole forest canopy, while Brunet et al. (1994) suggested that pressure transport is a source above the canopy, but

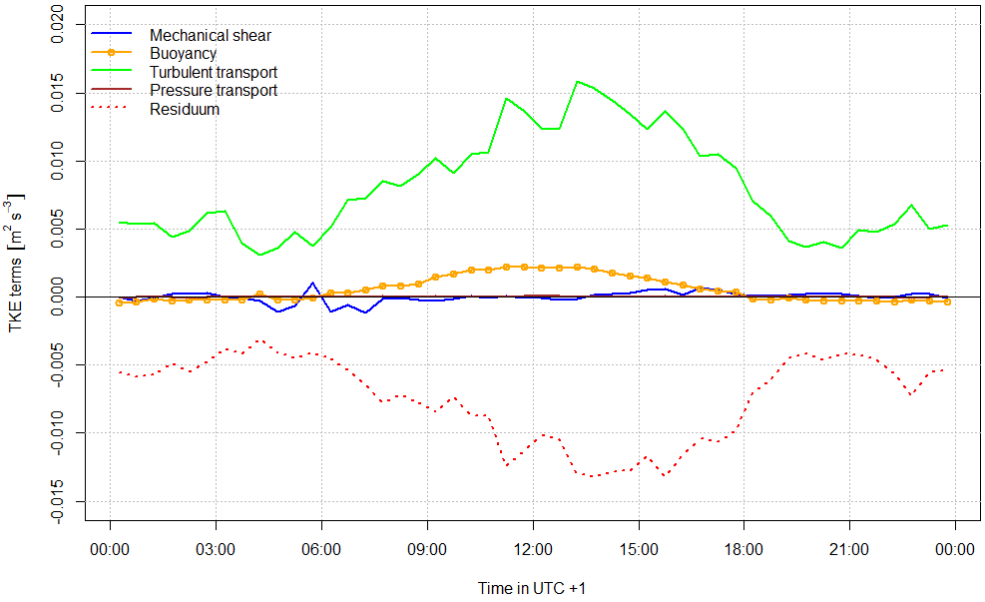

FIGURE 5.2.4: Ensemble averages of the TKE terms of the canopy layer of the dense forest. Mechanical shear (solid blue line), buoyancy production (orange line with filled circles), turbulent transport (solid green line), pressure transport (solid brown line) and the residual term (dashed red line) are plotted versus the time of the day. The TKE tendency was left out as the term was very small, but can be seen in Figure 5.1.7

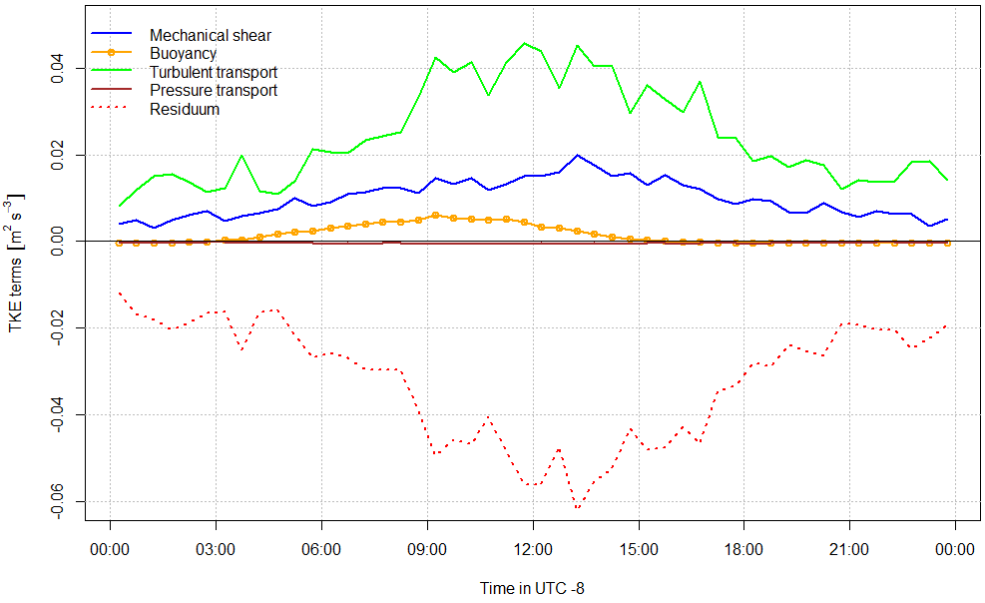

FIGURE 5.2.5: Ensemble averages of the TKE terms of the canopy layer of the sparse forest. Mechanical shear (solid blue line), buoyancy production (orange line with filled circles), turbulent transport (solid green line), pressure transport (solid brown line) and the residual term (dashed red line) are plotted versus the time of the day. The TKE tendency was left out as the term was very small, but can be seen in Figure 5.2.9

a loss of TKE within the forest. The results of this study indicate that both are right, because the pattern of the pressure transport term was strongly dependent on the forest architecture. In the dense Norway spruce forest of the Waldstein site pressure transport was mainly a source for turbulence kinetic energy at all three layers of the canopy, but was actually only important in the subcanopy (see Figure 5.2.1). There, the pressure transport acted a source for TKE comparable to the magnitude of buoyancy production in the subcanopy layer (see Figure 5.2.7). In contrast to that, the pressure transport was very small compared to the other terms of the TKE budget in the upper two layers of the dense forest. In the Ponderosa pine forest, pressure transport was no continuous source for TKE in contrast to that (see Figure 5.2.1). The pressure transport was a source for turbulence kinetic energy in the subcanopy and at the top of the canopy, but acted as a sink for TKE in the canopy layer, where it was greatest, too. In the sparse forest the pressure transport was also decreasing in the subcanopy layer by one order of magnitude (see Table 5.2.1), while in the dense Norway spruce forest the term laid in the same order of magnitude for all layers (see Table 5.1.1). So in the subcanopy of the sparse forest the pressure transport had only 12% of the value above the crown, while in the forest with the dense spruce crown the pressure transport had 44% of the magnitude at the top of the canopy.

Pressure transport was greatest at the top of the canopy of both forests, but in the sparse pine forest the pressure transport term was overall greater (see Figure 5.2.1). At the top of the canopy pressure transport was a constant source of TKE throughout the day with a peak around 09:00 of approximately 5.5x10^{-4} m^2s^{-3} (see Figure 5.2.6).

Pressure transport was a small, but nevertheless the second largest sink for TKE in the canopy layer of the sparse forest with a mean of -4.2x10^{-4} m^2s^{-3} (see Table 5.2.1), while it was a small source in the dense one. The course of pressure transport in the canopy of the sparse pine forest was almost inversely to the pressure transport term in the upper layer with a minimum around 11:00 and lower values at night (see Figure 5.2.6). This indicates that TKE is exported from the canopy layer of the open crown into the top of the canopy layer.

In the subcanopy of the pine forest the pressure transport term was twice as high in the subcanopy layer of the dense forest with 4.4x10^{-5} m^2s^{-3} (see Table 5.2.1). It was also a small source of TKE during the day and leveled around zero at night (see Figure 5.2.6), but as the other terms of the subcanopy TKE budget at the Ponderosa pine forest were greater than the TKE terms of the dense spruce forest, pressure transport was more important in the subcanopy layer of the dense

forest (see Figure 5.2.7, Figure 5.2.8). This vertical pattern of pressure transport is in contrast to what Dwyer et al. (1997) predicted in their LES study. They supposed that pressure transport extracts TKE from the top of the canopy and thereby supplies lower regions of the forest with turbulence kinetic energy. This could be the case in this study for the subcanopy, but the major part of TKE is redistributed upwards. An aspect that seems to be depicted correctly in the LES of Dwyer et al. (1997) is that pressure transport decreases only slowly towards the surface in contrast to turbulent transport. This was clearly true especially for the layers of the dense forest. Because of this Shaw and Zhang (1992) and Dwyer et al. (1997) assume that turbulence in the subcanopy of a forest is largely induced by pressure perturbations. The results of this study relativize these assumptions. Apparently, the pressure transport term is only important in the subcanopy of dense forests where other terms of the TKE budget are also small. Interestingly, the vertical distribution of the pressure transport term is inversely to the vertical profile of turbulent transport for both forest, whereby it is more distinct for the open forest (see Figure 5.2.1). This was predicted by Mcbean and Elliott (1975) who supposed that pressure transport has to be of opposite sign to the turbulent flux divergence.

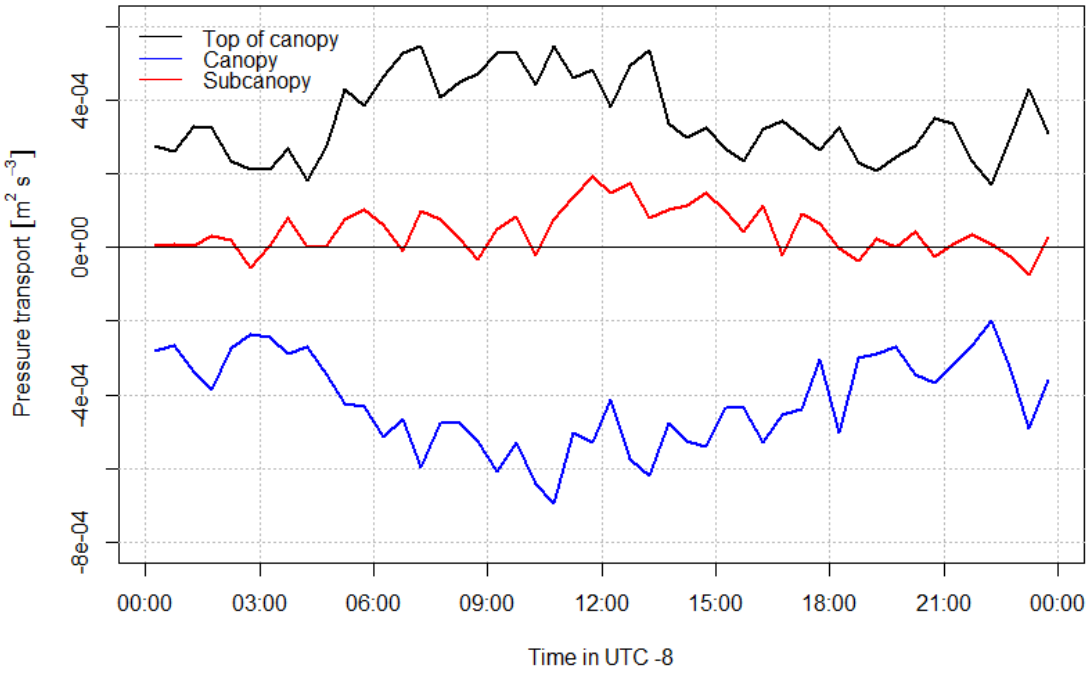

FIGURE 5.2.6: Ensemble averages of the pressure transport at top of the canopy (black line), canopy (blue line) and subcanopy layer (red line) of the sparse pine forest.

The residual was the dominant sink of TKE for all layers of the dense Norway spruce forest, whereby its magnitude decreased almost linearly towards the canopy top (see Figure 5.2.1). The residuum was also the ultimate sink for TKE across the all layers of the Ponderosa pine forest (see Figuree 5.2.1). In the open crown the residual also decreased in the lower part of the canopy and then increased again towards the canopy top.
In the top of the canopy layer the dissipation term was the largest sink for TKE with -2.1 10^{-2} m^2s^{-3} except for a period during the day between 4:30 and 14:00 during the day (see Table 5.2.1, Figure 5.2.3), when turbulent transport exceeded the residuum. There was also a clear diurnal cycle apparent at the top of the canopy (see Figure 5.2.3). The residual term was however a more important sink in the dense canopy, where it was the only negative TKE budget term (see Table 5.1.1). Furthermore the mean at in the top of the canopy layer of the dense spruce forest was greater than in the pine stand (see Figure 5.2.1).
In the canopy layer the residuum term was by far the largest source for TKE in the open Pine forest (see Figure 5.2.5). This is in absolute agreement with the residual of the dense spruce stand (see Figure 5.2.4). The residuum within the canopy of the Ponderosa pine forest showed furthermore a diel cycle with a negative peak around -6x10^{-2} m^2s^{-3} (see Figure 5.2.5).
The viscous dissipation in the subcanopy of the sparse pine forest of one order of magnitude greater than in the dense forest with a mean value of -2.6x10^{-3} m^2s^{-3} (see Table 5.2.1). This makes the dissipation term to the greatest sink for TKE in the subcanopy layer of the sparse forest. The pine forest showed a distinct diel cycle like the other canopy layers and the dense forest (see Figure 5.2.8).
All in all, the residual term in the sparse Ponderosa pine forest is very similar to the dense Norway spruce stand. The residuum was the dominant sink for turbulence kinetic energy and appeared to be not influenced by forest architectures.

Despite the clear differences in the processes that contribute to the production or consumption of TKE, the mean turbulence kinetic energy of the two different forests were quite similar. The TKE increased with increasing height being greatest at the top of the canopy with a mean of 1.7 m^2s^{-2} for the sparse Ponderosa pine forest (see Table 5.2.1) and 1.4 m^2s^{-2} for the dense spruce forest (see Table 5.1.1). TKE had a diel cycle for all layers at the sparse forest (see Figure 5.2.9), which was also observed for the dense spruce stand, but the were most distinct at 36 m (see Figure 5.2.9).
In the canopy layer the TKE was higher for the sparse Pine forest with 0.96 m^2s^{-2} compared to 0.37 m^2s^{-2} for the dense Norway spruce forest. This is a difference of

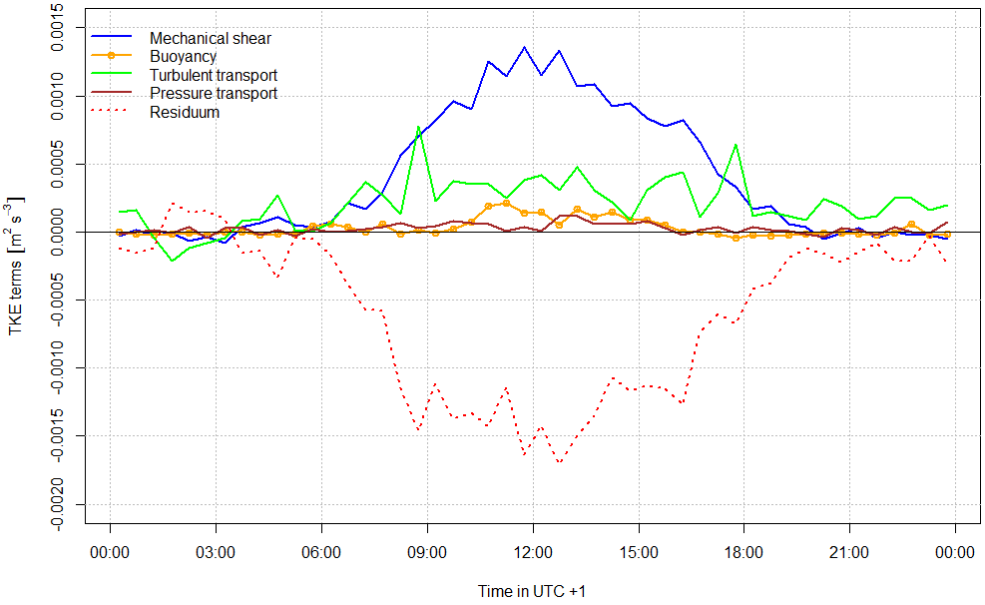

FIGURE 5.2.7: Ensemble averages of the TKE terms of the subcanopy layer of the dense forest. Mechanical shear (solid blue line), buoyancy production (orange line with filled circles), turbulent transport (solid green line), pressure transport (solid brown line) and the residual term (dashed red line) are plotted versus the time of the day. The TKE tendency was left out as the term was very small, but can be seen in Figure 5.1.7

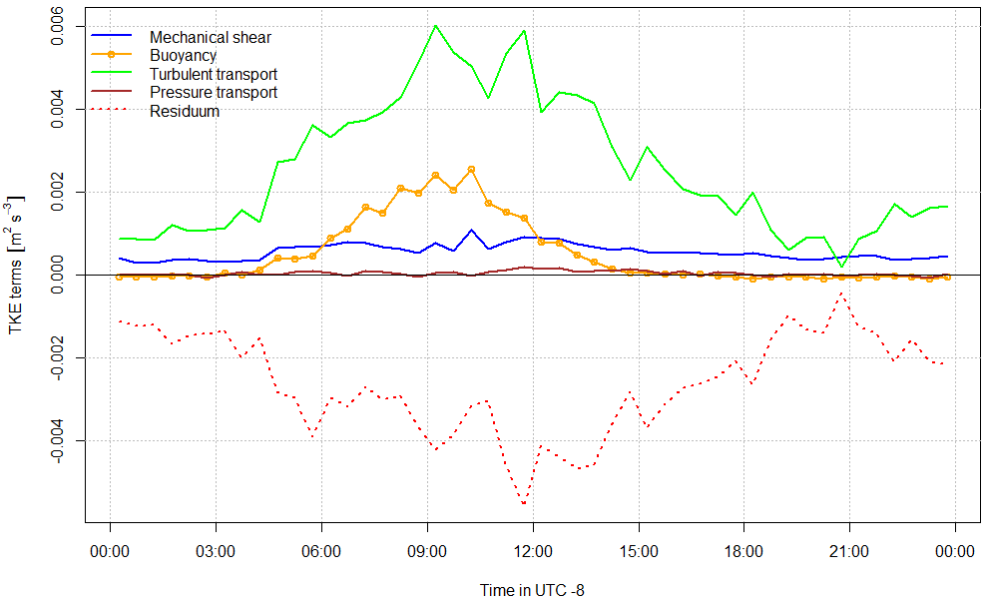

FIGURE 5.2.8: Ensemble averages of the TKE terms of the subcanopy layer of the sparse forest. Mechanical shear (solid blue line), buoyancy production (orange line with filled circles), turbulent transport (solid green line), pressure transport (solid brown line) and the residual term (dashed red line) are plotted versus the time of the day. The TKE tendency was left out as the term was very small, but can be seen in Figure 5.2.9

39% between the canopy layers of the different forest sites. A reason for this difference could be that the shear generation and turbulent transport produce more TKE in the sparse Ponderosa pine forest than in the dense canopy of the Norway spruce forest.
The mean turbulence kinetic in the subcanopy was almost equal again with 0.17 m^2s^{-2} for the sparse forest (see Table 5.2.1) and 0.16 m^2s^{-2} for the dense Norway spruce stand (see Table 5.1.1). The TKE in the subcanopy of both forests was only 10% and 12% of the mean turbulence kinetic energy at the top of the canopy of the sparse and dense forest, respectively. This results correspond well with the findings of Vickers and Thomas (2013) who found a value of 11% for the lower layer of the same pine forest site and Meyers and Baldocchi (1991) who found a reduction of TKE to approximatly 10% at z/h $<$ 0.75 in a dense deciduous forest. All in all, the TKE in the subcanopy space seems to be around 10% of the TKE at the top of the forest despite the forest architecture. The mean TKE was quite similar for the two forest except for the canopy layer, where the TKE of the dense stand was lower. This difference might be due to the small mechanical shear term in the canopy layer of the Norway spruce forest. The positive peak of TKE also occurred earlier throughout the whole canopy of the sparse pine stand at around 11:00, while in the dense forest the maximum was reached around 14:00. This delay is probably caused by the more southern location of the Ponderosa pine forest and the fact that the buoyancy term also peaks earlier in the open stand.

The TKE tendency of the dense forest was positive in the subcanopy and then decreased with increasing height getting negative in the top of the canopy layer. In the Ponderosa pine forest the TKE tendency increased from the subcanopy to the canopy layer and than became negative at the top of the canopy. For both forests the TKE tendency term was greatest at the top of the canopy (see Table 5.1.1, Table 5.2.1). Nevertheless, the TKE tendency in the sparse forest showed smaller differences between the layers (see Figure 5.2.1).
The TKE tendency at the top of the canopy of the sparse forest was only 53% of the TKE tendency in the top layer of the dense Norway spruce forest (see Table 5.2.1). The TKE tendency was positve during the increase of mean TKE in the morning and then got decreased and changed sign as soon as the mean TKE decreased (see Figure 5.2.9).
The TKE tendency in the canopy layer was also higher in the sparse Ponderosa Pine forest compared to the dense spruce stand with a mean of 2.7x10^{-7} m^2s^{-3} and had also 70% of the magnitude of the TKE tendency at the top of the canopy (see Table 5.2.1), while in the dense forest the canopy TKE tendency had only

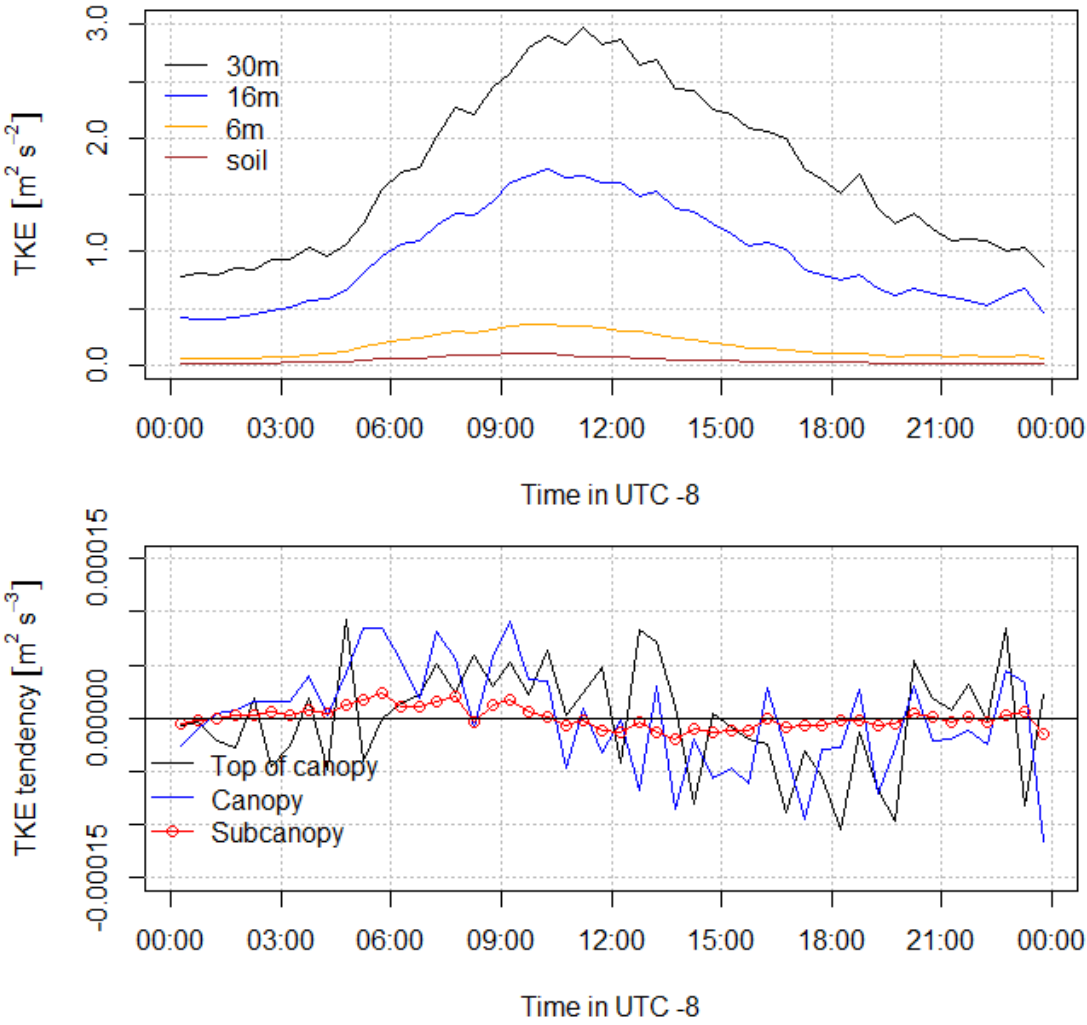

FIGURE 5.2.9: Ensemble average of the mean TKE of the sparse forest for the four measurement heights (upper plot) plotted as diel cycle. The lower plot shows the TKE tendency for the three canopy layers. A increasing TKE is associated with positive TKE tendency and reversely. Please note that the y-axis of the plots differ.

25% of the TKE tendency at the top see Table 5.1.1. The diel course of the TKE tendency in the canopy layer was similar to the one at the top, but smaller in magnitude.
The TKE tendency in the subcanopy of the sparse Pine forest was only one third of the subcanopy TKE tendency in the Norway spruce forest (see Table 5.2.1, Figure 5.2.1). The magnitude of the subcanopy TKE tendency of sparse forest compared to the dense spruce stand was also smaller with 28% compared to 43% in the subcanopy layer of the Norway spruce forest.

So all in all, the forest architecture had a major influence on the TKE budget as was also found by Meyers and Baldocchi (1991). The top layers of the dense and sparse forest were comparable with mechanical shear and buoyancy being the major sources and the residuum and turbulent transport being the largest sinks for TKE (see Figure 5.2.10b). Pressure transport was so low at the top of the canopy of both forests compared to the other terms of the TKE budget that it was almost negligible in the top of the canopy. The lower parts of the forests had much less similarities. Within the canopy of the dense Norway spruce forest the shear generation was understandably very low, while in the sparse forest mechanical shear was the second largest source for turbulence kinetic energy in the canopy layer. Analogously to the top of the canopy, the pressure transport term was also very small in the canopy layers of both forests compared to the dominate TKE terms, but the differences of pressure transport were interesting. While in the dense forest the pressure transport was an overall source for TKE in all layers, in the sparse Ponderosa pine forest pressure transport seemed to be redistributed upwards from the mid of the canopy and a small amount is apparently transported downwards into the subcanopy. The subcanopies of the contrasting forests differed also quite drastically. In the trunk space of the sparse pine forest, turbulent transport, buoyancy production and mechanical shear dominated, while in the dense forest the shear generation and turbulent transport term were largest. The buoyancy and pressure transport term acted as small sources for TKE.

The second hypothesis stated that the denser the forest, the more efficiently is TKE transported through pressure flux divergence between the canopy layers as the dense crown passes the pressure pulse through the canopy. This hypothesis can be partly accepted, as the pressure transport term in the dense forest was very similar in magnitude at all canopy layers. But the transfer of TKE through pressure transport is apparently also working in sparse forest canopies, where TKE was clearly redistributed by pressure transport and the magnitude of pressure transport was even higher in the open crown compared to the dense forest. Nevertheless,

pressure transport is more important in the subcanopy of a dense forest than in the trunk space of a sparse forest because under the dense canopy the magnitude of all fluxes is smaller and therefore the pressure transport term is more significant.

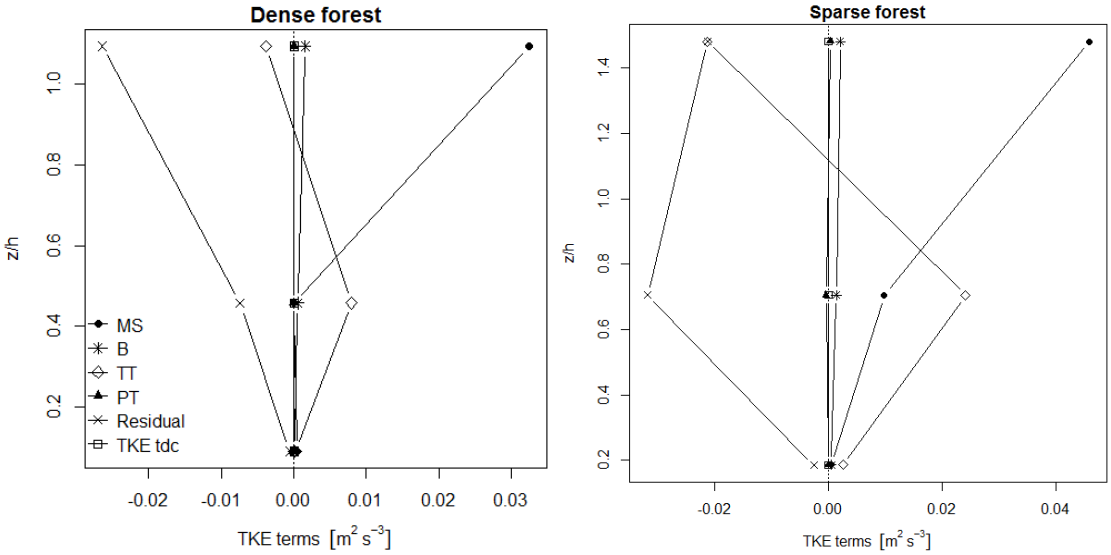

(A) Vertical profile of all TKE terms across the dense forest canopy.

(B) Vertical profile of all TKE terms across the open forest canopy.

FIGURE 5.2.10: Vertical profile of all TKE budget terms of the two forests. The legend in plot (A) is also valid for (B). Please note that the x-axis and y-axis of the plots differ.

5.3 Dynamic stability regimes

In this section the influence of dynamic stability of the atmosphere to the TKE budget terms is investigated. Several studies proposed that atmospheric stability is important for the magnitude and sign of the terms of the turbulence kinetic energy budget (Eigenmann et al., 2009; Leclerc et al., 1990). Stable conditions are expected to occur mostly at night and show only low wind speeds, while near-neutral conditions are characterized by high wind speeds and low values of net radiation (Baldocchi and Hutchison, 1987). Unstable conditions are in turn defined by high incoming radiation during the day, which leads to high buoyancy fluxes. The Figure 5.3.1, Figure 5.3.2 show the vertical distribution of each TKE budget term in the dense and sparse forest, respectively. The three points in every plot are the midpoint between two observation levels, which is the middle of respective layer of the canopy.

In case of the mechanical shear term, dynamic stability had a distinct influence at the top of the canopy, while the shear generation is very similar in the canopy and subcanopy layer (Figure 5.3.1). Beginning in the canopy layer the mechanical shear term increased towards the top of the forest. The mechanical shear term was largest in the top of the canopy layer under neutral conditions with a mean of 4.2x10^{-2} m^2s^{-3}, followed by shear generation under unstable conditions with 3.2x10^{-2} m^2s^{-3} in the dense forest (see Figure 5.3.1). The sparse pine forest showed a similar vertical profile, but the increase occurred already in the lower region of the canopy and the magnitude was greater. The largest values were also reached at the canopy top under neutral stratifications with 1.5x10^{-1} m^2s^{-3} and under the unstable regime with 2.6x10^{-2} m^2s^{-3} (see Figure 5.3.2). The mechanical shear was lowest under the stable regime (see Figure 5.3.1, Figure 5.3.2), which is not surprising as stable conditions are characterized by low wind speeds. These findings contradicts the results of Leclerc et al. (1990) who found that the mechanical shear term in a sparse deciduous forest canopy increased dramatically with the onset of stable conditions. Additionally, the shear generation of the neutral regime was lowest in their study. In contrast to the pattern observed in the upper canopy, the mechanical shear was largest in the subcanopy of the dense forest under unstable conditions, probably because more turbulence is generated near the surface under unstable conditions due to incoming solar radiation. This is interestingly in line with what Leclerc et al. (1990) with observed in the lower two-thirds of the sparse deciduous forest. The results in this study correspond well with Leclerc et al. (1990) who also identified a decrease of shear generation with

increasing stability parameter z/L. They even observed that mechanical shear was a very weak sink of TKE under very stable conditions. This indicates that TKE is converted back into mean kinetic energy during stable regimes.

While the influence of atmospheric stability on mechanical shear was mostly limited to the top of the canopy, the buoyancy terms seemed to be sensitive to atmospheric conditions throughout the whole canopy. Buoyancy production had the largest magnitude and was increasingly important with increasing canopy height under unstable conditions with the greatest positive value of 4.5x10^{-3} m^2s^{-3} at the canopy top of the dense forest and 5.1x10^{-3} m^2s^{-3} in the top layer of the open pine forest (see Figure 5.3.1, Figure 5.3.2). The buoyancy term is known to contribute to the production of TKE in a forest canopy under the unstable regime (Leclerc et al., 1990). That buoyancy term is occasionally a sink for TKE under unstable regimes and a source under stable conditions (Leclerc et al., 1990) could not be observed in this study. So there is apparently no heat flux within the canopy opposite the one at the canopy top. Instead the buoyancy production increased nearly linear towards the top of the dense forest in the unstable regime. Under neutral conditions the buoyancy term was small and leveled around zero, but showed a slight increase towards the top of the canopy with a mean of 1.5x10^{-4} m^2s^{-3} at the top of the dense canopy. In the sparse Ponderosa pine forest the mechanical shear was a small source for TKE in the whole canopy increasing slightly towards the top with a mean of 5.010^{-4} m^2s^{-3} (see Figure 5.3.2). This was perhaps caused by the relatively low net radiation under neutral conditions. Leclerc et al. (1990) also observed a very small buoyancy production under neutral regime. Stable conditions led to a negative buoyancy term, which further decreased with increasing canopy height in both forests (see Figure 5.3.1 and Figure 5.3.2). This supports former findings by Leclerc et al. (1990). Stable conditions occur mostly at night, when the buoyancy term is typically a sink for TKE. No matter what sigh the buoyancy term has it contributes significantly to the TKE budget for all dynamic stability regimes. In contrast to that, in a twenty year old pine forest the buoyancy term under different stability conditions was so small in comparison with the other TKE terms that it was neglected (Lesnik, 1974). Buoyancy production here may be relatively small under neutral conditions, but during the day in the unstable regime it was a major source and during nighttime under stable conditions it was an important sink for TKE.

Turbulent transport was sensitive to atmospheric stability in the upper two layers of the forest, but the differences were most distinct in upper portion of the canopy. The stable regime caused the lowest turbulent transport term in all layers of both

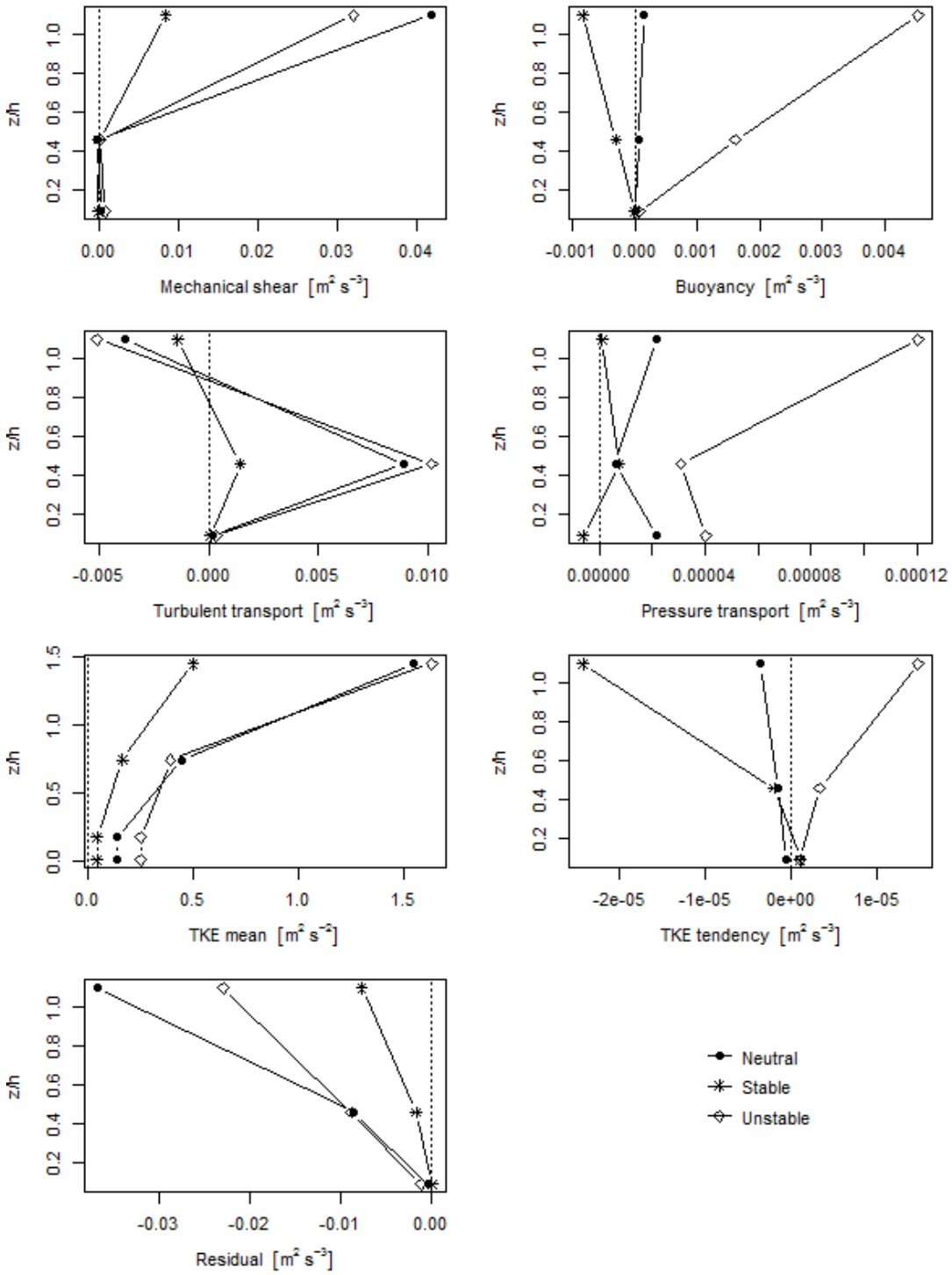

FIGURE 5.3.1: Vertical profile of the TKE terms of the dense forest under different stability regimes. The symbols indicate the mean of the respective layer and are located at the midpoint of each layer. The filled circles (•) represent the neutral, the asterisk (∗) the stable and the open diamonds (◇) stand for the unstable regime. Measurement height z is normalized by the canopy height h.

forests, whatever the sign of the term was (see Figure 5.3.1, Figure 5.3.2). Nevertheless, even under stable conditions turbulent transport of TKE still occurred within the canopy, in contrast to what Leclerc et al. (1990) found. Turbulent transport in the canopy layer were very similar, but highest for unstable conditions followed by near-neutral conditions in the dense canopy (see Figure 5.3.1). In the sparse forest the turbulent transport was higher under neutral conditions, followed by the unstable regime (see Figure 5.3.2). The LES results of Dwyer et al. (1997) were also sensitive to atmospheric stability. At near-neutral conditions the source within the canopy and the sink above the crown were almost equal, besides opposite in sign. Here it was observed that the source in the canopy layer of the dense forest was about twice as high with a mean of 1.0x10^{-2} m^2s^{-3} compared to the sink at the canopy top with a value of -5.1x10^{-3} m^2s^{-3} (see Figure 5.3.1). The sparse pine stand showed a similar pattern (see Figure 5.3.2). With increasingly unstable conditions it is expected that the source within the tree crown attenuates, while the sink at the top of the canopy became more negative like it did in the LES of Dwyer et al. (1997). Consistent with the results of this study Leclerc et al. (1990) identified turbulent transport as a source for TKE within the canopy for all three stability regimes, but the turbulent transport was only a sink at the of the canopy for stable and unstable conditions. They also found that the largest flux of turbulent transport occurred at thermally unstable conditions.
All in all, the turbulent transport was more distinct under neutral and unstable conditions and was only of minor importance in the stable regime. Nevertheless, under all stability regimes the turbulent transport term showed a maximum in the canopy layer and a minimum at the top of the canopy.

The third hypothesis stated that pressure transport is most important under unstable or free-convective conditions. The influence of dynamic stability on the pressure transport term was, in contrast to the other TKE budget terms, also very distinct in the subcanopy layer of the dense forest (see Figure 5.3.1). For neutral and unstable regimes, the pressure transport term decreased from the subcanopy to the canopy layer and then increased again towards the top of the canopy of the Norway spruce forest. Under stable conditions pressure transport showed a reverse pattern with an increase from the surface to the canopy layer and then a decrease again towards the top of the dense forest. The pressure transport was most important under unstable conditions with a mean at the canopy top of 1.2x10^{-4} m^2s^{-3} compared to 2.1x10^{-5} m^2s^{-3} under neutral and 8.6x10^{-7} m^2s^{-3} under the stable regime (see Figure 5.3.1)). This result supports the predictions of

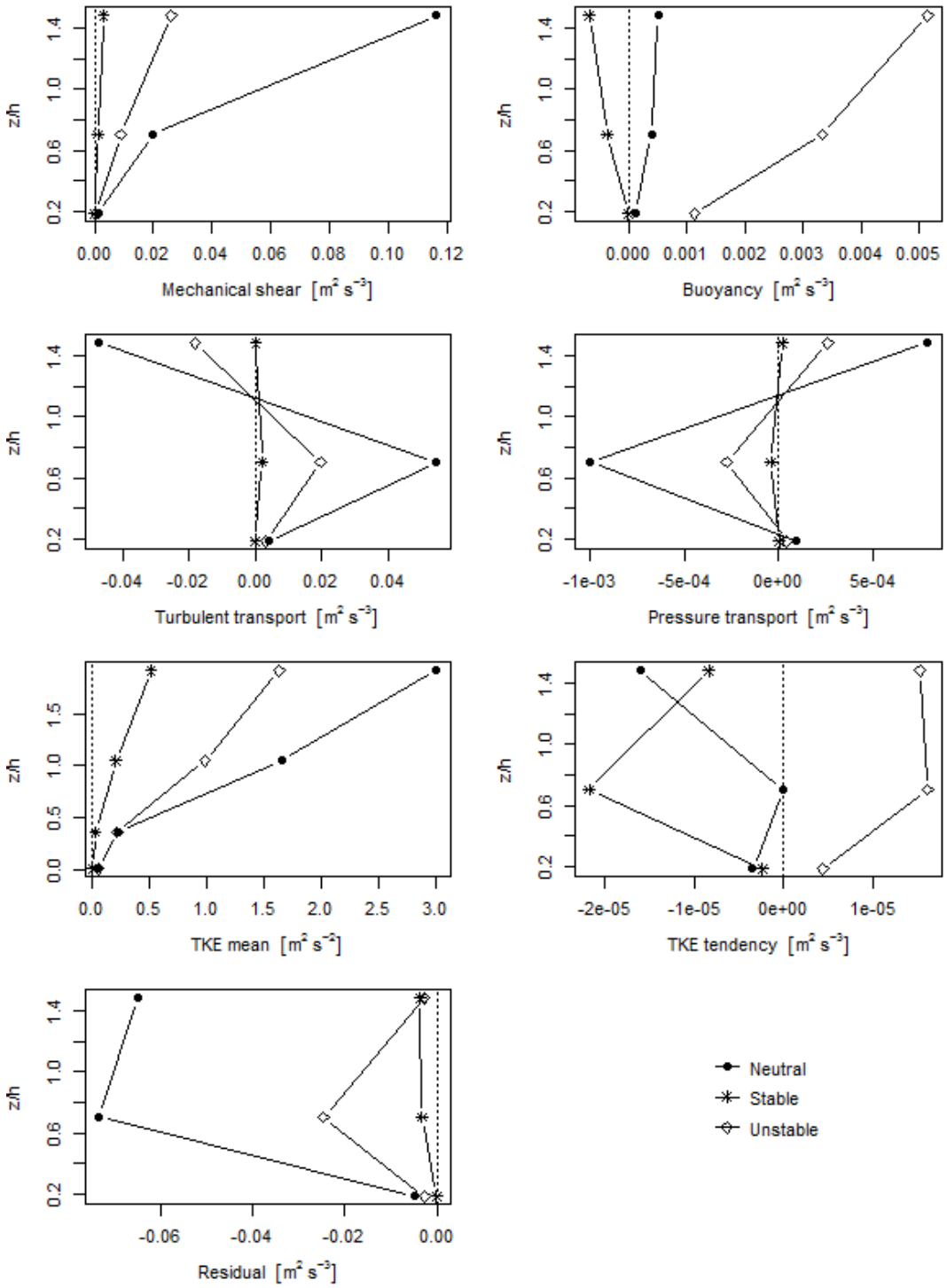

FIGURE 5.3.2: Vertical profile of the TKE terms of the sparse forest under different stability regimes. The symbols indicate the mean of the respective layer and are located at the midpoint of each layer. The filled circles (•) represent the neutral, the asterisk (∗) the stable and the open diamonds (◇) stand for the unstable regime. Measurement height z is normalized by the canopy height h.

Dwyer et al. (1997) who found in their LES that pressure transport gets more important with increasing atmospheric instability. The results for pressure transport across the sparse forest were contradicting though. The pressure transport was highest under the neutral regime with 9.2x10^{-5} m^2s^{-3} in the subcanopy, -1.0x10^{-3} m^2s^{-3} in the canopy layer and 7.9x10^{-4} m^2s^{-3} at the canopy top, followed by the pressure transport term under unstable stratification with 2.6x10^{-4} m^2s^{-3} in the subcanopy, -2.7x10^{-4} m^2s^{-3} within the canopy and 2.6x10^{-4} m^2s^{-3} above the sparse crown (see Figure 5.3.2). So all in all, the hypothesis that pressure transport is largest under convective conditions can only be accepted partly and the canopy architecture has to be considered in every case.

Generally, the residual decreased with increasing height in the dense forest and the residual term was largest at the canopy top (see Figure 5.3.1), whereas in the sparse pine forest the residuum was larger in the canopy layer (see Figure 5.3.2). The residual is quite similar in the subcanopy layer, still it is slightly higher under stable conditions. In the canopy layer the differences between the dynamic stability regimes got more distinct in both forests. The residuum under near-neutral and unstable conditions were almost equal and much more negative than under the stable regime of the dense forest, but showed a large difference between the stability regimes in the open pine stand. At the top of the canopy the differences between the three regimes have been largest at both forest sites. The stable regime had the lowest residuum with -7.7x10^{-3} m^2s^{-3} at the top of the canopy, followed by the residuum under unstable conditions with -2.3x10^{-2} m^2s^{-3} and the residual term of the near-neutral regime, which was around five times higher with -3.7x10^{-2} m^2s^{-3} than the value under stable conditions (see Figure 5.3.1). In comparison to that the residual was largest under neutral regime in the canopy layer with -7.3x10^{-2} m^2s^{-3}, followed by -2.5x10^{-2} m^2s^{-3} under unstable stratification and -3.4x10^{-3} m^2s^{-3} under stable conditions. The residual of a sparse deciduous forest in a study of Leclerc et al. (1990) showed a different pattern with the highest residual under stable regime, while under unstable and neutral conditions the residual was only one-third of the magnitude of the stable regime. However, the pressure transport was included in their residual, so the results are difficult to compare.

The mean turbulence kinetic energy is already dependent on dynamic stability in the subcanopy. In the subcanopy, TKE is smallest under stable conditions, slightly higher for the neutral regime and even higher under unstable conditions of the dense forest (see Figure 5.3.1). Turbulence kinetic energy was steady in the subcanopy layer and then increased towards the canopy. In the sparse forest the differences between the dynamic stability regimes in the subcanopy were less

distinct (see Figure 5.3.2). Leclerc et al. (1990) also observed an increase from the surface to the canopy top. This increase was steepest for neutral conditions, which slightly exceeded the TKE of the unstable regime. At the top of the canopy the discrepancy between stable and the other two stability regimes got larger. TKE under stable conditions was lowest in the top of the canopy layer of the dense forest with 0.50 m^2s^{-2} (see Figure 5.3.1). The values of TKE at the canopy top were relatively similar with 1.55 m^2s^{-2} under near-neutral conditions and 1.63 m^2s^{-2} for the unstable regime. In the sparse forest the TKE was highest under the neutral regime with 3.0 m^2s^{-2}, followed by unstable conditions with 1.6 m^2s^{-2} (see Figure 5.3.2). The TKE was lowest in both forest under stable regime with a mean of 0.5 m^2s^{-2} for the dense and 0.5 m^2s^{-2} for the sparse forest, respectively. That the TKE is lower under stable conditions is comprehensive as the regime is characterized by low wind speeds and net radiation and so simply less turbulence is generated.

The TKE tendency was also influenced by dynamic stability of the atmosphere. Under near-neutral conditions the TKE tendency was smallest being slightly negative. There was also a slight decrease with increasing canopy height apparent for the neutral conditions reaching its minimum at the top of the canopy with -3.5x10^{-6} m^2s^{-3} (see Figure 5.3.2). The other stability regimes were affected more strongly by dynamic stability. Under unstable conditions the TKE tendency was always positive in the whole forest canopy and increased towards the top of the canopy reaching its maximum at 1.5x10^{-5} m^2s^{-3} (see Figure 5.3.1). The TKE tendency under stable conditions had the highest magnitude and was positive in the subcanopy of the dense forest (see Figure 5.3.1). In the upper region of the canopy the TKE tendency of the stable regime became negative and reached its minimum at -2.4x10^{-5} m^2s^{-3} (see Figure 5.3.1). The sparse forest showed a similar pattern concerning the sign of the TKE tendency, but differences were higher in the canopy layer (see Figure 5.3.2).

Dynamic stability of the atmosphere significantly influenced all TKE budget terms, the mean turbulence kinetic energy and the TKE tendency. Especially in the upper part of the forest canopy dynamic stability is an important factor that determines the characteristics of turbulence within the forest (see Figure 5.2.10a, Figure 5.2.10a). A reason for this observation is probably the turbulent fluxes are simply higher at the top of the canopy due to high wind speeds and large net radiation. The vertical distribution patterns were quite similar for each forest, but the magnitude differed strongly among the dynamic stability regimes.

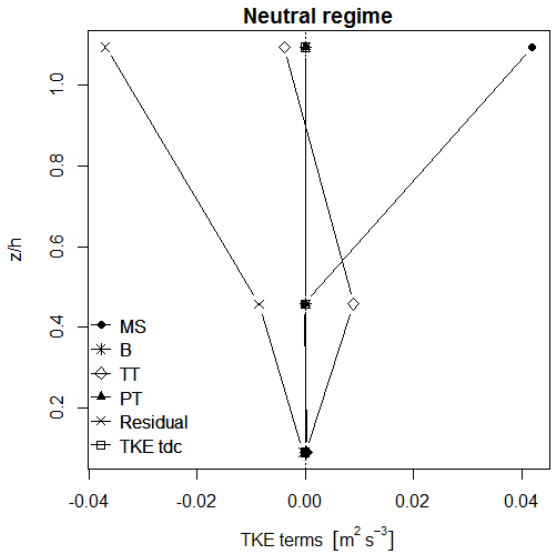

(A) Vertical profile of all TKE terms under neutral stratification.

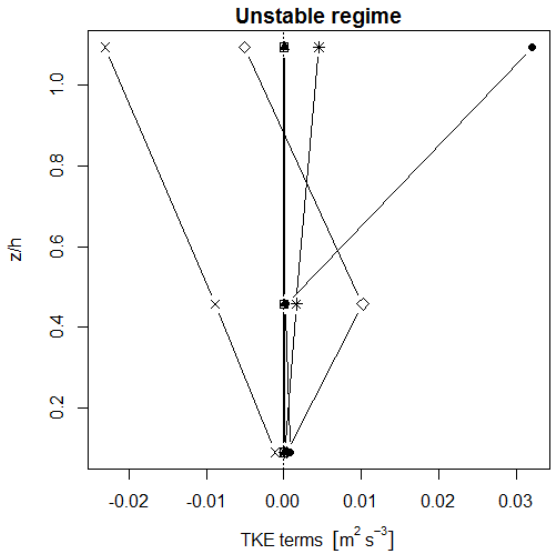

(B) Vertical profile of all TKE terms under unstable stratification.

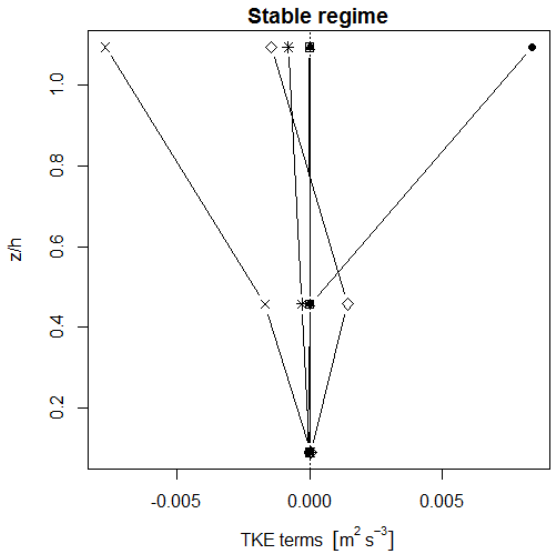

(C) Vertical profile of all TKE terms under stable stratification.

FIGURE 5.3.3: Vertical profile of all TKE budget terms of the dense forest. The legend in plot (A) is also valid for (B) and (C). Please note that the x-axis of the plots differ.

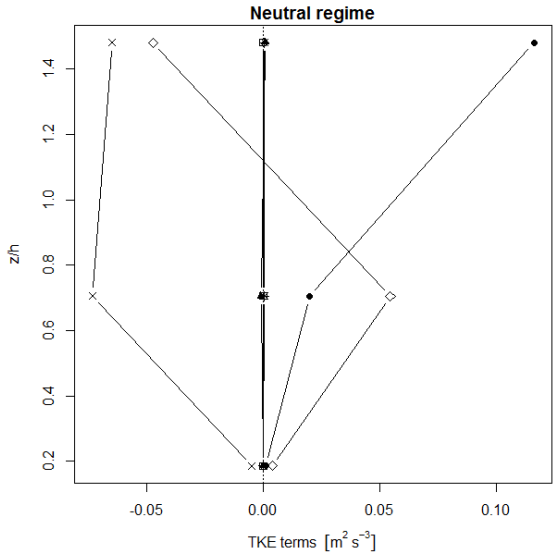

(A) Vertical profile of all TKE terms under neutral stratification.

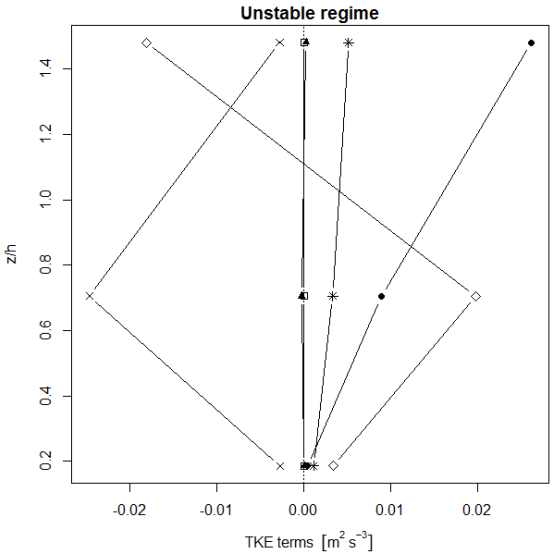

(B) Vertical profile of all TKE terms under unstable stratification.

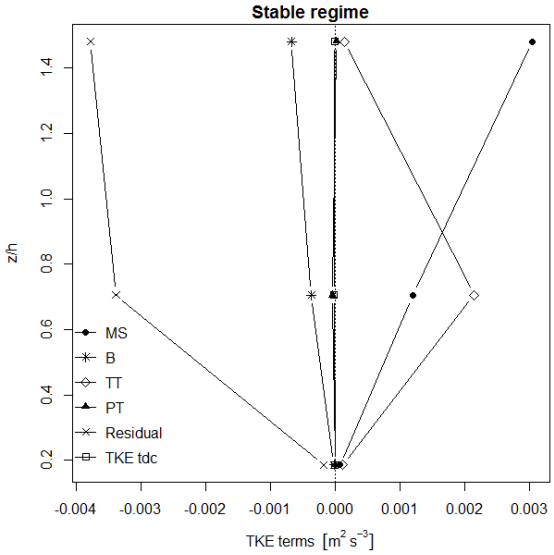

(C) Vertical profile of all TKE terms under stable stratification.

FIGURE 5.3.4: Vertical profile of all TKE budget terms of the sparse forest. The legend in plot (B) is also valid for (A) and (C). Please note that the x-axis of the plots differ.

5.4 Weak-wind and strong-wind regimes

Additionally to the three dynamic stability regimes, the influence of wind speed on the TKE budget was investigated. Two wind regimes were defined using the threshold of 0.6 $m\ s^{-1}$ applied to the subcanopy layer to distinguish between weak- and strong-winds. This was the threshold for the weak-wind conditions at the subcanopy layer identified by Tobias Wunder (see his master thesis on coherent structures in forest canopies for details). Mechanical shear is strongly driven by wind speed. This was evident for the vertical profile of the shear term. In the subcanopy and canopy layers the wind speeds are low due to the high foliage density of the crown. Therefore, the differences of the mechanical shear in the lower parts of the forest were only low (see Figure 5.4.1). In contrast to that the difference due to wind regime in the top of the canopy layer was massive. Under the strong-wind regime the mean at the canopy top was 5.5x10^{-2} m^2s^{-3} compared to 2.0x10^{-2} m^2s^{-3} under weak-wind conditions.

The buoyancy term was also influenced by wind regime, especially in the upper parts of the forest canopy (see Figure 5.4.1). In the subcanopy the differences of buoyancy production were relatively low. This is due to the dense tree crown, which prevents the wind from mixing the subcanopy space and thereby allows the development of buoyant motions. So overall the wind regime is only of minor important in the trunk space, as was expected for this dense canopy. In the upper canopy the buoyancy term under strong winds increased almost linearly with height reaching 2.0x10^{-3} m^2s^{-3} at the top of the canopy. Under weak-wind conditions the buoyancy production showed also a nearly-linear increase towards the top of the canopy with a maximum value of 1.3x10^{-3} m^2s^{-3}. The low wind speeds within the crown due to the high foliage density of the Norway spruce forest inhibit the mixing of the canopy layer and lead to a maximum above tree crown for both wind regimes. Besides, independent of the wind regime the net radiation is naturally highest at the canopy top.

Turbulent transport was also influenced by wind speed in the upper part of the canopy. The two wind regimes showed generally the same vertical distribution pattern with a positive turbulent transport term in the canopy and a negative one at the top of the canopy, but the magnitude of turbulent transport varied depending on the wind regime (see Figure 5.4.1). Strong wind speeds led to a higher turbulent transport compared to the weak-wind regime in the canopy and top of the canopy layer. In the subcanopy the effect due to wind speed was apparently weaker. This is clearly due to the high foliage density for the

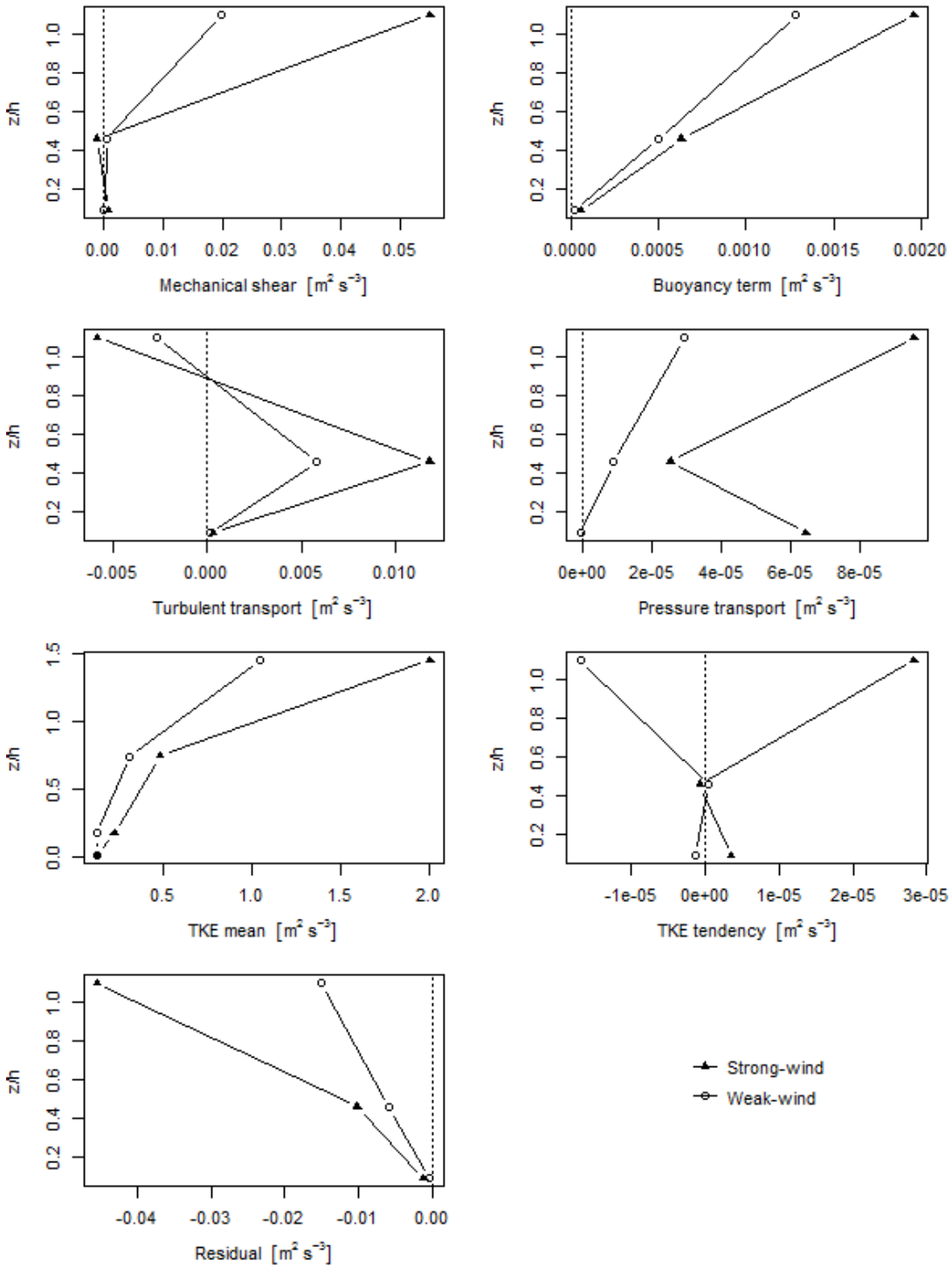

FIGURE 5.4.1: Vertical profile of the TKE terms across different wind regimes. The threshold = 0.6 $m\ s^{-1}$ was only applied to the subcanopy layer in this scenario. The symbols indicate the mean of the respective layer and are located at the midpoint of each layer. The filled triangles (▲) represent the strong-wind conditions and the open circles (○) stand for the weak-wind regime. Measurement height z is normalized by the canopy height h.

Norway spruce crown, which decouples the subcanopy of the dense forest from the influence of wind speed. Turbulent transport was largest in the canopy layer with a mean of 1.2x10^{-2} m^2s^{-3} under the strong-wind regime. At the top of the canopy the turbulent transport was negative with a value of -3.9x10^{-3} m^2s^{-3} for the strong-wind regime compared to a value at the canopy top of 5.8x10^{-3} m^3s^{-3}. Apparently, stronger wind lead to a more distinct downward transfer of TKE from the canopy top into the canopy layer.

Pressure transport was strongly dependent on the wind speed at all heights of the forest canopy (see Figure 5.4.1). Under weak-wind conditions the pressure transport term was slightly negative in the subcanopy, then the magnitude of the pressure transport increased almost linearly with height. The maximum value was reached at the canopy with a mean of 2.9x10^{-5} m^2s^{-3}. The pattern under strong wind speeds was very different from the weak-wind regime. The highest pressure transport was observed at the top of the canopy with 9.6x10^{-5} m^2s^{-3}, then the pressure transport term decreased in the canopy layer to a value of 2.6x10^{-5} m^2s^{-3}. Towards the subcanopy space pressure transport strongly increased again to 6.5x10^{-5} m^2s^{-3}. The pressure transport under the strong-wind conditions exceeded at all levels of the canopy the values of the weak-wind regime. Dupont et al. (2012) found in contrast to the findings of this study that pressure transport in their LES was a source within the crown layer of their sparse pine forest and a sink above the crown. It it interesting however that the vertical profiles of the two wind regimes are quite similar to the vertical distribution of the pressure transport in the sparse pine forest. This indicates that the influence of the forest architecture on the wind regime directly influences the vertical profile of pressure transport.

The residuum was also sensitive for the wind speed. Under weak-wind conditions the residuum was almost zero in the subcanopy and further decreased until it reached its minimum in the top of the canopy layer with -1.5x10^{-2} m^2s^{-3} (see Figure 5.4.1). For the strong-wind regime the residuum term was also decreasing with increasing height being negative throughout the whole canopy, but the magnitude was greater. The minimum value was reached at the top of the canopy with -4.6x10^{-2} m^2s^{-3}. As the other terms of the TKE budget are greater during the strong-wind regime, it is only comprehensive that the residuum term is also larger because it compensates for the other TKE terms.

The mean turbulence kinetic energy was strongly influenced by wind regime. Except for the subcanopy layer, where the magnitude of TKE was similar for

both regimes, the TKE was always greater under strong-wind conditions (see Figure 5.4.1). Nelson et al. (2007) also found that the turbulence intensity increases with higher wind speeds. This is logical as strong winds lead to higher mechanical shear, buoyancy and turbulent transport, which are the most important sources for TKE in this forest canopy. Under both wind regimes the TKE increased from the subcanopy to the canopy top. The weak-wind regime showed a steeper increase, but the maximum value reached at the top of the canopy was relatively low with 1.0 m^2s^{-2}. The TKE under strong-wind conditions increased slower, but eventually a peak of 2.0 m^2s^{-2} was reached, which was twice as high as the turbulence kinetic energy under weak-wind conditions.

The wind regime influenced also the TKE tendency, which showed completely different patterns for weak- and strong-winds, respectively. Under weak-wind conditions the TKE tendency was negative in the subcanopy and top of the canopy layer and was slightly positive in the canopy layer. It increased towards the canopy and then decreased again towards the canopy top. The minimum that was eventually reached at the top of the canopy with -1.7x10^{-5} m^2s^{-3}. The strong-wind regime was in contrast to that positive in the subcanopy and top of the canopy and negative in the canopy layer. The TKE tendency decreased from the subcanopy to the canopy layer and increased from there on towards the top of the canopy reaching its maximum at 2.8x10^{-5} m^2s^{-3}. The vertical profiles of the TKE tendency dependent on the wind regime were mirror-inverted. These differences of TKE tendency dependent on the wind regime indicate that under weak-winds the sources for TKE are underestimated, while the sinks appear to be underestimated for the strong-wind regime.

5.5 Evaluation of methods and outlook

Field studies like the INTRAMIX experiment are always valuable as they show the actual physical properties of the turbulent flow and are not dependent on our expectations like simulations and models are. This is especially important for quantities whose role is still unclear like the pressure transport term. Still, there are of course problems as well. One error source in field studies are the instruments due to wrong calibration, drifting or specific limitations of the instrument lead to measurement errors. Pressure sensor P4 was e.g. only sampled at 10 Hz

instead of 20 Hz due to data logger limitations. This led to frequent data gaps as the sensor had to be connected via RS232 at a lower sample frequency. But as mainly the pressure transport in the atmospheric layers within and directly above the forest were of interest, this discontinuity in the data was accepted to guarantee a reliable GPS signal for all fast-response sensors. The open-path sonic anemometers, which were used for this study, have for example the problem that they do not measure correctly when it rains. During the measurement period, occasional thunderstorms with heavy rainfalls took place, which certainly inhibited the performance of the sensor head. Additionally, some sensors were placed in the canopy, where maybe obstacles like branches or leaves may have blocked the measurement path of the sensor head resulting in unreasonable measurements. To evaluate the influence of the type of sensor comparable measurements have to be made with different types of sensors.
But not only the type of sensor, also the placement of the sensors influences the turbulent flow measured. Turbulence is very heterogeneous on a spatial and temporal scale and appears on very small scales, so the placement of the instruments influences what is measured. For example, differences in the structure of the crown or understory vegetation change the airflow and turbulence motions and thereby create artefacts (Leclerc et al., 1990). Even sites that appear to be quite similar regarding their physical properties can show significant differences in the measured fluxes as Vickers and Thomas (2013) demonstrated impressively when they studied the heterogeneity of subcanopy fluxes. In the INTRAMIX experiment, therefore three subcanopy stations were established at different types of understory vegetation to account for spatial heterogeneity. Tobias Wunder will look upon heterogeneity of measurements due to differences in understory structure. In future studies the heterogeneity of the pressure transport within the subcanopy could be studied. To overcome difficulties with temporal heterogeneity, the 20Hz measurements were averaged in 30 minute periods. All these errors contribute to the dissipation term of the TKE budget, which could not be measured directly and is therefore estimated as a residual. Therefore, the viscous dissipation has to be interpreted with additional care and under reserve.

This master thesis was the first experimental evaluation of the pressure transport term, so understandably more studies on the properties of the pressure transport and its importance to the TKE budget have to be done to fully understand turbulence kinetic energy. Moreover, different ecosystem and vegetation types have to be investigated to understand the influence of vegetation and surface roughness for the TKE budget equation. As the forest architectures seems to play a major

role on the TKE budget, it would be valuable to investigate a broad range of forest types to determine the role of foliage distribution and stand density. Here two coniferous forests were investigated, so it would be interesting what role the pressure transport plays in deciduous forests. Broad-leaved forests are known to have a different foliage distribution where 75% of the leaves are concentrated in the upper 20% of the canopy at around z/h = 0.85 and the extent of the canopy is less great than in a needle leaf forest (Hutchison et al., 1986). Several studies for deciduous forests (Gao et al., 1989; Meyers and Baldocchi, 1991) and tropical forests (Thompson and Pinker, 1975) confirm this structural feature. It would be interesting how the extensive trunk space influences the pressure transport term. It is expected that gradient of first-, second-, and third-order velocity moments are very large in deciduous canopies (Meyers and Baldocchi, 1991). Dwyer et al. (1997) proposed based on a LES that above 1.3 times the canopy height turbulent transport and pressure transport are opposed to each other and reverse sign at twice the canopy height. So it may be also interesting for future studies to accurately measure pressure perturbations well above the forest canopy.

6. Summary and conclusion

The INTRAMIX experiment was conducted to examine the relevance of the pressure transport term to the TKE budget of forest ecosystems. Therefore, a set-up of 12 fast-response sensors was established in a mountainous central European Norway spruce forest, which measured wind speed and direction, static pressure perturbations, temperatures, CO_2 and water vapor concentrations. The results revealed that the pressure transport term was of the same magnitude throughout the whole dense forest canopy, but was especially important in the subcanopy layer, while in the canopy and above the crown it is of only minor importance. In the top of the canopy mechanical shear and buoyancy production were the dominant sources for TKE, while turbulent transport and the residual term were the major sink terms. Turbulent transport and the buoyancy term were the dominant sources for TKE in the underlying canopy layer and the residuum was the major sink there. In the subcanopy of the dense forest mechanical shear was interestingly the largest source due to a second wind maximum, followed by turbulent transport. Buoyancy and pressure transport were also small sources for TKE in the subcanopy layer. Besides the differences between the canopy layers, pressure transport is a continuous source of TKE throughout the whole forest canopy during the day and a slight sink at night at the dense Norway spruce forest.
The pressure transport in the sparse Ponderosa Pine forest was in contrast to that a source term for TKE in the top of the canopy and subcanopy layer, but was a sink within the canopy. This indicates that TKE is exported from the canopy layer into the top of the canopy and subcanopy. Nonetheless, the pressure transport was less important in the sparse forest canopy due to the high magnitude of the remaining TKE terms. These distinct differences between the forests show clearly that forest architecture significantly influences the TKE budget.
Dynamic stability had also a great impact on the TKE budget and especially on the pressure transport term. Pressure transport was largest under unstable atmospheric conditions in the dense forest being a source for TKE, while under near-neutral or stable conditions the pressure transport term was slightly positive

or negative, respectively. In the Ponderosa pine forest pressure transport was in contrast to that largest under the neutral regime, followed by the unstable conditions. Pressure transport showed a minimum in the canopy layer and a maximum at the top of the canopy for all stability regimes.
Under weak-winds less than 0.6 m s-1 the pressure transport increased with canopy height, while for the strong-wind regime pressure transport showed a minimum in the canopy layer. The pattern pressure transport under the strong-wind regime was remarkably similar to vertical profile of pressure transport in the sparse pine forest indicating that the differences of the pressure transport term were mainly caused by the influence of the respective forest architecture on wind speeds in the canopy. In the sparse pine forest higher wind speeds occurred leading to the sink of pressure transport within the canopy that was also observed for the strong-wind regime.

Acknowledgements

I want to thank my supervisor Prof. Dr. Christoph Thomas for his valuable input and continuous help with writing this master thesis. I also thank Dr. Wolfgang Babel for helping with his expertise whenever it came to software problems and troubleshooting with instrumentation or R. I'm thanking Tobias Wunder for the good collaboration during our experiment and the countless hours we spent in 032. My thanks also go to Johannes Olesch who helped us with the preparation and setup of the field experiment. Last but not least, I want to thank my lecturers for valuable discussions and feedback on my master thesis.

Bibliography

American Meteorological Society. virtual potential temperature, 2017. URL http://glossary.ametsoc.org/wiki/Virtual_potential_temperature.

B. D. Amiro. Comparison of turbulence statistics within three boreal forest canopies. *Boundary-Layer Meteorology*, 51(1-2):99–121, 1990. ISSN 0006-8314. doi: 10.1007/BF00120463.

D. Anfossi, D. Oettl, G. Degrazia, and A. Goulart. An analysis of sonic anemometer observations in low wind speed conditions. *Boundary-Layer Meteorology*, 114(1):179–203, 2005. ISSN 00068314. doi: 10.1007/s10546-004-1984-4.

D. Baldocchi and B. A. Hutchison. Turbulence in an almond orchard: Vertical variations in turbulent statistics. *Boundary-Layer Meteorology*, (40):127–146, 1987. ISSN 00068314.

BayCEER. Bayceer: Forschung und lehre: De-bay: Waldstein-weidenbrunnen (de-bay), 2011. URL https://www.bayceer.uni-bayreuth.de/bayceer/de/forschung/proj/m_detail.php?id_obj=78292.

Y. Brunet, J. J. Finnigan, and M. R. Raupach. A wind tunnel study of air flow in waving wheat: Single point velocity measurements. *Boundary-Layer Meteorology*, (70):95–132, 1994. ISSN 00068314.

Bundesamt für Kartographie und Geodäsie. Karte der fichtelgebirgsregion in oberfranken, deutschland., 2005.

G. Burba, D. K. McDermitt, Grelle Achim, and Anderson Daniel J. : Addressing the influence of instrument surface heat exchange on the measurements of co 2 flux. *Global Change Biology*, 14(8):1854–1876, 2008. ISSN 13541013.

A. Christen, M. Rotach, and R. Vogt, editors. *Experimental determination of the turbulent kinetic energy budget within and above an urban canopy*, 2004.

A. Christen, M. W. Rotach, and R. Vogt. The budget of turbulent kinetic energy in the urban roughness sublayer. *Boundary-Layer Meteorology*, 131(2):193–222, 2009. ISSN 0006-8314. doi: 10.1007/s10546-009-9359-5.

R. M. Cionco. Intensity of turbulence within canopies with simple and complex roughness elements. *Boundary-Layer Meteorology*, 2(4):453–465, 1972. ISSN 0006-8314. doi: 10.1007/BF00821548.

S. Dupont, M. R. Irvine, J.-M. Bonnefond, E. Lamaud, and Y. Brunet. Turbulent structures in a pine forest with a deep and sparse trunk space: Stand and edge regions. *Boundary-Layer Meteorology*, 143(2):309–336, 2012. ISSN 0006-8314. doi: 10.1007/s10546-012-9695-8.

M. J. Dwyer, E. G. Patton, and R. H. Shaw. Turbulent kinetic energy budgets from large-eddy simulation of airflow above and within a forest canopy. *Boundary-Layer Meteorology*, 84(1):23–43, 1997. ISSN 00068314. doi: 10.1023/A:1000301303543.

R. Eigenmann, S. Metzger, and T. Foken. Generation of free convection due to changes of the local circulation system. *Atmospheric Chemistry and Physics*, 9 (21):8587–8600, 2009. ISSN 1680-7324. doi: 10.5194/acp-9-8587-2009.

J. Finnigan. Turbulence in plant canopies. *Annual Review of Fluid Mechanics*, 32 (1):519–571, 2000. ISSN 0066-4189. doi: 10.1146/annurev.fluid.32.1.519.

T. Foken. 50 years of the monin–obukhov similarity theory. *Boundary-Layer Meteorology*, 119(3):431–447, 2006. ISSN 0006-8314. doi: 10.1007/s10546-006-9048-6.

T. Foken and K. Staudt. Documentation of reference data for the experimental areas of the bayreuth cenre for ecology and environmental reesearch (bayceer) at the waldstein site, 2007. URL https://epub.uni-bayreuth.de/625/1/ARBERG035.pdf.

W. Gao, R. H. Shaw, and K. T. Paw U. Observation of organized structure in turbulent flow within and above a forest canopy. In R. E. Munn, editor, *Boundary Layer Studies and Applications*, pages 349–377. Springer Netherlands, Dordrecht, 1989. ISBN 978-94-010-6928-1. doi: 10.1007/978-94-009-0975-5{\textunderscore}22.

M. Giometto, A. Christen, J. Fang, and M. B. Parlange. Large-eddy simulations to characterize the role of turbulent and dispersive production, transport and dissipation of tke over and within a realistic urban canopy. *International Association For Urban Climate*, 2015.

B. A. Hutchison, D. R. Matt, R. T. McMillen, L. J. Gross, S. J. Tajchman, and J. M. Norman. The architecture of a deciduous forest canopy in eastern

tennessee, u.s.a. *The Journal of Ecology*, 74(3):635, 1986. ISSN 00220477. doi: 10.2307/2260387.

M. Y. Leclerc, R. H. Shaw, G. D. Hartog, and H. H. Neumann. The influence of atmospheric stability on the budgets of the reynolds stress and turbulent kinetic energy within and above a deciduous forest. *Journal of Applied Meteorology*, 29(9):916–933, 1990. ISSN 0894-8763. doi: 10.1175/1520-0450(1990)029{\textless}0916:TIOASO{\textgreater}2.0.CO;2.

X. Lee, W. Massman, and B. Law, editors. *Handbook of Micrometeorology*. Atmospheric and Oceanographic Sciences Library. Kluwer Academic Publishers, Dordrecht, 2005. ISBN 1-4020-2264-6. doi: 10.1007/1-4020-2265-4.

B. J. Legg and J. L. Monteith. Heat and mass transfer within plant canopies. *Heat and Mass Transfer in the Biosphere*, pages 167–186, 1975.

G. E. Lesnik. Results of measurement of turbulent energy balance components in a layer vegetation. *Atmospheric and Oceanic Physics*, (10):625–655, 1974.

H. Liu, G. Peters, and T. Foken. New equations for sonic temperature variance and buoyancy heat flux with an omnidirectional sonic anemometer. *Boundary-Layer Meteorology*, 100(3):459–468, 2001. ISSN 00068314. doi: 10.1023/A:1019207031397.

L. Mahrt. Weak-wind mesoscale meandering in the nocturnal boundary layer. *Environmental Fluid Mechanics*, 7(4):331–347, 2007. ISSN 1567-7419. doi: 10.1007/s10652-007-9024-9.

T. Maitani and T. Seo. Estimates of velocity-pressure and velocity-pressure gradient interactions in the surface layer over plant canopies. *Boundary-Layer Meteorology*, 33(1):51–60, 1985. ISSN 0006-8314. doi: 10.1007/BF00137035.

E. Matzner. *Biogeochemistry of forested catchments in a changing environment: A German case study*, volume volume 172 of *Ecological studies*. Springer, Berlin and New York, 2004. ISBN 3642059007.

G. A. Mcbean and J. A. Elliott. The vertical transports of kinetic energy by turbulence and pressure in the boundary layer. *Journal of the Atmospheric Sciences*, 32(4):753–766, 1975. ISSN 0022-4928. doi: 10.1175/1520-0469(1975)032{\textless}0753:TVTOKE{\textgreater}2.0.CO;2.

T. P. Meyers and D. D. Baldocchi. The budgets of turbulent kinetic energy and reynolds stress within and above a deciduous forest. *Agricultural and Forest*

Meteorology, 53(3):207–222, 1991. ISSN 01681923. doi: 10.1016/0168-1923(91)90058-X. URL https://nature.berkeley.edu/biometlab/pdf/Meyers%20+%20ddb%201991%20Agformet%20v53.pdf.

C. J. Moore. Frequency response corrections for eddy correlation systems. *Boundary-Layer Meteorology*, 37(1-2):17–35, 1986. ISSN 0006-8314. doi: 10.1007/BF00122754.

M. A. Nelson, E. R. Pardyjak, J. C. Klewicki, S. U. Pol, and M. J. Brown. Properties of the wind field within the oklahoma city park avenue street canyon. part i: Mean flow and turbulence statistics. *Journal of Applied Meteorology and Climatology*, 46(12):2038–2054, 2007. ISSN 1558-8424. doi: 10.1175/2006JAMC1427.1.

M. R. Raupach, P. A. Coppin, and B. J. Legg. Experiments on scalar dispersion within a model plant canopy part i: The turbulence structure. *Boundary-Layer Meteorology*, 35(1-2):21–52, 1986. ISSN 0006-8314. doi: 10.1007/BF00117300.

M. R. Raupach, J. J. Finnigan, and Y. Brunet. Coherent eddies and turbulence in vegetation canopies: The mixing-layer analogy. In J. R. Garratt and P. A. Taylor, editors, *Boundary-Layer Meteorology 25th Anniversary Volume, 1970-1995*, pages 351–382. Springer Netherlands, Dordrecht, s.l., 1996. ISBN 978-90-481-4740-3. doi: 10.1007/978-94-017-0944-6{\textunderscore}15.

R. H. Shaw. Secondary wind maxima inside plant canopies. *Journal of Applied Meteorology*, (16):514–521, 1977.

R. H. Shaw and X. J. Zhang. Evidence of pressure-forced flow in a forest. *Boundary-Layer Meteorology*, (58):47–64, 1992. ISSN 00068314.

R. H. Shaw, K. T. U Paw, X. J. Zhang, W. Gao, G. Den Hartog, and H. H. Neumann. Retrieval of turbulent pressure fluctuations at the ground surface beneath a forest. *Boundary-Layer Meteorology*, 50(1-4):319–338, 1990. ISSN 0006-8314. doi: 10.1007/BF00120528.

J. T. Sigmon, K. R. Knoerr, and E. J. Shaughnessy. Microscale pressure fluctuations in a mature deciduous forest. *Boundary-Layer Meteorology*, 27(4):345–358, 1983. ISSN 0006-8314. doi: 10.1007/BF02033744.

R. Stull and C. D. Ahrens. *Meteorology for scientists and engineers*. Brooks/Cole, Pacific Grove, Calif., 2. ed. edition, 2000. ISBN 0534372147.

O. E. Thompson and R. T. Pinker. Wind and temperature profile characteristics in a tropical evergreen forest in thailand. *Tellus*, 27(6):562–573, 1975. ISSN 0040-2826. doi: 10.3402/tellusa.v27i6.10184.

D. Vickers and L. Mahrt. Quality control and flux sampling problems for tower and aircraft data. *Journal of Atmospheric and Oceanic Technology*, 14(3):512–526, 1997. ISSN 0739-0572. doi: 10.1175/1520-0426(1997)014{\textless}0512:QCAFSP{\textgreater}2.0.CO;2.

D. Vickers and C. K. Thomas. Some aspects of the turbulence kinetic energy and fluxes above and beneath a tall open pine forest canopy. *Agricultural and Forest Meteorology*, 181:143–151, 2013. ISSN 01681923. doi: 10.1016/j.agrformet.2013.07.014.

J. M. Wilczak, S. P. Oncley, and S. A. Stage. Sonic anemometer tilt correction algorithms. *Boundary-Layer Meteorology*, 99(1):127–150, 2001. ISSN 00068314. doi: 10.1023/A:1018966204465.

N. R. Wilson and R. H. Shaw. A higher order closure model for plant canopies. *Journal of Applied Meteorology*, (16):1197–1205, 1977.

J. C. Wyngaard and O. R. Coté. The budgets of turbulent kinetic energy and temperature variance in the atmospheric surface layer. *Journal of the Atmospheric Sciences*, 28(2):190–201, 1971. ISSN 0022-4928. doi: 10.1175/1520-0469(1971)028{\textless}0190:TBOTKE{\textgreater}2.0.CO;2.

Appendix

Additional Tables

TABLE 6.0.1: Overview of the total number of 30-min intervals and percentage of the respective wind regime in all layer. The threshold is applied to each layer.2

Wind regime	**Number of 30-min intervals**	**Relative percentage**
Subcanopy		
Weak-wind	1668	0.64
Strong-wind	941	0.36
Canopy		
Weak-wind	1877	0.72
Strong-wind	731	0.28
Top of canopy		
Weak-wind	20	0.008
Strong-wind	2589	0.992

Additional Figures

FIGURE 6.0.1: Satellite station b) with sonic anemometer S6 at the location with low understory vegetation.

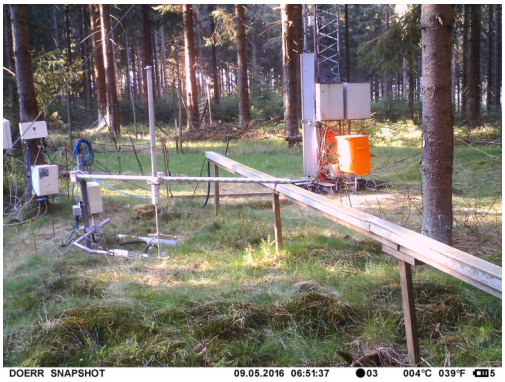

(A) Early morning around 07:00 after sunrise (photo: trail camera).

(B) Morning around 09:00 with full sun at the site (photo: trail camera).

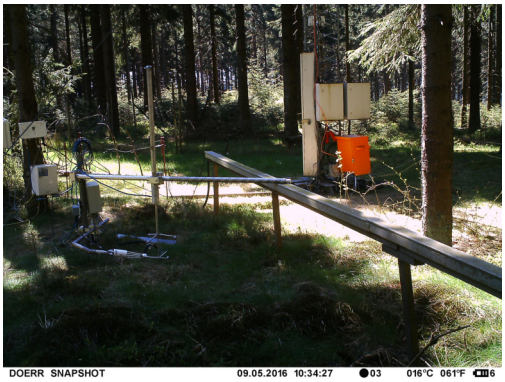

(C) Late morning around 11:00 with shading (photo: trail camera).

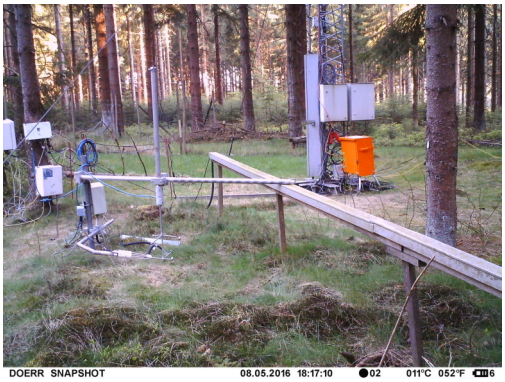

(D) Evening around 18:15 with indirect radiation (photo: trail camera).

FIGURE 6.0.2: Soil measurement complex from another point of view consisting of a USA-1, a Li-7500 and a pressure transducer within the soil. The different figures show the soil measurement complex at different times of day to illustrate the variability of net radiation in the subcanopy.

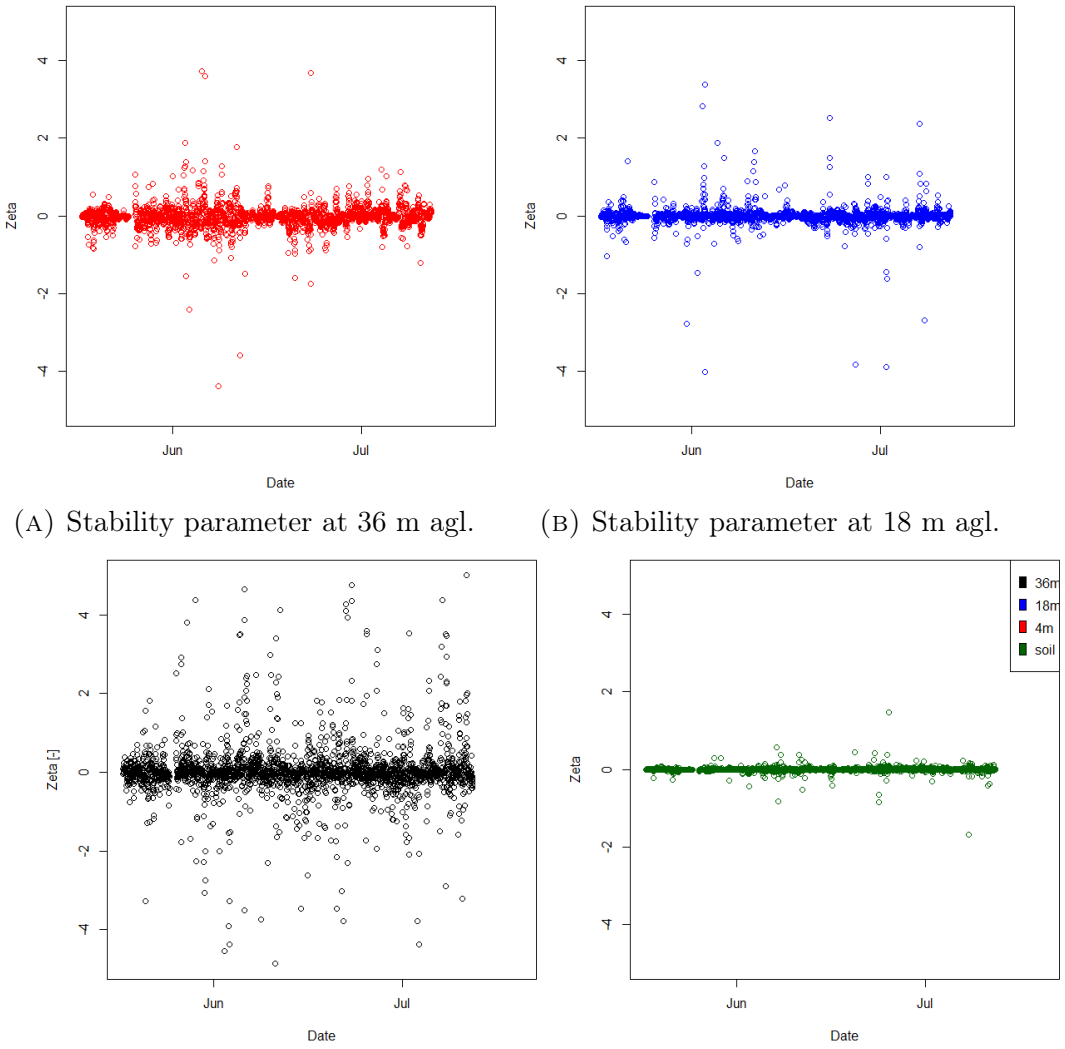

(A) Stability parameter at 36 m agl.

(B) Stability parameter at 18 m agl.

(C) Stability parameter at 4 m agl.

(D) Stability parameter at soil.

FIGURE 6.0.3: Time series of ζ four all four measurement heights of the dense Norway spruce forest.

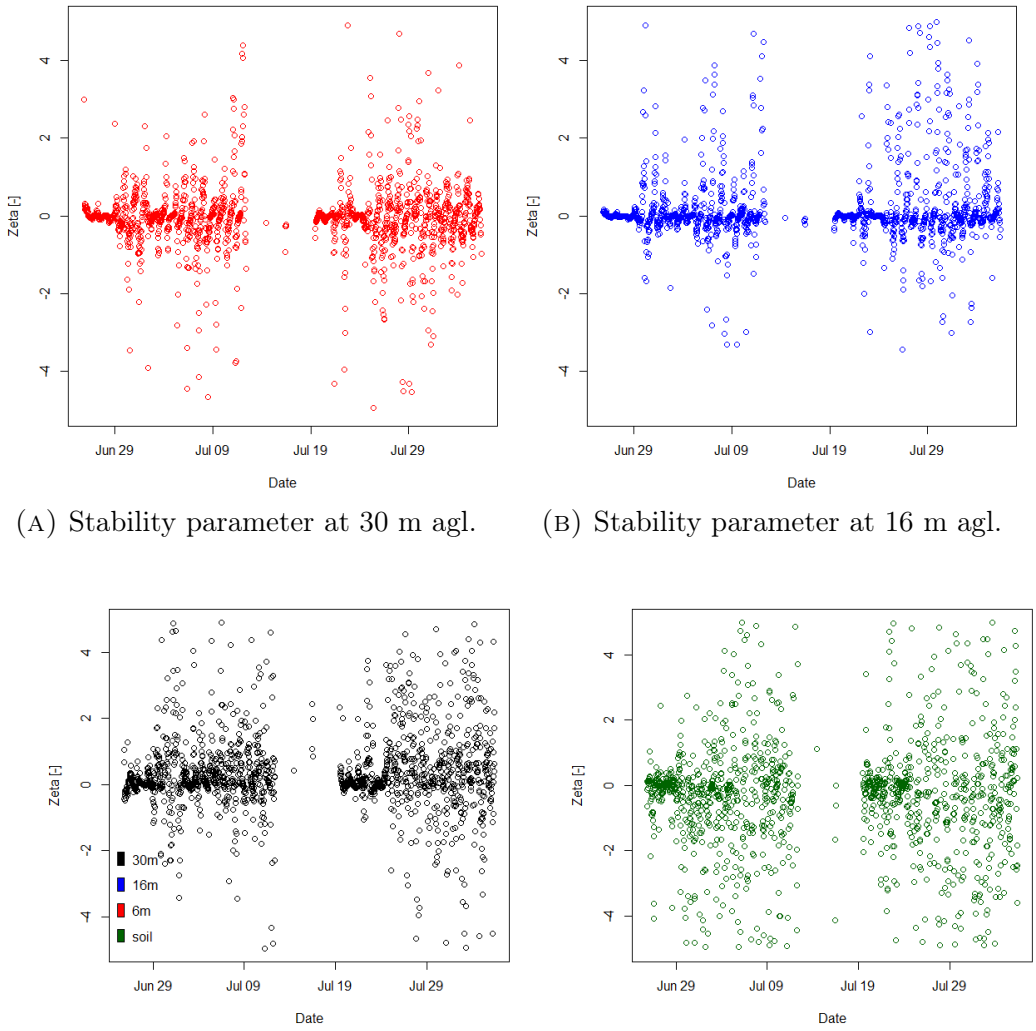

(A) Stability parameter at 30 m agl.

(B) Stability parameter at 16 m agl.

(C) Stability parameter at 6 m agl.

(D) Stability parameter at soil.

FIGURE 6.0.4: Time series of ζ four all four measurement heights of the sparse Ponderosa pine forest.

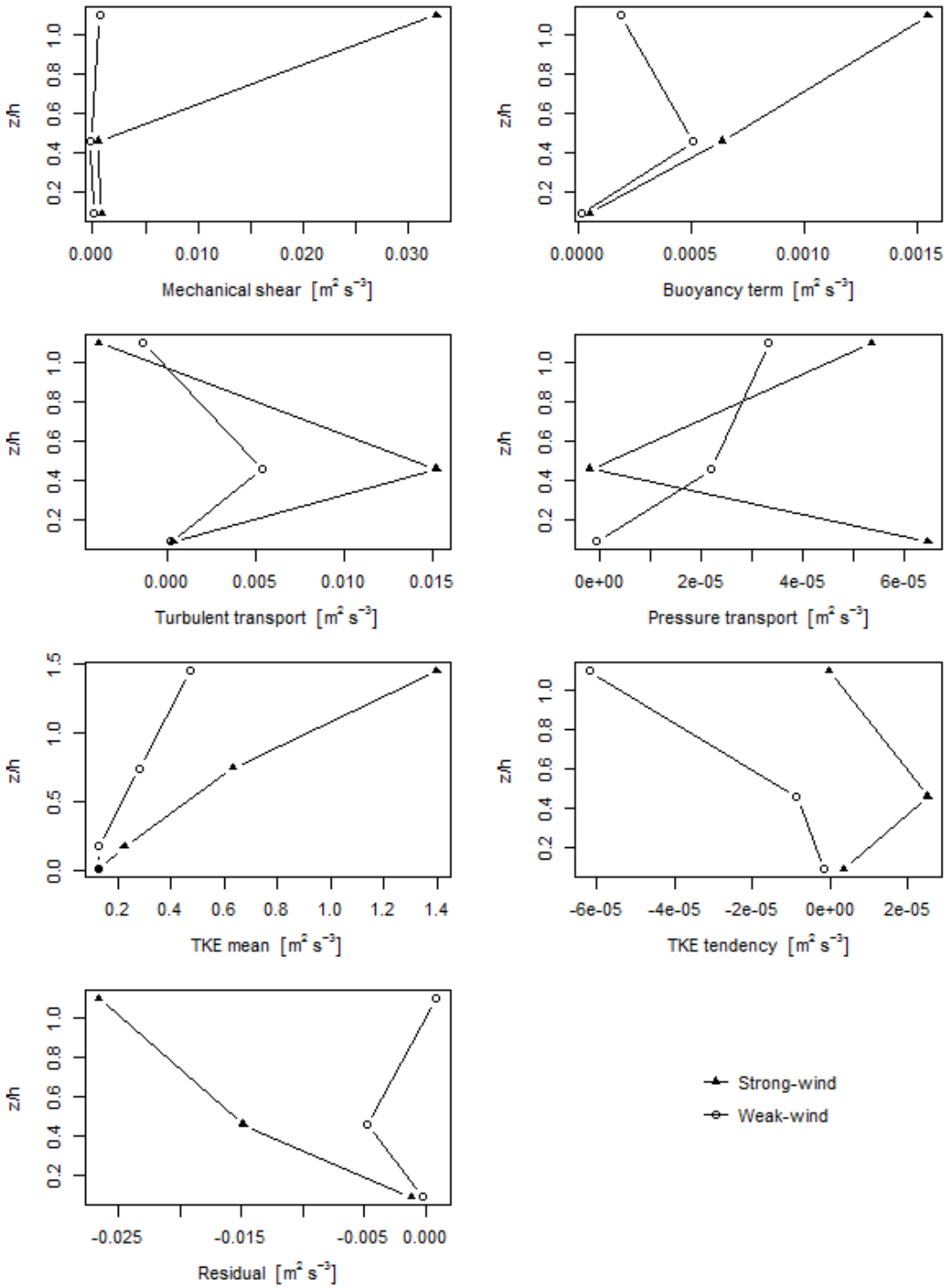

FIGURE 6.0.5: Vertical profile of the TKE terms of the wind regimes. The threshold = 0.6 $m\ s^{-1}$ was applied to the top of the canopy and canopy layer, too (In contrast to Figure 5.4.1). The symbols indicate the mean of the respective layer and are located at the midpoint of each layer. The filled circles (•) represent the dense forest, while the open diamonds (◇) stand for the sparse canopy. Measurement height z is normalized by the canopy height h.